ATOMIC AND MOLECULAR PHYSICS

PHAS2224

2015 – 2016

Dr. Stephen Hogan
Department of Physics and Astronomy
University College London

09.04.2016

General Information

Dr. Stephen Hogan

Office: Room E20 Physics Building
Email: s.hogan@ucl.ac.uk
Phone: 34324

Course outline:

1. Structure and spectra of atoms
2. Lasers and laser cooling
3. Molecular structure - diatomic molecules
4. Atoms in magnetic and electric fields
5. Particle scattering

Recommended text books:[1]

- *Introduction to the Structure of Matter*, J. J. Brehm and W. J. Mullins, Wiley & Sons (1989)
- *Quantum Physics of Atoms, Molecules, Solids, Nuclei and Particles*, R. Eisberg and R. Resnick, Wiley & Sons (1985)
- *Spectra of Atoms and Molecules*, P. F. Bernath, Oxford University Press, 2nd Edition (2005)
- *Physics of Atoms and Molecules*, B. H. Bransden and C. J. Joachain, Prentice Hall, 2nd Edition (2003)

[1]The first three books listed here cover particular parts in the course at the appropriate level, with a greater emphasis on molecular structure in the third book. The last book listed covers everything encountered in the course, but generally in more depth than is required.

Contents

Part I

Atomic Structure

Chapter 1

Introduction

The main objective of this course is to provide a detailed overview of the structure of atoms and small diatomic molecules, and their interactions with electric, magnetic and electromagnetic fields.

This information is of importance in many areas of research including, for example[1]:

1. Tests of fundamental physics: Comparison of high precision experimental measurements of the energy-level structure of H, He, H_2 and other simple atoms and molecules, with the results of calculations provide a basis for fundamental tests of atomic and molecular quantum mechanics. For example, at present very precise measurements of energy intervals in the hydrogen atom suggest that the radius of the proton may be different from that which has been determined up to now[2]. This is motivating new precision spectroscopy experiments involving hydrogen-like atoms which may help understand the origins of this discrepancy.

2. Investigations of matter-antimatter asymmetries: Comparison studies of the energy level structure of the hydrogen (H) and anti-hydrogen ($\overline{\mathrm{H}}$) atoms are currently being developed with the aim of investigating why our

[1] Note: the following list is only a very small subset of the research areas in which the content of this course if of importance.

[2] *The Proton Radius Puzzle*, J. C. Bernauer and R. Pohl, Scientific American, February 2014.

observable Universe appears to composed predominantly of matter, even though at the time of Big Bang it is thought that equal amounts of matter and antimatter should have been created. In this area, studies involving the hydrogen-like positronium atom (Ps), composed of an electron bound to its antiparticle, the positron, may also provide insight.

3. Studies of extrasolar planets: Accurate measured or calculated spectra of small molecules are of importance in many areas of research ranging from environmental sensing, to searches for signs of life on planetary objects outside the solar system (extrasolar planets, or exoplanets). Comparison of these spectra with those observed in emission or absorption from such planets allow the molecular composition of their atmospheres to be determined. By precisely identifying the atmospheric composition it may be possible to identify signs of life.

4. Atomic clocks: At present the second is defined with respect to the inverse of the frequency of the electromagnetic radiation required to drive a microwave transition between to energy levels in the caesium (Cs) atom. However, more precise clocks have now been developed in which optical transitions are driven in, e.g., strontium (Sr) atoms or aluminium (Al^+) ions. A detailed knowledge of the energy level structure of these atoms and their susceptibility to electric and magnetic fields is essential for the identification of appropriate transitions for the further development of more precise atomic clocks such as these.

5. Quantum computing: Efforts in many laboratories around the world to develop new quantum technologies, including those related to quantum computation, center around the use of pairs of energy levels in neutral atoms [e.g., helium (He) or rubidium (Rb)], or in atomic ions [e.g., the calcium ion (Ca^+)], as quantum bits (qubits). A precise knowledge of the lifetimes of these energy levels, and their sensitivity to electric, magnetic and electromagnetic fields is crucial to take advantage of the opportunities that these systems offer in this area.

Chapter 2

One-electron atoms

To begin we consider atoms and atomic ions with one electron bound to a nucleus, or ion core, with a charge $q = +Z_{\text{core}}e$, where e is the charge of the electron. Many of these atoms exist and include those listed in the table below.

System	Symbol	Composition	Z_{core}
Hydrogen atom	H	$p^+ - e^-$	$+1e$
Deuterium atom	D	$np^+ - e^-$	$+1e$
Positronium atom	Ps	$e^+ - e^-$	$+1e$
He^+ ion	He^+	$He^{2+} - e^-$	$+2e$
Li^{2+} ion	Li^{2+}	$Li^{3+} - e^-$	$+3e$

2.1 Hamiltonian

The two particles in these systems, the electron with a charge $-e$ and the ion core with charge $+Z_{\text{core}}e$, interact via the Coulomb interaction for which the potential energy is given by

$$V(r) = \frac{-Z_{\text{core}}e^2}{4\pi\epsilon_0 r}, \tag{2.1}$$

where ϵ_0 is the permittivity of the vacuum, and $r = |\vec{r}|$ is the inter-particle separation.

In this situation, if the ion core A^+ (see Figure 2.1) is considered to be

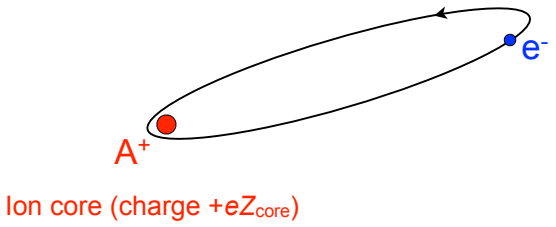

Figure 2.1: A one electron atom in which a single electron is bound to a nucleus, or ion core, of charge $+eZ_{\text{core}}$.

infinitely heavy, the Hamiltonian governing the motion of the electron is

$$\hat{H} = -\frac{\hbar^2}{2m_{\text{e}}}\nabla^2 - \frac{Z_{\text{core}}e^2}{4\pi\epsilon_0 r}, \tag{2.2}$$

where $\hbar = h/(2\pi)$ with h the Planck constant, and m_{e} is the mass of the electron.

2.2 Energy levels

The energy eigenvalues, E, associated with this quantum system can be obtained by solving the Schrödinger equation

$$\hat{H}\,\Psi = E\,\Psi, \tag{2.3}$$

where Ψ are the wavefunctions of the electronic states. This leads to a set of energy eigenvalues, E_n, of the form

$$E_n = -\frac{m_{\text{e}}\,Z_{\text{core}}^2 e^4}{32\pi^2\epsilon_0^2\hbar^2 n^2}, \tag{2.4}$$

where $n = 1, 2, 3, \ldots \infty$ is the *principal quantum number* (see Figure 2.2).

Equation 2.4 leads to an energy of the $n = 1$ ground state of the H atom of

$$E_{n=1}^{\text{calc}} = -2.17991 \times 10^{-18}\ \text{J}. \tag{2.5}$$

However, the experimentally measured value for this ground state energy is

$$E_{n=1}^{\text{expt}} = -2.17872 \times 10^{-18}\ \text{J}. \tag{2.6}$$

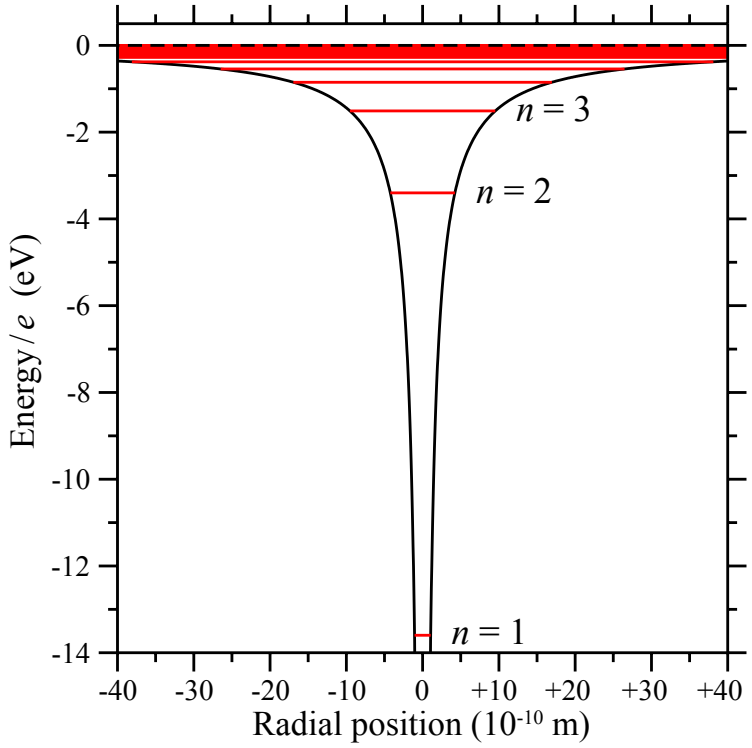

Figure 2.2: Electronic energy levels (red horizontal lines - see Equation 2.4) and Coulomb potential (black curves) associated with the H atom.

The discrepancy between these calculated and measured values is result of the assumption that in this simplified description of the H atom, the ion core (proton) is treated as being infinitely heavy.

2.2.1 Emission and absorption spectra

Early emission spectra of H atoms were recorded by generating an electric discharge in a cell containing hydrogen gas. The energies of the emitted photons observed corresponded to the energy differences between the discrete electronic energy levels of the atoms (see Figure 2.3).

In emission, if E_{n_i} is the energy of the initial state with principal quantum number n_i, and E_{n_f} is the energy of the lower-lying, final state, n_f, where

$$E_{n_\mathrm{i}} = -\frac{m_\mathrm{e} Z_\mathrm{core}^2 e^4}{32\pi^2 \epsilon_0^2 \hbar^2} \frac{1}{n_\mathrm{i}^2} \tag{2.7}$$

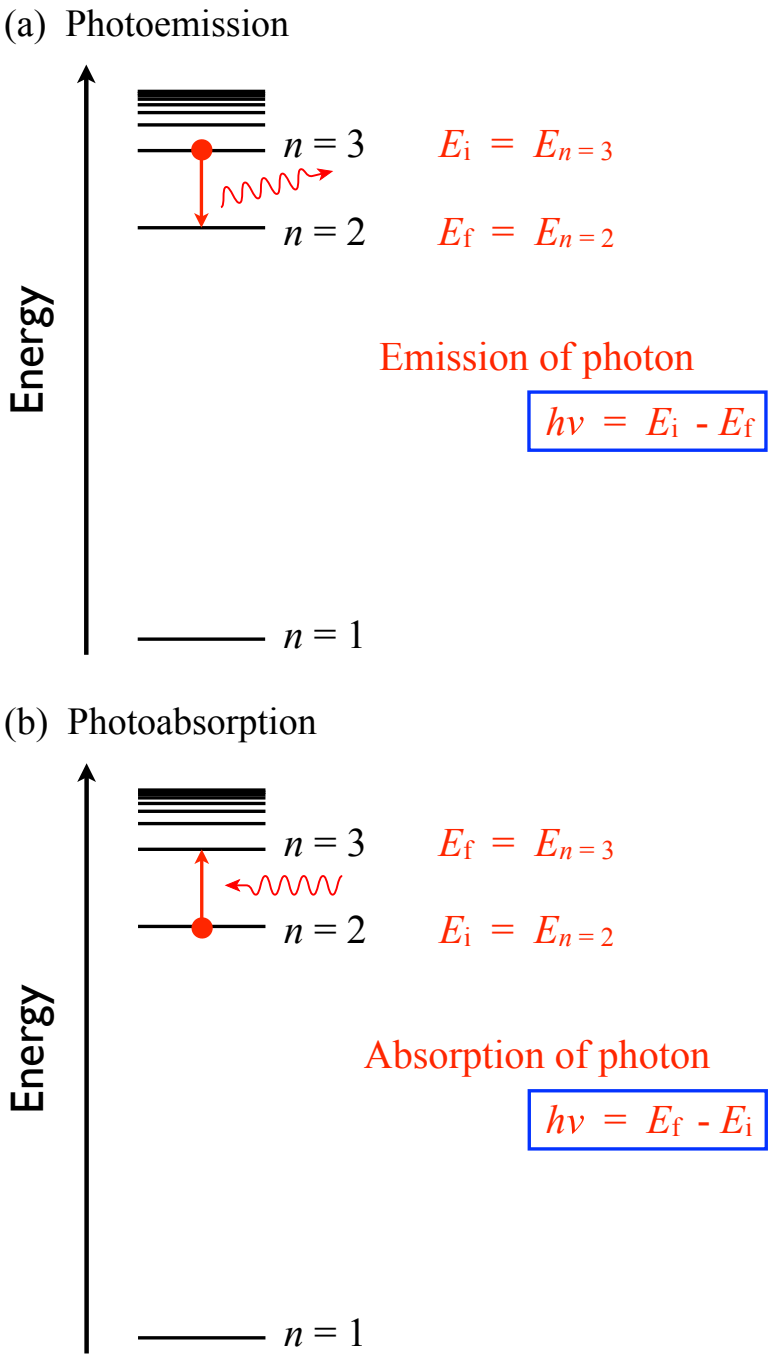

Figure 2.3: The processes of (a) emission, and (b) absorption of a photon by a H atom.

and

$$E_{n_\mathrm{f}} = -\frac{m_\mathrm{e} Z_\mathrm{core}^2 e^4}{32\pi^2 \epsilon_0^2 \hbar^2} \frac{1}{n_\mathrm{f}^2}, \tag{2.8}$$

the energy of the emitted photon is equal to the energy difference, $\Delta E_{\mathrm{i}\,\mathrm{f}}$, between the two states

$$\Delta E_{\mathrm{i}\,\mathrm{f}} = E_{n_\mathrm{i}} - E_{n_\mathrm{f}} = \frac{m_\mathrm{e} Z_\mathrm{core}^2 e^4}{32\pi^2 \epsilon_0^2 \hbar^2} \left(\frac{1}{n_\mathrm{f}^2} - \frac{1}{n_\mathrm{i}^2} \right). \tag{2.9}$$

If $n_\mathrm{i} > n_\mathrm{f}$ a photon is emitted [Figure 2.3(a)], while if $n_\mathrm{i} < n_\mathrm{f}$ a photon can be absorbed by the atom [Figure 2.3(b)].

Regular series of sharp spectral lines were first identified in H atom emission spectra by Johann Balmer in 1885. Balmer realised that these sharp lines indicated that photoemission must occur following transitions between discrete energy levels within the atoms.

Following this, in 1888 Johannes Rydberg found an empirical formula linking the wavelengths of the observed spectral lines, $\lambda_{\mathrm{i}\,\mathrm{f}}$, with the quantum numbers of the states involved in the transitions

$$\frac{1}{\lambda_{\mathrm{i}\,\mathrm{f}}} = R \left(\frac{1}{n_\mathrm{f}^2} - \frac{1}{n_\mathrm{i}^2} \right), \tag{2.10}$$

where R is a constant.
Since

$$\begin{aligned} \Delta E_{\mathrm{i,f}} &= h\nu_{\mathrm{i}\,\mathrm{f}} \\ &= \frac{hc}{\lambda_{\mathrm{i}\,\mathrm{f}}}, \end{aligned} \tag{2.11}$$

where $\nu_{\mathrm{i}\,\mathrm{f}}$ is the transition frequency, and c is the speed of light in vacuum, by comparing Equation 2.9 and Equation 2.10

$$R = \frac{m_\mathrm{e} Z_\mathrm{core}^2 e^4}{64\pi^3 \epsilon_0^2 \hbar^3 c}, \tag{2.12}$$

and is known as the *Rydberg constant*.

Because this expression (Equation 2.12) for the Rydberg constant results from the comparison of Rydberg's formula (Equation 2.10) with an equation obtained for a hydrogen atom in which the electron is considered to be

bound to an infinitely heavy ion core, when $Z_{\text{core}} = +1$ this value of the Rydberg constant is denoted R_∞, such that

$$\begin{aligned} R_\infty &= \frac{m_e e^4}{64\pi^3 \epsilon_0^2 \hbar^3 c} \\ &= 10\,973\,731.6\ \text{m}^{-1} \\ &= 109\,737.316\ \text{cm}^{-1} \end{aligned} \tag{2.13}$$

2.2.2 Accounting for the finite mass of the ion core

In the above treatment of one-electron atoms the single electron of mass $m_e = 9.109 \times 10^{-31}$ kg is considered to be bound to an infinitely heavy ion core. The result of this is that the motion of the electron does not affect the center-of-mass motion.

This is generally not a bad approximation since, e.g., for the H atom the mass of the ion core $M_{\text{core}} = m_p$, where $m_p = 1.673 \times 10^{-27}$ kg, so

$$m_p \gg m_e. \tag{2.14}$$

and

$$\frac{m_p}{m_e} = 1836. \tag{2.15}$$

However, corrections to the energy level structure arising from the finite mass of the ion core are important. These effects give rise to energy level shifts for different isotopes of the same atomic species, e.g., H, D, and T, and as a result different transitions frequencies.

To treat the finite mass of the ion core in a one-electron atom we must consider the *reduced mass*, μ_M of the two-body system. This is the effective mass of the system in the frame of reference associated with the center-of-mass.

In the case of the H atom, the forces acting on the electron and the proton in this frame of reference are indicated in Equation 2.4, where

$$\vec{r} = \vec{r}_e - \vec{R}_p \tag{2.16}$$

and

$$\vec{F}_{pe} = -\vec{F}_{ep}. \tag{2.17}$$

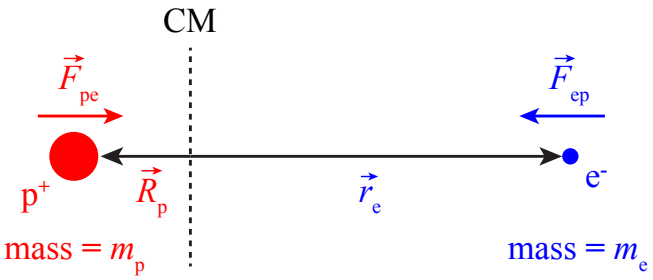

Figure 2.4: The forces acting on the electron and proton in the H atom in the frame of reference associated with the center-of-mass (CM) of the system.

Given that

$$\vec{F}_{pe} = m_p \frac{d^2\vec{R}_p}{dt^2} \qquad \text{and} \qquad \vec{F}_{ep} = m_e \frac{d^2\vec{r}_e}{dt^2},$$

$$\frac{\vec{F}_{pe}}{m_p} = \frac{d^2\vec{R}_p}{dt^2} \qquad \text{and} \qquad \frac{\vec{F}_{ep}}{m_e} = \frac{d^2\vec{r}_e}{dt^2}. \tag{2.18}$$

With the result that

$$\frac{\vec{F}_{ep}}{m_e} - \frac{\vec{F}_{pe}}{m_p} = \frac{d^2\vec{r}_e}{dt^2} - \frac{d^2\vec{R}_p}{dt^2} \tag{2.19}$$

$$= \frac{d^2\vec{r}}{dt^2}. \tag{2.20}$$

Using Equation 2.17 this leads to

$$\vec{F}_{ep}\left(\frac{1}{m_e} + \frac{1}{m_p}\right) = \frac{d^2\vec{r}}{dt^2}. \tag{2.21}$$

If

$$\frac{1}{\mu_M} = \frac{1}{m_e} + \frac{1}{m_p}, \tag{2.22}$$

an expression for the equation of motion of the two-body system is obtained:

$$\vec{F}_{ep} = \mu_M \frac{d^2\vec{r}}{dt^2}, \tag{2.23}$$

in terms of the *reduced mass*

$$\mu_M = \frac{m_e m_p}{m_e + m_p}. \tag{2.24}$$

For the above treatment of a one-electron atom with an infinitely heavy ion core, the reduced mass is

$$\mu_\infty = \lim_{m_p \to \infty} \frac{m_e m_p}{m_e + m_p} \tag{2.25}$$

$$= m_e, \tag{2.26}$$

and therefore Equation 2.13 can also be expressed in the form

$$R_\infty = \frac{\mu_\infty e^4}{64\pi^3 \epsilon_0^2 \hbar^3 c}. \tag{2.27}$$

To account for the effect of the finite mass of the proton in the H atom the Rydberg constant, R_H, must be determined, where

$$R_H = \frac{\mu_H e^4}{64\pi^3 \epsilon_0^2 \hbar^3 c}, \tag{2.28}$$

and

$$\begin{aligned} \mu_H &= \frac{m_e m_p}{m_e + m_p} \\ &= 0.999456\, m_e. \end{aligned} \tag{2.29}$$

Therefore

$$\begin{aligned} R_H &= R_\infty \frac{\mu_H}{m_e} \\ &= 0.999456\, R_\infty \\ &= 109\,677.583\ \text{cm}^{-1}. \end{aligned} \tag{2.30}$$

Or more generally for a one-electron atom of mass M, with an ion core of charge $+e\,Z_{core}$,

$$R_M = R_\infty \frac{\mu_M}{m_e} Z_{core}^2. \tag{2.31}$$

2.2.3 Spectroscopic units

The Rydberg constant[1], R_∞, is defined as a wave number in units of m^{-1}, or cm^{-1}, as

$$\begin{aligned} R_\infty &= 10\,973\,731.568\,508 \pm 0.000\,065\ \mathrm{m}^{-1} \\ &= 109\,737.315\,685\,08 \pm 0.000\,000\,65\ \mathrm{cm}^{-1}. \end{aligned} \tag{2.32}$$

It is most common in atomic and molecular spectroscopy to quote the wave number, $\tilde{\nu}$, of the radiation emitted or absorbed, such that

$$\tilde{\nu} = \frac{1}{\lambda}, \tag{2.33}$$

where λ is the wavelength of the radiation. The wave number is therefore is the number of wavelengths per unit length (i.e., per meter, or per centimeter).

Although SI units will generally be used throughout this course, there are some occasions where it is convenient to express quantities in atomic units. In this unit system

The atomic unit of mass is the electron mass, m_e

The atomic unit of charge is the charge of the electron, e

The atomic unit of length is the Bohr radius, a_0

The atomic unit of energy is $2hcR_M$

and therefore

$$\hbar = 4\pi\epsilon_0 = a_0 = e = m_\mathrm{e} = 1. \tag{2.34}$$

For example, in this system of units the Coulomb potential associated with the interaction of the electron and the proton in the hydrogen atom

$$V(r) = -\frac{e^2}{4\pi\epsilon_0\, r} \tag{2.35}$$

can be expressed as

$$V(r) = -\frac{1}{r}. \tag{2.36}$$

[1]CODATA Internationally recommended 2014 values of the fundamental physical constants (http://physics.nist.gov/cuu/Constants)

2.2.4 Example exam question

2014

Section A

Question 2.[2]

The experimentally recorded spectrum below represents a portion of a Rydberg series of a neutral atom. Determine, giving your reasoning, what the atom is. **[6]**

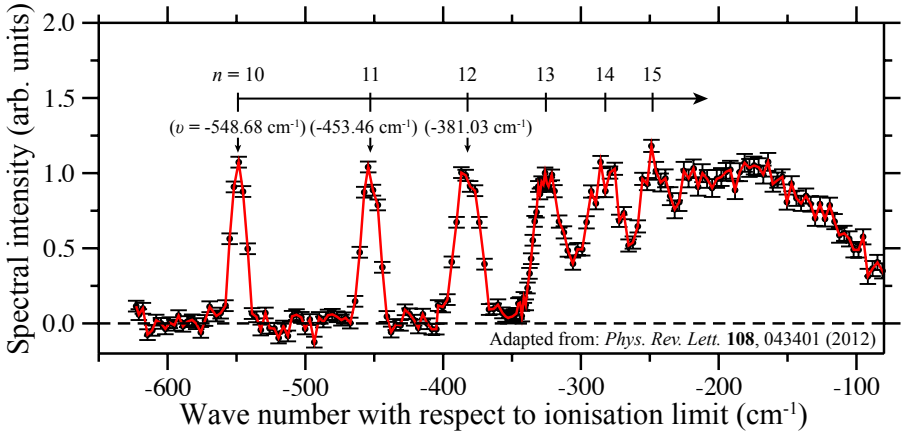

[2]The data presented in this exam question was adapted from a recent publication: D. B. Cassidy, T. H. Hisakado, H. W. K. Tom, and A. P. Mills, Jr., Efficient Production of Rydberg Positronium, *Phys. Rev. Lett.* **108**, 043401 (2012)

2.3 Wavefunctions

The Shrödinger equation associated with the Hamiltonian in Equation 2.2 when expressed in spherical polar coordinates (r, θ, ϕ), where

$$x = r\sin(\theta)\cos(\phi) \tag{2.37}$$

$$y = r\sin(\theta)\sin(\phi) \tag{2.38}$$

$$z = r\cos(\theta), \tag{2.39}$$

results in wavefunctions $\Psi(r, \theta, \phi)$, that are separable into radial, $R(r)$, and angular, $Y(\theta, \phi)$, components such that

$$\Psi(r, \theta, \phi) = R(r)\,Y(\theta, \phi). \tag{2.40}$$

2.3.1 Angular momentum in quantum mechanics

The classical orbital angular momentum, $\vec{L} = (L_x, L_y, L_z)$, of a particle can be expressed in terms of the radial position vector, $\vec{r} = (x, y, z)$, and the linear momentum, $\vec{p} = (p_x, p_y, p_z)$ as

$$\vec{L} = \vec{r} \times \vec{p}. \tag{2.41}$$

therefore

$$L_x = yp_z - zp_y \tag{2.42}$$

$$L_y = zp_x - xp_z \tag{2.43}$$

$$L_z = xp_y - yp_x. \tag{2.44}$$

From the Correspondence Principle

$$\vec{p} \Rightarrow \hat{\vec{p}} = -i\hbar\hat{\vec{\nabla}} \tag{2.45}$$

and

$$\vec{r} \Rightarrow \hat{\vec{r}}. \tag{2.46}$$

Therefore the quantum mechanical operators associated with angular momentum are

$$\hat{\vec{L}} = -i\hbar(\hat{\vec{r}} \times \hat{\vec{\nabla}}) \tag{2.47}$$

$$\hat{L}_x = -i\hbar\left(\hat{y}\frac{\partial}{\partial z} - \hat{z}\frac{\partial}{\partial y}\right) \tag{2.48}$$

$$\hat{L}_y = -i\hbar\left(\hat{z}\frac{\partial}{\partial x} - \hat{x}\frac{\partial}{\partial z}\right) \tag{2.49}$$

$$\hat{L}_z = -i\hbar\left(\hat{x}\frac{\partial}{\partial y} - \hat{y}\frac{\partial}{\partial x}\right) \tag{2.50}$$

and

$$\hat{\vec{L}}^2 = \hat{L}_x^2 + \hat{L}_y^2 + \hat{L}_z^2. \tag{2.51}$$

This set of angular momentum operators obey the commutation relation

$$\begin{aligned}\left[\hat{L}_i, \hat{L}_j\right] &= \hat{L}_i\hat{L}_j - \hat{L}_j\hat{L}_i \\ &= i\hbar\hat{L}_k,\end{aligned} \tag{2.52}$$

where $i, j, k \equiv x, y, z$.

Consequently, the individual x, y or z components of $\hat{\vec{L}}$ cannot be assigned definite values simultaneously unless $\vec{L} = (0, 0, 0)$.

However, the operator $\hat{\vec{L}}^2$ does commute any one of the individual components of $\vec{L}$, i.e.,

$$\left[\hat{\vec{L}}^2, \hat{L}_j\right] = 0, \tag{2.53}$$

$$\text{E.g.,} \quad \left[\hat{\vec{L}}^2, \hat{L}_z\right] = 0. \tag{2.54}$$

Therefore it is possible to have simultaneous eigenfunctions of $\hat{\vec{L}}^2$ and one individual component of $\hat{\vec{L}}$. By convention the component $\hat{L}_z$ is chosen.

Under these conditions the angular momentum vector $\vec{L}$ can be considered to precess about the z-axis (see Figure 2.5). This precessional motion preserves $\hat{\vec{L}}^2$ and $\hat{L}_z$ while the time-averaged values of $\hat{L}_x$ and $\hat{L}_y$ are zero.

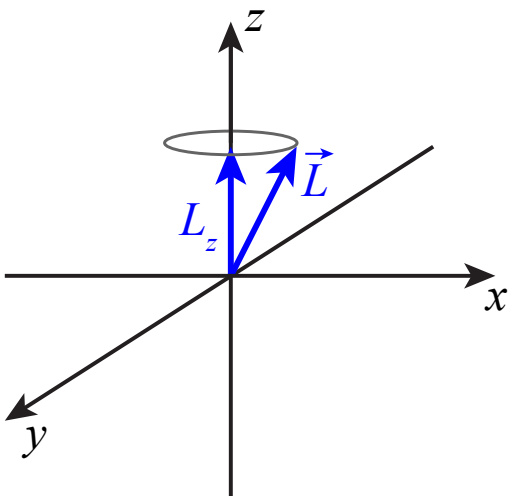

Figure 2.5: Precession of the angular momentum vector $\vec{L}$ about the z-axis.

Converting the expressions in Equation 2.48 – Equation 2.51 into spherical polar coordinates leads to

$$\hat{L}_z = -i\hbar\left(\hat{x}\frac{\partial}{\partial y} - \hat{y}\frac{\partial}{\partial x}\right) = -i\hbar\frac{\partial}{\partial \phi} \tag{2.55}$$

$$\hat{\vec{L}}^2 = \hbar^2\left[\frac{1}{\sin\theta}\frac{\partial}{\partial\theta}\left(\sin\theta\frac{\partial}{\partial\theta}\right) + \frac{1}{\sin^2\theta}\frac{\partial^2}{\partial\phi^2}\right]. \tag{2.56}$$

The simultaneous eigenfunctions of the eigenvalue equations involving the operators $\hat{L}_z$ and $\hat{\vec{L}}^2$ are the *spherical harmonic* functions, $Y_{\ell,m}(\theta,\phi)$.

$$\hat{\vec{L}}^2\, Y_{\ell,m}(\theta,\phi) = \ell(\ell+1)\hbar^2\, Y_{\ell,m}(\theta,\phi) \tag{2.57}$$

$$\hat{L}_z\, Y_{\ell,m}(\theta,\phi) = m\hbar\, Y_{\ell,m}(\theta,\phi). \tag{2.58}$$

$\ell = 0, 1, 2, 3, \ldots$ is the *orbital angular momentum quantum number*

$m = 0, \pm1, \pm2, \cdots \pm\ell$ is the *azimuthal quantum number*

The discrete values of these quantum numbers indicate that the electron orbital angular momentum is quantised. The value of m corresponds to the projection of the electron orbital angular momentum vector, $\vec{\ell}$, onto the z-axis, and is also often referred to as the *magnetic quantum number*.

2.3.2 Spherical harmonic functions

The spherical harmonic functions, $Y_{\ell,m}(\theta,\phi)$, are separable functions, i.e.,

$$Y_{\ell,m}(\theta,\phi) \quad = \quad \Phi_m(\phi)\,\Theta_{\ell,m}(\theta). \tag{2.59}$$

The two components of these functions are

$$\Phi_m(\phi) \quad = \quad \frac{1}{\sqrt{2\pi}}\,\mathrm{e}^{im\phi}, \tag{2.60}$$

and

$$\Theta_{\ell,m}(\theta) \quad \propto \quad \mathrm{P}_\ell^m(\cos\theta), \tag{2.61}$$

where the functions $\mathrm{P}_\ell^m(\cos\theta)$ are *associated Legendre polynomials*.

The complete set of normalised spherical harmonic functions can be expressed explicitly as

$$Y_{\ell,m}(\theta,\phi) \quad = \quad \frac{1}{\sqrt{2\pi}}\,\mathrm{e}^{im\phi}\left[\frac{(2\ell+1)(\ell-|m|)!}{2(\ell+|m|)!}\right]^{1/2}\mathrm{P}_\ell^{|m|}(\cos\theta), \tag{2.62}$$

with examples for low values of ℓ and m in Table 2.1 below, and in Figure 2.6.

ℓ	m	$Y_{\ell,m}(\theta,\phi)$
0	0	$Y_{0,0} = \frac{1}{\sqrt{4\pi}}$
1	0	$Y_{1,0} = \sqrt{\frac{3}{4\pi}}\cos\theta$
	±1	$Y_{1,\pm1} = \mp\sqrt{\frac{3}{8\pi}}\sin\theta\,\mathrm{e}^{\pm i\phi}$
2	0	$Y_{1,0} = \sqrt{\frac{5}{16\pi}}\left(3\cos^2\theta-1\right)$
	±1	$Y_{2,\pm1} = \mp\sqrt{\frac{15}{8\pi}}\sin\theta\cos\theta\,\mathrm{e}^{\pm i\phi}$
	±2	$Y_{2,\pm2} = \sqrt{\frac{15}{32\pi}}\sin^2\theta\,\mathrm{e}^{\pm 2i\phi}$

Table 2.1: Spherical harmonic functions with $\ell = 0, 1$ and 2, and $m = 0, \pm1$ and ±2 as indicated.

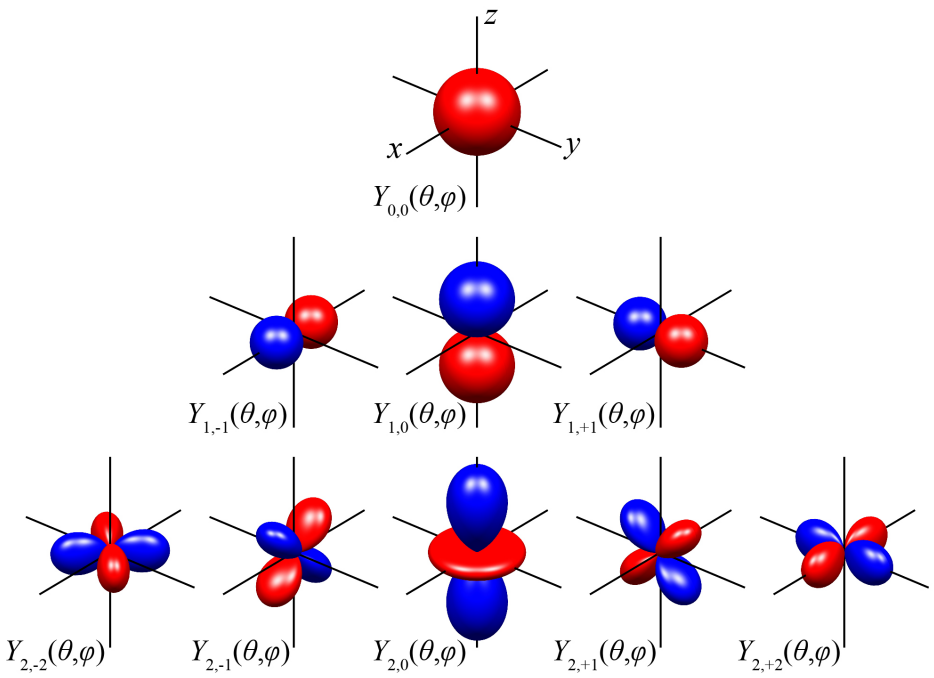

Figure 2.6: Angular probability distributions represented by the spherical harmonic functions, $Y_{\ell,m}(\theta,\phi)$, for which $\ell = 0, 1$ and 2. In each panel, the sign of the function is indicated by the colour - positive values are indicated in red while, negative values are indicated in blue.

2.3.3 Parity

Parity is an important symmetry in atomic and molecular systems. When applied to a function expressed in spherical polar coordinates, the parity transformation is an inversion of the function through the origin such that $\vec{r} \rightarrow -\vec{r}$. When the parity operator, $\hat{P}$, associated with this transformation is applied to a function $f(\vec{r})$, the result can therefore be expressed as

$$\hat{P}f(\vec{r}) \quad = \quad f(-\vec{r}). \tag{2.63}$$

i. If $\hat{P}f(\vec{r}) = f(\vec{r})$

i.e., if $f(-\vec{r}) = f(\vec{r})$

$\Rightarrow$ the function $f(\vec{r})$ is said to have *even* parity.

ii. If $\hat{P}f(\vec{r}) = -f(\vec{r})$

i.e., if $f(-\vec{r}) = -f(\vec{r})$

$\Rightarrow$ the function $f(\vec{r})$ is said to have *odd* parity.

When applied to the spherical harmonic functions, $Y_{\ell,m}(\theta,\phi)$, in Equation 2.62:

The parity of $e^{im\phi}$ is given by $(-1)^m$

The parity of $P_\ell^m(\cos\theta)$ is given by $(-1)^{\ell-m}$

Therefore

$$\hat{P}\, Y_{\ell,m}(\theta,\phi) \quad = \quad (-1)^\ell\, Y_{\ell,m}(\theta,\phi), \tag{2.64}$$

and the parity of $Y_{\ell,m}(\theta,\phi)$ is given by $(-1)^\ell$ so that

If $(-1)^\ell = +1$, the corresponding spherical harmonic has *even* parity

If $(-1)^\ell = -1$, the corresponding spherical harmonic has *odd* parity

2.3.4 Spectroscopic notation

In the spectroscopic notation used to label one-electron orbitals in atoms, the orbital angular momentum quantum number, ℓ, is represented by a lower case letter.

$\ell =$	0	1	2	3	4	5	...
	s	p	d	f	g	h	...

This labelling system arose from early observations of atomic spectra in which emission from excited states with $\ell = 0$ was seen to give rise to *sharp* spectral features leading to these states been labelled as s-states. The strongest, *principal*, features in such spectra arose from emission from excited states with $\ell = 1$, hence these states were labelled as p-states, while the emission from states with $\ell = 2$ was seen to be more *diffuse*, leading to the labelling of these states as d-states.

For example:

- The ground state of the H atom has $n = 1$, $\ell = 0$, $m = 0$ and is therefore denoted the 1s state
- The excited state of the H atom for which $n = 2$, $\ell = 1$, $m = 0$ is therefore denoted the 2p state (see Figure 2.7)

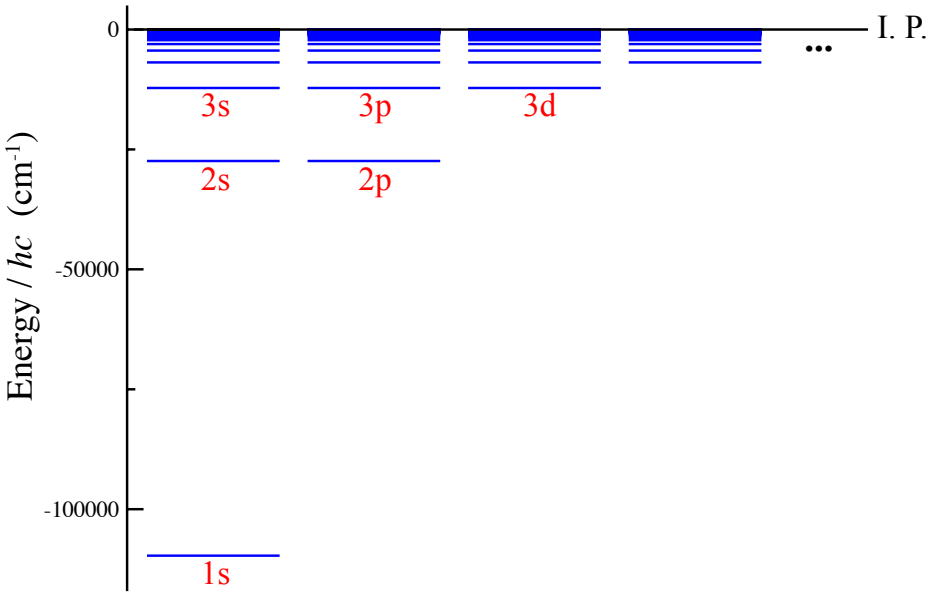

Figure 2.7: Energy levels of the H atom labelled according to the spectroscopic notation for one-electron atomic orbitals.

2.3.5 Radial wavefunctions

For a one electron atom such as the H atom, the radial component, $R(r)$, of the total wavefunctions in Equation 2.40 can be determined analytically[3], and take the form

$$R_{n,\ell}(r) = N_{n,\ell}\left[\frac{2Z_{\text{core}}}{na_0}r\right]^{\ell}\exp\left(-\frac{2Z_{\text{core}}}{na_0}r\right)\mathrm{L}^{2\ell+1}_{n-\ell-1}\left(\frac{2Z_{\text{core}}}{na_0}r\right), \quad (2.65)$$

where $N_{n,\ell}$ is a normalisation constant,

$$N_{n,\ell} = \left(\frac{2Z_{\text{core}}}{na_0}\right)^{3/2}\sqrt{\frac{(n-\ell-1)!}{2n(n+\ell)!}}, \quad (2.66)$$

[3] *Quantum Mechanics of One- and Two-Electron Atoms* H. A. Bethe and E. E. Salpeter, Springer, Berlin, 1957

$\mathrm{L}_a^b(x)$ are the *associated Laguerre polynomials* which take the form

$$\mathrm{L}_a^b(x) \quad = \quad \sum_{k=0}^{a} (-1)^k \frac{(a+b)!}{(a-b)!\,(b+k)!\,k!} x^k, \tag{2.67}$$

and a_0 is the Bohr radius for the H atom, where

$$a_0 \quad = \quad \frac{4\pi\epsilon_0\hbar^2}{e^2\, m_\mathrm{e}}. \tag{2.68}$$

The radial wavefunctions in a one-electron atom therefore only depend on the principal quantum number n, and the electron orbital angular momentum quantum number ℓ. Some examples of radial wavefunctions for low values of n and ℓ are given in Table 2.2 below.

n	ℓ	$R_{n,\ell}(r)$
1	0	$R_{1,0} = 2\left(\frac{Z_\mathrm{core}}{a_0}\right)^{3/2} \mathrm{e}^{-\frac{Z_\mathrm{core} r}{a_0}}$
2	0	$R_{2,0} = 2\left(\frac{Z_\mathrm{core}}{2a_0}\right)^{3/2} \left(1 - \frac{Z_\mathrm{core} r}{2a_0}\right) \mathrm{e}^{-\frac{Z_\mathrm{core} r}{2a_0}}$
	1	$R_{2,1} = \frac{1}{\sqrt{3}} \left(\frac{Z_\mathrm{core}}{2a_0}\right)^{3/2} \left(\frac{Z_\mathrm{core} r}{a_0}\right) \mathrm{e}^{-\frac{Z_\mathrm{core} r}{2a_0}}$

Table 2.2: Radial wavefunctions for states with $n = 1$ and 2, and $\ell = 0$ and 1 in one-electron atoms.

For each of these radial wavefunctions, as $r \to \infty$ the exponential term dominates, as a result for all n and ℓ,

$$R_{n,\ell}(r) \to 0 \quad \text{as} \quad r \to \infty \tag{2.69}$$

Again from the exponential term in Equation 2.65, it can be seen that:

- As the value of Z_core is increased for a selected value of n, the amplitude of the wavefunctions reduce more rapidly with increasing r

  $\Rightarrow$ The electron is therefore localised more closely to the ion core when the core is more highly charged

- As the value of n is increased for a selected value of Z_core, the amplitude of the wavefunctions reduces more slowly with increasing r

⇒ The charge of the electron is therefore extended over a longer range in more highly excited states

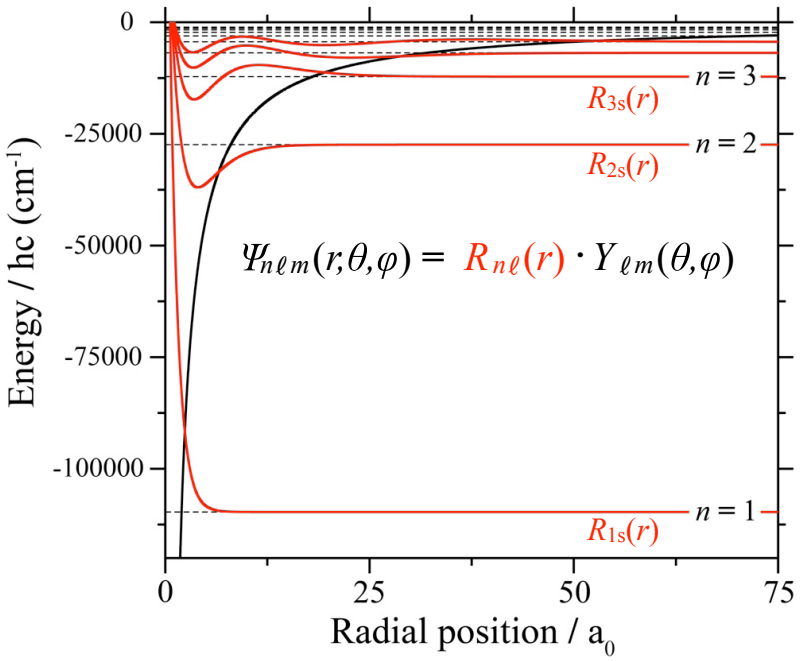

Figure 2.8: Radial wavefunctions of the 1s, 2s and 3s states of the H atom displayed at the location of each energy level (dashed horizontal lines) in the Coulomb potential (black curves) associated with the interaction between the electron and the proton.

2.3.6 Wavefunction normalisation

The total wavefunctions for the one-electron atom must be normalized so that

$$\int \left|\Psi_{n,\ell,m}(r,\theta,\phi)\right|^2 \mathrm{d}\tau \quad = \quad 1, \tag{2.70}$$

therefore

$$\int_0^\infty \left|R_{n,\ell}(r)\right|^2 r^2 \mathrm{d}r \int_0^{2\pi}\int_0^{\pi} \left|Y_{\ell,m}(\theta,\phi)\right|^2 \sin\theta \mathrm{d}\theta \mathrm{d}\phi \quad = \quad 1. \tag{2.71}$$

Since the spherical harmonic functions are normalised such that

$$\int_0^{\pi} \left|Y_{\ell,m}(\theta,\phi)\right|^2 \sin\theta \mathrm{d}\theta \mathrm{d}\phi \quad = \quad 1, \tag{2.72}$$

the function $P_{n,\ell}(r) = \left|R_{n,\ell}(r)\right|^2 r^2$, gives the radial probability distribution of the electron. This is the probability of finding the electron at a distance r from the ion core. Some examples of these radial probability distributions for selected values of n and ℓ in the H atom are displayed in Figure 2.9.

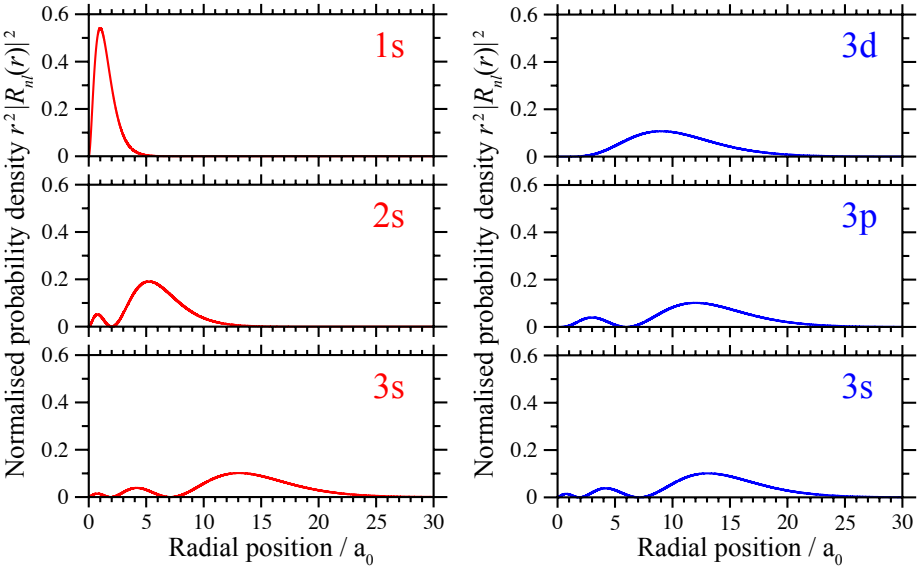

Figure 2.9: Electron radial probability distributions associated with the 1s, 2s, 3s, 3p, and 3d states in the H atom as indicated.

As can be seen from this figure, for a selected value of ℓ (left column) the spatial extent of the electron charge distribution increases with increasing values of n. For a selected value of n (right column), the probability of finding the electron near to the ion core decreases with increasing values of ℓ. This occurs because the centrifugal barrier experienced by the orbiting electron pushes it outwards to larger radial positions. As a result, low-ℓ orbitals (e.g., the s- or p-orbitals) are said to be more *core-penetrating* than orbitals with higher values of ℓ (e.g., the d-orbital).

The radial probability density distribution associated with the 1s ground state of a hydrogen-like atom can be expressed explicitly in the form

$$P_{n,\ell}(r) \quad = \quad \left|R_{n,\ell}(r)\right|^2 r^2 = \left[2\left(\frac{Z_{\text{core}}}{a_0}\right)^{3/2} \exp\left(\frac{-Z_{\text{core}} r}{a_0}\right)\right]^2 r^2. \qquad (2.73)$$

From Figure 2.9 it can be seen that this function has a single intensity

maximum. The position of this intensity maximum corresponds to the most probably radial position, r_{prob}, of the electron. By calculating the point in this function where the derivative with respect to r is zero, it is found that

$$r_{\text{prob}} = \frac{a_0}{Z_{\text{core}}}. \tag{2.74}$$

Therefore, in the ground state of the H atom, for which $Z_{\text{core}} = +1$, the orbital radius of the electron determined in the semiclassical Bohr model corresponds to the radius at which it is most likely to find the electron in the quantum treatment of the atom.

The average radial position of the electron is given by the expectation value, $\langle r \rangle$, where

$$\langle r \rangle = \int \Psi^*_{n,\ell,m}(r,\theta,\phi)\, \hat{r}\, \Psi_{n,\ell,m}(r,\theta,\phi)\, \mathrm{d}\tau \tag{2.75}$$

$$= \int_0^\infty r\, P_{n,\ell}(r)\, \mathrm{d}r, \tag{2.76}$$

and, after integration, for any $n\ell$ state in a hydrogen-like atom is

$$\langle r \rangle = \frac{a_0}{2\, Z_{\text{core}}} \Big[3n^2 - \ell(\ell+1) \Big]. \tag{2.77}$$

For the 1s state in the hydrogen atom with $Z_{\text{core}} = +1$,

$$\langle r_{1,0} \rangle = \frac{3\, a_0}{2}. \tag{2.78}$$

This average radial position of the electron in the ground state of the H atoms is larger than the r_{prob} (see Equation 2.74) because of the long tail in the radial probability distribution toward large values of r.

2.3.7 Energy level degeneracy

In a one-electron atom the energy eigenvalues, E_n, given by the Rydberg formula

$$\frac{E_n}{hc} = \frac{E_{\text{ion}}}{hc} - \frac{R_M}{n^2}, \tag{2.79}$$

depend only on the value of the principal quantum number n. For each value of n, there exist n corresponding values of ℓ [i.e., $\ell = 0, 1, 2, \ldots (n-1)$], and $2\ell + 1$ values of m (i.e., $m = 0, \pm 1, \pm 2, \cdots \pm \ell$).

As a result the total number of degenerate eigenstates, i.e., states with the same energy, E_n, in a one-electron atom is

$$\sum_{\ell=0}^{n-1}(2\ell+1) \quad = \quad n^2. \tag{2.80}$$

and there is complete energy degeneracy with respect to ℓ and m.

m-degeneracy: The m-degeneracy of the eigenstates in a one-electron atom is a feature of a central potential. Such a potential, V, depends on the magnitude of $\vec{r}$ but not its direction, i.e., $V = V(r)$.

ℓ-degeneracy: The ℓ-degeneracy of the eigenstates in a one-electron atom is a characteristic of a potential, such as the Coulomb potential, that depends on $1/r$. The ℓ-degeneracy in the atom is removed if the dependence of the potential experienced by the electron on r is modified.

2.3.8 Electron spin

In addition to its orbital angular momentum when bound within an atom, a relativistic treatment of a one-electron atom leads to an additional quantised quantity associated with the electron. This is its intrinsic *spin* angular momentum, $\vec{s}$.

As in the case of the orbital angular momentum operators $\hat{\vec{L}}^2$ and $\hat{L}_z$, the operators associated with the square of the magnitude of the spin vector, $\hat{\vec{S}}^2$, and the projection of the spin vector in the z-dimension, $\hat{S}_z$, commute, i.e.,

$$\left[\hat{\vec{S}}^2, \hat{S}_z\right] \quad = \quad 0. \tag{2.81}$$

Considering the one-electron spin eigenfunctions, χ_{s,m_s}, where s is the electron spin quantum number, and m_s is the projection of the electron spin vector in the z-dimension,

$$\hat{\vec{S}}^2\chi_{s,m_s} \quad = \quad s(s+1)\,\hbar^2\,\chi_{s,m_s} \quad \text{with} \quad s = \frac{1}{2}, \tag{2.82}$$

and

$$\hat{S}_z\chi_{s,m_s} \quad = \quad m_s\,\hbar\,\chi_{s,m_s} \quad \text{with} \quad m_s = \pm s = \pm\frac{1}{2}. \tag{2.83}$$

The total electronic wavefunction of a one-electron atom including electron spin can therefore be expressed in the form

$$\Psi_{n,\ell,m_\ell,s,m_s}(r,\theta,\phi) = \overbrace{\underbrace{R_{n,\ell}(r)}_{\text{Radial}}\,\overbrace{Y_{\ell,m_\ell}(\theta,\phi)}^{\text{Angular}}}^{\text{Space}}\,\underbrace{\chi_{s,m_s}}_{\text{Spin}}, \tag{2.84}$$

where the projection of the orbital angular momentum, m, from Section 2.3.1 has been replaced by m_ℓ to distinguish it from the projection of the spin angular momentum, m_s.

2.3.9 Transitions between energy levels

In all quantum systems transitions between different eigenstates resulting from emission or absorption of electromagnetic radiation are only allowed to occur if they fulfill an appropriate set of *selection rules*. These selection rules arise following the treatment of the interaction of the atom with an electromagnetic field which will be discussed later in the course.

In a one-electron atom the selection rules for transitions between different eigenstates require that:

- Δn = any value**:** The value of n can change by any value when a photon is emitted or absorbed.
- $\Delta \ell = \pm 1$**:** The value of ℓ must change by +1, or by −1 upon the emission or absorption of a photon to conserve angular momentum.
- $\Delta m_\ell = 0, \pm 1$**:** The value of m_ℓ can change by 0 or by ±1 upon the emission or absorption of a photon.

Examples of transitions in the H atom that fulfill these selection rules are indicated by the arrows in Figure 2.10.

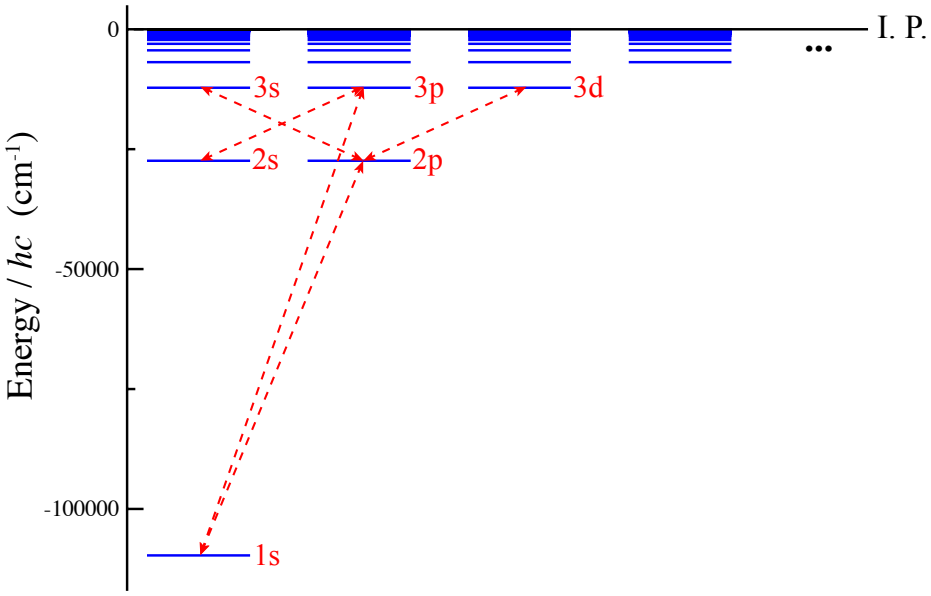

Figure 2.10: Examples of allowed transitions between $n\ell$ states of the H atom.

2.3.10 Example exam question

2014

Section B

Question 8.

The wavefunction, $\Psi_{n,\ell,m}$, of the hydrogen atom can be written as:

$$\Psi_{n,\ell,m}(\vec{r}) = R_{n,\ell}(r)\, Y_{\ell,m}(\theta,\phi)$$

in spherical polar coordinates (r,θ,ϕ).

(i) What is the function $Y_{\ell,m}(\theta,\phi)$? Illustrate your answer with a sketch of two examples of this wavefunction giving the associated quantum numbers. **[4]**

(ii) For a state with principal quantum number n, what are the possible values of the quantum numbers ℓ and m? **[2]**

(iii) What further quantum numbers (if any) are required to completely specify the state of the electron in the hydrogen atom? **[2]**

(iv) Use the wavefunction in the equation above to derive an expression for the radial probability distribution of the electron in the hydrogen atom. **[4]**

(v) Sketch radial distributions for three sets of (n, ℓ) quantum numbers, sampling wavefunctions which differ in both n and ℓ. How many nodes does the radial probability distribution of the wavefunction $\Psi_{n,\ell,m}(\vec{r})$ have?

Use these sketches to explain what is meant by 'electron penetration' when hydrogenic wavefunctions are used to describe the behaviour of many-electron atoms. What are the consequences of this for the order in which the orbitals are occupied in such atoms? **[8]**

Chapter 3

Many-electron atoms

For one-electron atoms such as the H atom the electronic Schrödinger equation can be solved analytically. For more complex atoms with many electrons, only numerical solutions to the Schrödinger equation are possible. However, using simple models it is possible to estimate the energies of, and classify, the eigenstates of atoms with more than one electron.

3.1 Hamiltonian for many-electron atoms

The electronic Hamiltonian for an atom with N electrons takes the form

$$\hat{H}(\vec{r}_1, \vec{r}_2, \vec{r}_3, \ldots \vec{r}_N) = \sum_{i=1}^{N} \Bigg[\overbrace{-\frac{\hbar^2}{2m_e}\nabla_i^2}^{\text{Single e}^- \text{ K.E.}} - \overbrace{\frac{Z_{\text{nucl}}\, e^2}{4\pi\epsilon_0 r_i}}^{\text{e}^- - \text{nucleus attraction}} \Bigg] + \ldots + \underbrace{\sum_{i=1}^{N}\sum_{j=i+1}^{N} \frac{e^2}{4\pi\epsilon_0 r_{ij}}}_{\text{e}^- - \text{e}^- \text{ repulsion}}, \tag{3.1}$$

where $r_{ij} = |\vec{r}_i - \vec{r}_j|$ is the separation between electron-i and electron-j.

For example, in the two-electron He atom, the electron-electron repulsion term, V_{rep}, is

$$V_{\text{rep}} = \frac{e^2}{4\pi\epsilon_0 r_{12}}, \tag{3.2}$$

while in the three-electron Li atom,

$$V_{\text{rep}} = \frac{e^2}{4\pi\epsilon_0 r_{12}} + \frac{e^2}{4\pi\epsilon_0 r_{13}} + \frac{e^2}{4\pi\epsilon_0 r_{23}}. \tag{3.3}$$

In general for an N-electron atom, V_{rep}, has $N(N-1)/2$ contributing terms.

The Hamiltonian for an N-electron atom, Equation 3.1, can therefore be expressed in the form of a sum over a set of single electron Hamiltonians, $\hat{h}(\vec{r}_i)$, plus a sum over the full set of electron-electron interaction terms, i.e.,

$$\hat{H}(\vec{r}) = \sum_i \hat{h}(\vec{r}_i) + \sum_{i,j>i} \frac{e^2}{4\pi\epsilon_0 r_{ij}}, \tag{3.4}$$

where $\hat{H}(\vec{r}) = \hat{H}(\vec{r}_1, \vec{r}_2, \vec{r}_3, \ldots \vec{r}_N)$.

Because the electron-electron repulsion term depends on the instantaneous positions of every pair of electrons, the Schrödinger equation associated with $\hat{H}(\vec{r})$ cannot be completely separated into single electron components and therefore cannot be solved analytically. However, it is possible to separate the single electron contributions within certain sets of approximations.

3.2 Approximate solutions to the Schrödinger equation for N-electron atoms

In the following, two approaches to obtaining approximate solutions to the Schrödinger equation for N-electron atoms will be considered. These are the *independent-particle model* and the *central-field approximation*.

3.2.1 Independent-particle model

In the independent-particle model of a many electron atom, the electron-electron repulsion is first ignored to obtain a very crude approximation for the energies of the eigenstates. The neglected interactions are then added to refine the result.

Without the electron-electron interaction term, the Hamiltonian for a N-electron atom (Equation 3.4) takes the form

$$\hat{H}(\vec{r}) = \sum_i \hat{h}(\vec{r}_i). \tag{3.5}$$

This operator is separable because the term associated with each electron, labelled with the index i, is dependent only on the position, $\vec{r}_i$, of that electron. The complete Hamiltonian is therefore the sum over N single-electron Hamiltonians, $\hat{h}(\vec{r}_i)$. Following from this each single-electron Hamiltonian will have corresponding eigenfunctions $\psi(\vec{r}_i)$, and eigenvalues E_i such that

$$\hat{h}(\vec{r}_i)\,\psi(\vec{r}_i) \quad = \quad E_i\,\psi(\vec{r}_i), \tag{3.6}$$

where, as in the one-electron atom, $\psi(\vec{r}_i) = R_{n_i,\ell_i}(r_i)\,Y_{\ell_i,m_i}(\theta_i,\phi_i)$ is separable into radial and angular components characterised by the single-electron principal quantum number n_i, angular momentum quantum number ℓ_i, and azimuthal quantum number m_i.

The total electronic wavefunction, $\Psi(\vec{r}_N)$, for the N-electron system is then the product of the N single-electron wavefunctions,

$$\Psi(\vec{r}_N) \quad = \quad \psi(\vec{r}_1)\,\psi(\vec{r}_2)\,\psi(\vec{r}_3)\,\times\cdots\times\,\psi(\vec{r}_N), \tag{3.7}$$

and the total energy, E, is the sum over the energies of the N single electrons,

$$E \quad = \quad E_1 + E_2 + E_3 + \cdots + E_N, \tag{3.8}$$

where each E_i is given by the Rydberg formula (Equation 2.79) for a one-electron atom.

To test the accuracy of this independent-particle model we use it to calculate the ground-state energy of the two-electron He atom, in which the two electrons are in the 1s orbital. The total energy of the system is therefore

$$E_{\text{gnd}}(\text{He}) \quad = \quad E_{n=1} + E_{n=1} \tag{3.9}$$

$$\frac{E_{\text{gnd}}(\text{He})}{hc} \quad = \quad -R_\infty\,Z_{\text{nucl}}^2\,\frac{\mu_{\text{He}^+}}{m_{\text{e}}} - R_\infty\,Z_{\text{nucl}}^2\,\frac{\mu_{\text{He}^+}}{m_{\text{e}}}, \tag{3.10}$$

where $Z_{\text{nucl}} = +2$ and

$$\mu_{\text{He}^+} \quad = \quad \frac{m_{\text{e}}\,m_{\text{He}^{2+}}}{m_{\text{e}} + m_{\text{He}^{2+}}}. \tag{3.11}$$

Therefore,

$$\frac{E_{\text{gnd}}(\text{He})}{hc} \quad = \quad -877\,778\ \text{cm}^{-1} \tag{3.12}$$

$$\quad \simeq \quad -8\,R_\infty. \tag{3.13}$$

However, the true ground state energy of the He atom determined from experimental measurements is

$$\frac{E_{\text{gnd}}(\text{He})}{hc} = -\frac{E_{\text{ion}}(\text{He})}{hc} - \frac{E_{\text{ion}}(\text{He}^+)}{hc}, \tag{3.14}$$

$$= -198\,311\ \text{cm}^{-1} - 438\,909\ \text{cm}^{-1}$$

$$= -637220\ \text{cm}^{-1} \tag{3.15}$$

$$\simeq -5.8\,R_\infty, \tag{3.16}$$

where $E_{\text{ion}}(\text{He})$ is the ground state ionisation energy of the neutral He atom, and $E_{\text{ion}}(\text{He}^+)$ is the ground state ionisation energy of the single-charged He^+ ion. Therefore, as might be expected, neglecting the effects of electron-electron repulsion when calculating the energy of the ground state of the He atom results in the electrons being too tightly bound.

To crudely correct for the electron-electron repulsion we can consider the typical separation between the two electrons in the 1s orbital of the He atom and approximate the repulsion energy. Since the most probable radial position of each individual electron in the 1s orbital is

$$r_{\text{prob}}(\text{He}^+\ 1\text{s}) = \frac{a_0}{Z_{\text{nucl}}} \tag{3.17}$$

$$= \frac{a_0}{2}, \tag{3.18}$$

where a_0 is the Bohr radius associated with the ground state of the H atom (see Equation 2.74), and because of the Coulomb repulsion between them we may expect to find them typically located on opposite sides of the nucleus, the most probably spatial separation between the two electrons is $r_{12} \simeq a_0$. Therefore the typical electron-electron repulsion energy is

$$E_{\text{rep}}(\text{He}) = V_{\text{rep}}(\text{He}) \tag{3.19}$$

$$\simeq \frac{e^2}{4\pi\epsilon_0 a_0} \tag{3.20}$$

and

$$\frac{E_{\text{rep}}(\text{He})}{hc} = 219\,475\ \text{cm}^{-1} \tag{3.21}$$

$$\simeq 2\,R_\infty. \tag{3.22}$$

Therefore adding this to the value obtained when the electron-electron repulsion is neglected (Equation 3.13), leads to the result that

$$\frac{E_{\text{gnd}}(\text{He})}{hc} = -877\,778\ \text{cm}^{-1} + \frac{e^2}{4\pi\epsilon_0 r_{12}}\frac{1}{hc} \tag{3.23}$$

$$= -877\,778\ \text{cm}^{-1} + 219\,475\ \text{cm}^{-1} \tag{3.24}$$

$$\simeq -6\,R_\infty \tag{3.25}$$

This is closer to the measured value of $\sim -5.8\,R_\infty$.

3.2.2 Central-field approximation

A more refined approach to the calculation of the electronic structure of atoms with many-electrons involves the introduction of a position-dependent correction to the electron-nucleus interaction for each individual electron. This approach is known as the central-field approximation, and allows the electron-electron interactions to be accounted for in a way that the motion of the individual electrons can still be separated.

To achieve this, we consider a single electron Hamiltonian, $\hat{h}(\vec{r}_i)$, as above, to which we add a central potential $V_\text{c}(r_i)$ that represents the average interaction of the electron labelled with the index i, with all of the other electrons. Therefore the complete N-electron Hamiltonian becomes

$$\hat{H}(\vec{r}_N) = \sum_i \hat{h}'(\vec{r}_i), \tag{3.26}$$

where

$$\hat{h}'(\vec{r}_i) = \hat{h}(\vec{r}_i) + V_\text{c}(r_i) \tag{3.27}$$

$$= -\frac{\hbar^2}{2m_\text{e}}\nabla^2 - \frac{Z_\text{nucl}e^2}{4\pi\epsilon_0 r_i} + V_\text{c}(r_i), \tag{3.28}$$

and

$$V_\text{c}(r_i) = \left\langle \frac{e^2}{4\pi\epsilon_0 r_{ij}} \right\rangle_{j\neq i}. \tag{3.29}$$

Therefore the central potential, $V_\text{c}(r_i)$, depends only on $r_{ij} = |\vec{r}_{ij}|$, the magnitude of $\vec{r}_{ij}$, and not on its direction. As a result this potential has no angular dependence.

To determine the electronic structure within this central-field approximation it is therefore necessary to solve N one-electron Schrödinger equations of the form

$$\hat{h}'(\vec{r}_i)\,\psi(\vec{r}_i) \;=\; E_i\,\psi(\vec{r}_i), \tag{3.30}$$

where $\psi(\vec{r}_i)$ are one-electron orbitals. The total electronic energy, E, is then

$$E \;=\; \sum_i E_i, \tag{3.31}$$

and, as in the independent-particle model, the total electronic wavefunction, $\Psi(\vec{r}_N)$, takes a product form,

$$\Psi(\vec{r}_N) \;=\; \psi(\vec{r}_1)\,\psi(\vec{r}_2)\,\psi(\vec{r}_3)\,\times\cdots\times\,\psi(\vec{r}_N). \tag{3.32}$$

The one-electron orbitals obtained using this central-field approximation are separable into radial, $F_{n_i,\ell_i}(r_i)$, and angular, $Y_{\ell_i,m_i}(\theta_i,\phi_i)$, parts, i.e.,

$$\psi(\vec{r}_i) \;=\; F_{n_i,\ell_i}(r_i)\,Y_{\ell_i,m_i}(\theta_i,\phi_i). \tag{3.33}$$

As in a one-electron atom, the angular functions are the set of spherical harmonic functions, however, because of the deviation of the potential from a pure Coulomb potentials following the introduction of the central-field, the radial functions differ from those obtained in the case of the one-electron atom.

Because the central potential, $V_c(r)$, modifies the Coulomb potential at short range, i.e., for small values of r, the ℓ-degeneracy associated with eigenstates with equal values of n that was seen in the case of a one-electron atom, is lifted. However, because the central potential depends only on the magnitude of $\vec{r}_{ij}$ and not its direction, the m-degeneracy of all states with the equal values of n and ℓ remains. Therefore

$$E_i \equiv E_{n_i,\ell_i}. \tag{3.34}$$

This above description of the electronic wavefunctions of many-electron atoms in terms of products of one-electron orbitals leads to the notation in which the occupation of each orbital in the many-electron atom is listed, e.g., in the case of the C atom, in the form

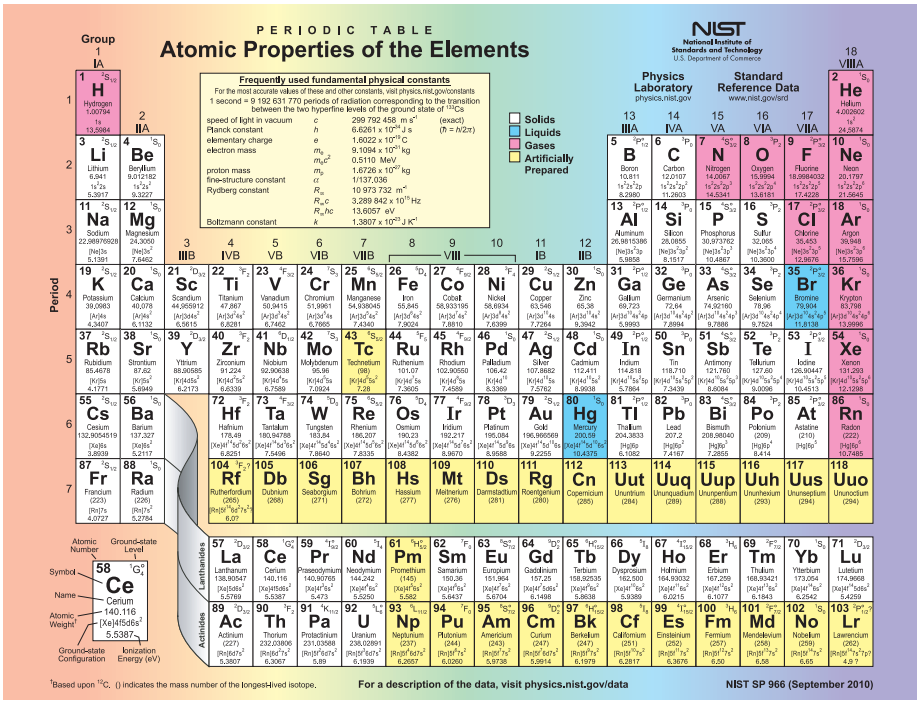

Figure 3.1: Periodic table of the elements, NIST[1].

C atom ground state: $1s^2\,2s^2\,2p^3$.

In this notation the number of electrons in each orbital is indicated in the right superscript. When listed in this way, the set of occupied orbitals is called the *electronic configuration*.

Applicability of the central-field approximation

- The central-field approximation is most applicable to atoms or atomic ions with a single electron occupying an outer orbital. These include:

  The *alkali metal atoms* in Group I of the periodic table, e.g., Li, Na, K, Rb,. . . (see Figure 3.1). These atoms have one single electron in an outer s-orbital:

  Li: $1s^2\,2s^1$

[1]R. A. Dragoset, A. Musgrove, C. W. Clark, and W. C. Martin, The National Institute of Standards and Technology (NIST), Physical Measurement Laboratory, 2010 (http://www.nist.gov/pml/data/periodic.cfm).

Na: $1s^2\,2s^2\,2p^6\,3s^1$

K: $1s^2\,2s^2\,2p^6\,3s^2\,3p^6\,4s^1$

Singly-ionised *alkaline earth metals* in Group II of the periodic table, e.g., Be^+, Mg^+, Ca^+,... (see Figure 3.1). These atomic ions have one single electron in an outer s-orbital:

Be^+: $1s^2\,2s^1$

Mg^+: $1s^2\,2s^2\,2p^6\,3s^1$

- Other atoms with one electron in a highly excited state, i.e., a state with a high value of n. Atoms, such as these, with one electron in a high-n states are often called *Rydberg atoms*.

In each of the these cases, $N-1$ electrons in the many-electron atom are tightly bound to the nucleus while one single electron is loosely bound. The central-field approximation is most appropriate for calculating the eigenfunctions and eigenvalues of the this one loosely bound electron.

In these cases the inner electrons as said to *screen* the charge of the nucleus such that

As $r_i \to 0$:

$$-\frac{Z_{\text{nucl}}e^2}{4\pi\epsilon_0 r_i} + V_{\text{c}}(r_i) \quad \longrightarrow \quad -\frac{Z_{\text{nucl}}e^2}{4\pi\epsilon_0 r_i} \tag{3.35}$$

As $r_i \to \infty$:

$$-\frac{Z_{\text{nucl}}e^2}{4\pi\epsilon_0 r_i} + V_{\text{c}}(r_i) \quad \longrightarrow \quad -\frac{e^2}{4\pi\epsilon_0 r_i} \tag{3.36}$$

Therefore when the one loosely-bound electron approaches $r_i = 0$, the Coulomb attraction of the positively charge nucleus dominates, while at larger distances the nucleus and core electrons appear from the perspective of this outer electron as a single charged object with an effective charge of $+1e$.

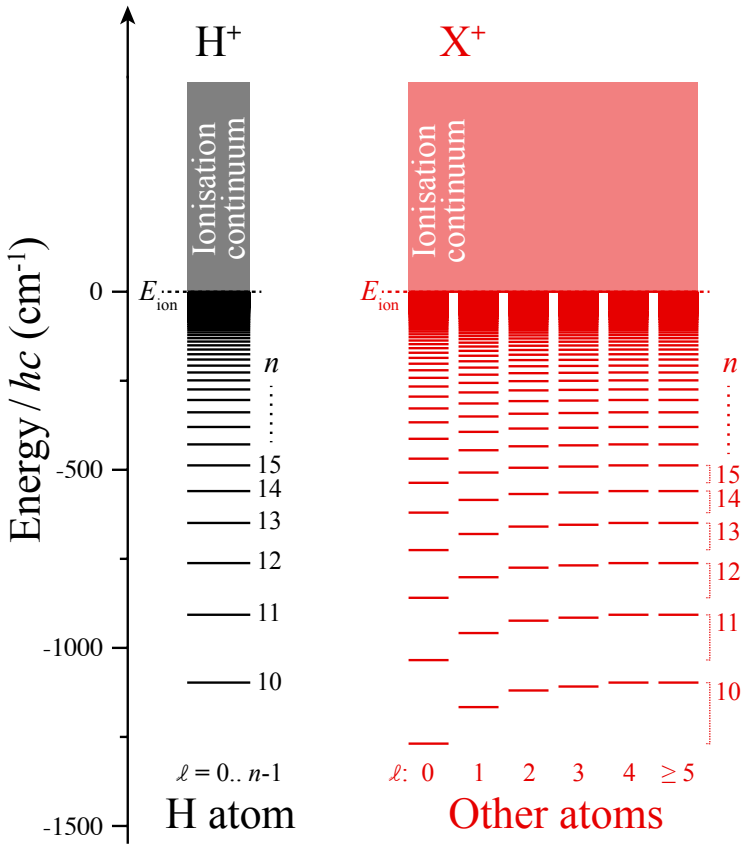

Figure 3.2: Series of eigenstates of the H atom in which the energies are only dependent on the value of n and independent of the value of ℓ, and in other non-hydrogenic many-electrons for which the energies depend on n and ℓ.

As can be seen from the radial probability density distributions associated with the one-electron orbitals in the H atom displayed in Figure 2.9, the proximity of the electron to the position of the screened charge of the nucleus depends on the value of n and the value of ℓ. Because an electron in a low-ℓ orbital is more core-penetrating than one in a higher-ℓ orbital with the same value of n, the effective charge of the nucleus and core electrons appear greater. On the other hand, electrons in higher-ℓ orbitals appear bound to an ion core with a charge of $+1e$ and their binding energies are similar to those of a one electron atom (see Figure 3.2).

Therefore:

H atom: $E_{1s} < E_{2s} = E_{2p} < E_{3s} = E_{3p} = E_{3d} \ldots$

He atom: $E_{1s} < E_{2s} < E_{2p} < E_{3s} < E_{3p} < E_{3d} \ldots$

3.2.3 Quantum defects

As discussed above, the central-field approximation is well suited to the calculation of the eigenfunctions and eigenvalues of many-electron atoms with a single (excited) out electron. Such an electron is often called an *optically active* electron since transitions involving it lie in the optical/visible regions of the electromagnetic spectrum.

Within the central-field approximation, the energy of a single active electron can be expressed as

$$\frac{E_{n,\ell}}{hc} = -\frac{R_M}{(n-\Delta_{n,\ell})^2}, \tag{3.37}$$

where

Z_{eff}: is the effective combined charge of the nucleus and core electrons

$\Delta_{n,\ell}$: is known as the *quantum defect*

$(n - \Delta_{n,\ell})$: is often described as the *effective principal quantum number*

and as in Section 2 the Rydberg constant

$$R_M = R_\infty Z_{\text{eff}}^2 \frac{\mu_M}{m_e}. \tag{3.38}$$

This expression (Equation 3.37) for the energy of the single active electron can be derived rigorously by solving the Schrödinger equation for a single electron in a central potential that deviates from its dependence on $1/r$ at small r.

The value of $\Delta_{n,\ell}$, the quantum defect in Equation 3.37 depends on how strongly the single active electron interacts with the non-hydrogenic ion core.

For high values of ℓ: $\Delta_{n,\ell} \rightarrow 0$

This is because the centrifugal barrier associated with the high angular momentum forces the electron away from the core and it therefore does not penetrate the cloud of inner electrons.

For low values of ℓ: $\Delta_{n,\ell} > 0$

This is because in lower-ℓ states the active electron penetrates the cloud of inner electrons more significantly.

As can be seen in Figure 3.2 the values of $\Delta_{n,\ell}$ are strongly dependent on ℓ and weakly dependent on the value of n. For example, in the case of a single active electron in low-n states of the helium atom the corresponding quantum defects are listed in the table below.

$\Delta_{n,\ell}$	$\ell = 0$	$\ell = 1$	$\ell = 2$	$\ell = 3$
$n = 2$	0.311	0.066	-	-
$n = 3$	0.302	0.066	0.002	-
$n = 4$	0.299	0.066	0.002	0.0003

Table 3.1: Quantum defects for the low-n triplet states of He.

3.2.4 Screening constant

An alternative, but less common, parameterisation of the energies of the eigenstates associated with the excitation of a single active electron in a many-electron atom involves the introduction of an effective screened nuclear charge

$$Z^* = Z_{\text{nucl}} - \sigma_{n,\ell}, \tag{3.39}$$

where $\sigma_{n,\ell}$ is a *screening constant* that accounts for the screening of the nuclear charge Z_{nucl} by the inner electrons. In this parameterisation the expression for the energies of the eigenstates associated with the single active electron

in Equation 3.37 becomes

$$\frac{E_{n,\ell}}{hc} = -\frac{R_M}{n^2}(Z^*)^2 \tag{3.40}$$

$$= -\frac{R_M}{n^2}(Z_{\text{nucl}} - \sigma_{n,\ell})^2. \tag{3.41}$$

3.3 Indistinguishable particles

In a quantum mechanical treatment of many-electron atoms, it is necessary to consider the effects that the indistinguishability of electrons has on the total electronic wavefunction.

Consider two particles that are indistinguishable by any measurement, e.g., two electrons, two photons, ... If the wavefunction of the two particle system is $\psi(1,2)$, then

$$|\psi(1,2)|^2 = |\psi(2,1)|^2. \tag{3.42}$$

This condition can be satisfied in two ways. If

$$\psi(1,2) = +\psi(2,1), \tag{3.43}$$

the wavefunction is said to be *symmetric* with respect to exchange of the two particles, while if

$$\psi(1,2) = -\psi(2,1), \tag{3.44}$$

the wavefunction is said to be *antisymmetric* with respect to exchange.

More generally any physically allowed wavefunction of a two-particle system must be either symmetric or antisymmetric with respect to exchange of the two particles.

3.3.1 The Pauli principle

To explain the way in which the one-electron orbitals are filled in a many-electron atom, Wolfgang Pauli postulated that

- Wavefunctions are *antisymmetric* with respect to exchange of identical Fermions (particles with 1/2 integer spins, e.g., e^-, p^+, n, . . .)

- Wavefunctions are *symmetric* with respect to exchange of identical Bosons (particles with integer spins, e.g., photon, α-particle, ^{4}He atom, ...)

For example, for two electrons (two Fermions),

$$\psi(1,2) = -\psi(2,1). \tag{3.45}$$

Within the orbital approximation, if ϕ_A and ϕ_B are two one electron orbitals, e.g., 1s, 2p, ... orbitals, then

$$\psi(1,2) = \phi_A(1)\,\phi_B(2), \tag{3.46}$$

and

$$\psi(2,1) = \phi_A(2)\,\phi_B(1), \tag{3.47}$$

where the numbers in brackets are arbitrary labels assigned to the two electrons, e.g., electron number 1 and electron number 2. Therefore, from Pauli's postulate for two Fermions

$$\phi_A(1)\,\phi_B(2) = -\phi_A(2)\,\phi_B(1), \tag{3.48}$$

which can only be true of

$$\phi_A \neq \phi_B. \tag{3.49}$$

Because the wavefunction ϕ_A cannot be the same as the wavefunction ϕ_B it must be concluded that no to electrons can occupy the same (spin-) orbital in a many-electron atom. For example, two electrons cannot occupy the 1s orbital unless they have opposite spins.

When normalised, a generalised two-electron wavefunction that fulfills the principle postulated by Pauli takes the form

$$\psi(1,2) = \frac{1}{\sqrt{2}}\left[\phi_A(1)\,\phi_B(2) - \phi_A(2)\,\phi_B(1)\right] \tag{3.50}$$

$$= -\psi(2,1). \tag{3.51}$$

3.4 Effect of the Pauli principle on atomic structure

Consider the case of the He atom with two-electrons (indistinguishable Fermions). The total wavefunction has the form

$$\Psi(1,2) = \underbrace{\Phi(\vec{r}_1,\vec{r}_2)}_{\text{Space}}\,\underbrace{\chi(\sigma_1,\sigma_2)}_{\text{Spin}} = -\Phi(\vec{r}_2,\vec{r}_1)\,\chi(\sigma_2,\sigma_1), \tag{3.52}$$

where σ_i represent the spin coordinates.

The function χ is an eigenfunction of the the operator $\hat{\vec{S}}^2$ associated with the square of the total electron spin, and the operator $\hat{S}_z$ associated with the projection of the total electron spin on the z-axis.

The total electron spin operator

$$\hat{\vec{S}} = \hat{\vec{s}}_1 + \hat{\vec{s}}_2, \tag{3.53}$$

where $\hat{\vec{s}}_1$ and $\hat{\vec{s}}_2$ are the spin operators associated with each individual electron, 1 and 2, and

$$\hat{S}_z = \hat{s}_{z_1} + \hat{s}_{z_2}. \tag{3.54}$$

3.4.1 Spin wavefunctions

For an individual electron the allowed value of the spin quantum number, s, is

$$s = \frac{1}{2}\hbar, \tag{3.55}$$

and is often simply written as

$$s = \frac{1}{2}. \tag{3.56}$$

This single electron spin can be aligned along the positive z-axis, in which case it is said to be *spin-up* and is denoted by the one-electron spin wavefunction

$$\alpha \quad \text{or} \quad \uparrow \tag{3.57}$$

and the azimuthal quantum number

$$m_s = +\frac{1}{2}\hbar \tag{3.58}$$

$$\equiv +\frac{1}{2}, \tag{3.59}$$

or can be aligned along the negative z-axis, in which case it is said to be *spin-down* and is denoted by the one-electron spin wavefunction

$$\beta \quad \text{or} \quad \downarrow \tag{3.60}$$

and the azimuthal quantum number

$$m_s = -\frac{1}{2}\hbar \tag{3.61}$$

$$\equiv -\frac{1}{2}, \tag{3.62}$$

i.e.,

$$\hat{S}_z\,\alpha = +\frac{1}{2}\hbar\,\alpha \tag{3.63}$$

$$\hat{S}_z\,\beta = -\frac{1}{2}\hbar\,\beta. \tag{3.64}$$

For a two-electron system the total spin vector, $\vec{S}$, is the sum of the two individual electron spin vectors, $\vec{s_1}$ and $\vec{s_2}$,

$$\vec{S} = \vec{s_1} + \vec{s_2}. \tag{3.65}$$

The total spin quantum number $S = |\vec{S}|$ can then take values in the range

$$S = |s_1 - s_2|, \ldots, |s_1 + s_2| \tag{3.66}$$

in steps of 1, where $s_i = |\vec{s_i}|$. The total electron spin of the atom is therefore quantised.

Since in the He atom $s_1 = 1/2$ and $s_2 = 1/2$,

$$S = \left|\frac{1}{2} - \frac{1}{2}\right|, \ldots, \left|\frac{1}{2} + \frac{1}{2}\right| \tag{3.67}$$

$$\tag{3.68}$$

$$= 0, \ldots, 1 \tag{3.69}$$

$$= 0 \text{ and } 1. \tag{3.70}$$

The spin quantum number $S = 0$ corresponds to the situation in which the two electron spins are aligned antiparallel to each other, while $S = 1$ corresponds to the case in which the two electrons spins are aligned parallel to each other.

In general the total electron spin in a many-electron atom is denoted by the uppercase letter $\vec{S}$, while the individual electron spins are denoted by the lowercase letter $\vec{s}$, i.e.,

$$\vec{S} = \sum_i \vec{s}_i. \tag{3.71}$$

The total spin quantum number and the projection of the total spin onto the z-axis are denoted by the upper case letters S and M_S, respectively.

Consider separately the cases in which $S = 0$ and $S = 1$.

$S = 1$: When $S = 1$, $M_S = -1, 0, +1$.

Because there are three values of M_S, the $S = 1$ state is known as a *triplet* spin state.

$M_S = +1$: The triplet state in which the spins of the two electrons are both aligned parallel to the z-axis has the wavefunction

$$\chi^{\mathrm{T}} = \alpha(1)\alpha(2). \tag{3.72}$$

$M_S = -1$: The triplet state in which the spins of the two electrons are both aligned antiparallel to the z-axis has the wavefunction

$$\chi^{\mathrm{T}} = \beta(1)\beta(2). \tag{3.73}$$

$M_S = 0$: The two wavefunctions above are both symmetric with respect to exchange of the two electrons. Therefore the wavefunction associated with the final triplet state, for which $M_S = 0$, is the symmetric combination of electron 1 with spin-up and electron 2 with spin-down, and electron 2 with spin-up and electron 1 with spin-down, i.e.,

$$\chi^{\mathrm{T}} = \frac{1}{\sqrt{2}}\left[\alpha(1)\beta(2) + \alpha(2)\beta(1)\right], \tag{3.74}$$

where the prefactor ensures that the two-particle wavefunction is normalised.

$\underline{S = 0}$**:** When $S = 0$, $M_S = 0$.

Because there is only one single value of M_S, the $S = 0$ state is known as a *singlet* spin state.

$\underline{M_S = 0}$: As above the singlet spin state with $M_S = 0$, is a combination of electron 1 with spin-up and electron 2 with spin-down, and electron 2 with spin-up and electron 1 with spin-down. Since the symmetric form of this function must correspond to the triplet state, it is the antisymmetric form that corresponds to the singlet state, i.e.,

$$\chi^{\mathrm{S}} = \frac{1}{\sqrt{2}}\left[\alpha(1)\beta(2) - \alpha(2)\beta(1)\right]. \tag{3.75}$$

3.4.2 He atom wavefunctions

Since the spatial part of the electronic wavefunction of the He atom can be expressed in a general form as

$$\Phi_{\pm}(\vec{r}_1, \vec{r}_2) = \frac{1}{\sqrt{2}}\left[\phi_{n\ell m_\ell}(\vec{r}_1)\phi_{n'\ell' m'_\ell}(\vec{r}_2) \pm \phi_{n\ell m_\ell}(\vec{r}_2)\phi_{n'\ell' m'_\ell}(\vec{r}_1)\right], \tag{3.76}$$

where under exchange of the two electrons

$$\Phi_{+}(\vec{r}_1, \vec{r}_2) \quad \Rightarrow \quad \text{symmetric}$$

$$\Phi_{-}(\vec{r}_1, \vec{r}_2) \quad \Rightarrow \quad \text{antisymmetric}$$

to satisfy the Pauli principle, that the total wavefunction of the two-electron system must be antisymmetric with respect to exchange of the two electrons, the symmetric spatial wavefunction can only occur when the spins form a singlet state, while the antisymmetric spatial wavefunction must only occur when the spins form a triplet state.

S			Spin	Space	Wavefunction
$S = 0$	$\Rightarrow$	Singlet	antisymmetric	symmetric	$\Phi_{+}(\vec{r}_1, \vec{r}_2)\,\chi^{\mathrm{S}}$
$S = 1$	$\Rightarrow$	Triplet	symmetric	antisymmetric	$\Phi_{-}(\vec{r}_1, \vec{r}_2)\,\chi^{\mathrm{T}}$

Ground state of He

$1s^2$: Two electrons in the 1s orbital.
The spatial part of the wavefunction for the ground state of the He atom can have the form

$$\Phi_+(\vec{r}_1,\vec{r}_2) = \frac{1}{\sqrt{2}}\left[\phi_{1s}(\vec{r}_1)\phi_{1s}(\vec{r}_2)+\phi_{1s}(\vec{r}_2)\phi_{1s}(\vec{r}_1)\right], \tag{3.77}$$

or

$$\Phi_-(\vec{r}_1,\vec{r}_2) = \frac{1}{\sqrt{2}}\left[\phi_{1s}(\vec{r}_1)\phi_{1s}(\vec{r}_2)-\phi_{1s}(\vec{r}_2)\phi_{1s}(\vec{r}_1)\right]$$

$$= 0. \tag{3.78}$$

Because $\Phi_-(\vec{r}_1,\vec{r}_2) = 0$, the ground state of the He atom can only be described by the $\Phi_+(\vec{r}_1,\vec{r}_2)$ spatial wavefunction which is symmetric with respect to exchange of the two electrons.

With a symmetric spatial component of the ground-state wavefunction, to satisfy the Pauli principle the spin part must be antisymmetric with respect to exchange of the two electrons, i.e., χ^S.

Therefore the wavefunction for the ground state of the He atom must be:

$$\text{He } 1s^2: \quad \Psi(1,2) = \Phi_+(\vec{r}_1,\vec{r}_2)\,\chi^S. \tag{3.79}$$

Excited states of the He atom

In excited states of the He atom, e.g., the 1s2s state, the spatial wavefunctions

$$\Phi_+(\vec{r}_1,\vec{r}_2) = \frac{1}{\sqrt{2}}\left[\phi_{1s}(\vec{r}_1)\phi_{2s}(\vec{r}_2)+\phi_{1s}(\vec{r}_2)\phi_{2s}(\vec{r}_1)\right], \tag{3.80}$$

and

$$\Phi_-(\vec{r}_1,\vec{r}_2) = \frac{1}{\sqrt{2}}\left[\phi_{1s}(\vec{r}_1)\phi_{2s}(\vec{r}_2)-\phi_{1s}(\vec{r}_2)\phi_{2s}(\vec{r}_1)\right] \tag{3.81}$$

are both non-zero. Therefore excited states in which the two electrons are in distinct orbitals can be either singlet or triplet states.

3.4.3 Spin multiplicity

As seen above, for spin states with $S = 1$, there are three possible values of M_S: -1, 0 and $+1$. From this it can be concluded that for any value of S there are $2S + 1$ associated values of M_S.

This value of the quantity $2S + 1$ is known as the *spin multiplicity* of the state. For $S = 1$, $2S + 1 = 3$ leading to such states being denoted *triplet states*. This nomenclature is also extended to all other values of $2S + 1$, i.e.,

$$\begin{aligned}
&\text{For } S = 0: && M_S = 0 \\
& && 2S + 1 = 1 \Rightarrow \textit{singlet} \text{ state} \\
&\text{For } S = 1/2: && M_S = -1/2, +1/2 \\
& && 2S + 1 = 2 \Rightarrow \textit{doublet} \text{ state} \\
&\text{For } S = 3/2: && M_S = -3/2, -1/2, +1/2, +3/2 \\
& && 2S + 1 = 4 \Rightarrow \textit{quartet} \text{ state}
\end{aligned}$$

3.5 Exchange

Consider a triplet state of the He atom. In this state $S = 1$ and the spin part of the wavefunction is χ^{T}, where

$$\chi^{\mathrm{T}} \quad \Rightarrow \quad \begin{array}{c} \alpha(1)\alpha(2) \\ \frac{1}{\sqrt{2}}\left[\alpha(1)\beta(2) + \alpha(2)\beta(1)\right] \\ \beta(1)\beta(2) \end{array}$$

The spatial parts of the triplet wavefunctions are antisymmetric with respect to exchange of the two electrons

$$\Phi(\vec{r}_1, \vec{r}_2) \quad = \quad \Phi_-(\vec{r}_1, \vec{r}_2) = \frac{1}{\sqrt{2}}\left[\phi_{\mathrm{a}}(\vec{r}_1)\phi_{\mathrm{b}}(\vec{r}_2) - \phi_{\mathrm{a}}(\vec{r}_2)\phi_{\mathrm{b}}(\vec{r}_1)\right]. \qquad (3.82)$$

However, if the two electrons are at the same position, i.e., $\vec{r}_1 = \vec{r}_2$, the expression in Equation 3.82 is equal to zero. Therefore in the triplet states of He the two electrons tend to avoid each other. As a result they do not screen the $+2e$ charge of the nucleus for each other as much as they would if they overlapped spatially. They are therefore more strongly bound (lower

in energy) than would be expected if the symmetry restrictions imposed by the Pauli principle were not considered.

On the other hand, in the singlet states of He, $S = 0$ and the spin part of the wavefunction is χ^{S}, where

$$\chi^{\mathrm{S}} \quad \Rightarrow \quad \tfrac{1}{\sqrt{2}}\left[\alpha(1)\beta(2) - \alpha(2)\beta(1)\right]$$

In this case the spatial parts of the wavefunctions are symmetric with respect to exchange of the two electrons

$$\Phi(\vec{r}_1, \vec{r}_2) = \Phi_+(\vec{r}_1, \vec{r}_2) \quad = \quad \frac{1}{\sqrt{2}}\left[\phi_{\mathrm{a}}(\vec{r}_1)\phi_{\mathrm{b}}(\vec{r}_2) + \phi_{\mathrm{a}}(\vec{r}_2)\phi_{\mathrm{b}}(\vec{r}_1)\right] \tag{3.83}$$

$$\neq \quad 0 \quad \text{if} \quad \vec{r}_1 = \vec{r}_2. \tag{3.84}$$

As a result there is a non-zero probability of finding the two electrons close to each other where they can each screen the other from the $+2e$ charge of the nucleus. Consequently, the singlet states are more weakly bound (higher in energy) than the triplet states as can be seen in Figure 3.3

The energy shifts that arise as a result of considering the effects of the Pauli principle on the electronic structure of an atom suggest that an interaction occurs between the electrons within the atom, the sign of which depends on the relative orientations of the their spins. This interaction is known as the *Exchange Interaction* and is a direct result of the requirement of the Pauli principle that the total wavefunction is antisymmteric with respect to exchange of identical Fermions.

3.5.1 Formal analysis of the Exchange Interaction

To treat the Exchange Interaction in a more formal way we must consider the effects of the symmetry of the total wavefunctions on the repulsion between the two electrons. The repulsive interaction, V_{rep}, takes the form

$$V_{\mathrm{rep}} \quad = \quad \frac{e^2}{4\pi\epsilon_0 r_{12}} = C\frac{1}{r_{12}}, \tag{3.85}$$

where C is a constant. The electron-electron repulsion therefore depends directly on the expectation value of r_{12}^{-1},

$$\left\langle \frac{1}{r_{12}} \right\rangle \quad = \quad \iint \psi^*(1,2)\,\frac{1}{r_{12}}\,\psi(1,2)\,\mathrm{d}V\,\mathrm{d}\sigma, \tag{3.86}$$

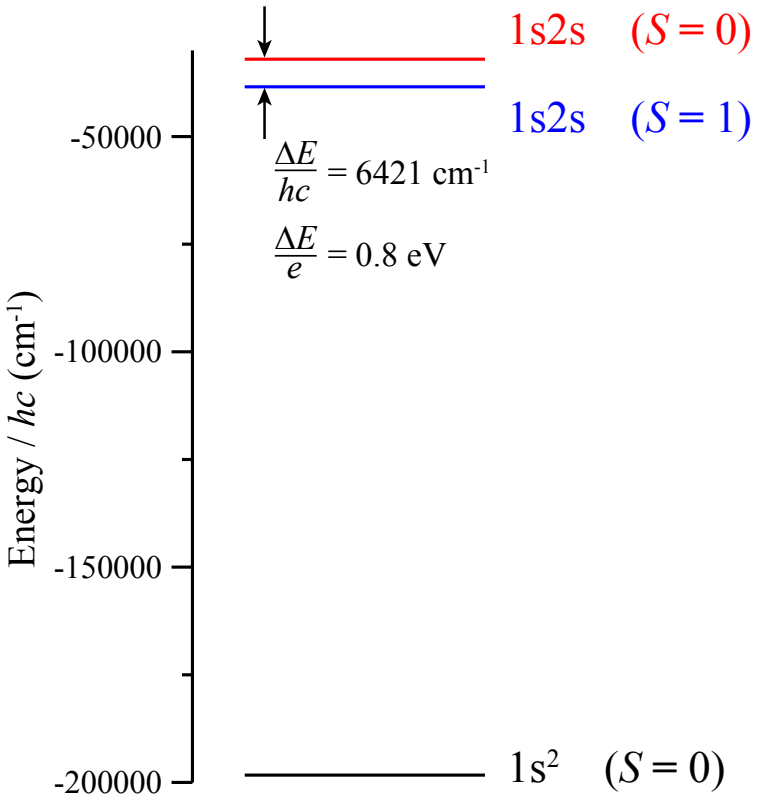

Figure 3.3: Energy splitting between the 1s2s singlet and triplet states of He resulting from the Exchange Interaction.

where $\vec{r}_1$ and $\vec{r}_2$ are denoted by the the numbers 1 and 2, and $\mathrm{d}V$ and $\mathrm{d}\sigma$ represent the sets of spatial coordinates and spin coordinates, respectively.

Considering first the singlet states, the total wavefunctions take the form

$$\Psi(1,2) \quad = \quad \Phi_+ \, \chi^{\mathrm{S}}, \tag{3.87}$$

and therefore

$$\begin{aligned}
\left\langle \frac{1}{r_{12}} \right\rangle \quad &= \quad \iint \Phi_+^* \, \chi^{\mathrm{S}\,*} \, \frac{1}{r_{12}} \, \Phi_+ \, \chi^{\mathrm{S}} \, \mathrm{d}V \, \mathrm{d}\sigma, \qquad (3.88) \\
&= \quad \iint \frac{1}{\sqrt{2}} \left[\phi_{\mathrm{a}}(1)\phi_{\mathrm{b}}(2) + \phi_{\mathrm{a}}(2)\phi_{\mathrm{b}}(1) \right]^* \times \ldots \\
&\qquad \times \frac{1}{\sqrt{2}} \left[\alpha(1)\beta(2) - \alpha(2)\beta(1) \right]^* \times \ldots \\
&\qquad \times \frac{1}{r_{12}} \times \ldots \\
&\qquad \times \frac{1}{\sqrt{2}} \left[\phi_{\mathrm{a}}(1)\phi_{\mathrm{b}}(2) + \phi_{\mathrm{a}}(2)\phi_{\mathrm{b}}(1) \right] \times \ldots \\
&\qquad \times \frac{1}{\sqrt{2}} \left[\alpha(1)\beta(2) - \alpha(2)\beta(1) \right] \mathrm{d}V \, \mathrm{d}\sigma. \qquad (3.89)
\end{aligned}$$

Because the operator r_{12}^{-1} only acts on the spatial parts of the wavefunctions and not the spin parts, the space and spin parts of Equation 3.89 can be separated, such that,

$$\begin{aligned}
\left\langle \frac{1}{r_{12}} \right\rangle \quad &= \quad \frac{1}{2} \int \left[\phi_{\mathrm{a}}(1)\phi_{\mathrm{b}}(2) + \phi_{\mathrm{a}}(2)\phi_{\mathrm{b}}(1) \right]^* \times \ldots \\
&\qquad \times \frac{1}{r_{12}} \left[\phi_{\mathrm{a}}(1)\phi_{\mathrm{b}}(2) + \phi_{\mathrm{a}}(2)\phi_{\mathrm{b}}(1) \right] \mathrm{d}V \times \ldots \\
&\qquad \times \frac{1}{2} \int \left[\alpha(1)\beta(2) - \alpha(2)\beta(1) \right]^* \times \ldots \\
&\qquad \times \left[\alpha(1)\beta(2) - \alpha(2)\beta(1) \right] \mathrm{d}\sigma. \qquad (3.90)
\end{aligned}$$

Since the spin wavefunction is normalised, i.e.,

$$\int \chi^{\mathrm{S}\,*} \, \chi^{\mathrm{S}} \, \mathrm{d}\sigma \quad = \quad 1, \tag{3.91}$$

expanding the spatial parts of Equation 3.90 leads to the result that

$$\left\langle \frac{1}{r_{12}} \right\rangle = \frac{1}{2}\left\{ \int \frac{\left[\phi_a(1)\phi_b(2)\right]^* \left[\phi_a(1)\phi_b(2)\right]}{r_{12}} \, dV + \ldots \right.$$
$$+ \int \frac{\left[\phi_a(1)\phi_b(2)\right]^* \left[\phi_a(2)\phi_b(1)\right]}{r_{12}} \, dV + \ldots$$
$$+ \int \frac{\left[\phi_a(2)\phi_b(1)\right]^* \left[\phi_a(1)\phi_b(2)\right]}{r_{12}} \, dV + \ldots$$
$$\left. + \int \frac{\left[\phi_a(2)\phi_b(1)\right]^* \left[\phi_a(2)\phi_b(1)\right]}{r_{12}} \, dV \right\} \tag{3.92}$$

and therefore

$$\left\langle \frac{1}{r_{12}} \right\rangle = \frac{1}{2}\left\{ \int \frac{|\phi_a(1)|^2 |\phi_b(2)|^2}{r_{12}} \, dV + \ldots \right.$$
$$+ \int \frac{\phi_a^*(1)\phi_b^*(2)\phi_a(2)\phi_b(1)}{r_{12}} \, dV + \ldots$$
$$+ \int \frac{\phi_a^*(2)\phi_b^*(1)\phi_a(1)\phi_b(2)}{r_{12}} \, dV + \ldots$$
$$\left. + \int \frac{|\phi_a(2)|^2 |\phi_b(1)|^2}{r_{12}} \, dV \right\} \tag{3.93}$$

$$= \int \frac{|\phi_a(1)|^2 |\phi_b(2)|^2}{r_{12}} \, dV + \int \frac{\phi_a^*(1)\phi_b^*(2)\phi_a(2)\phi_b(1)}{r_{12}} \, dV \tag{3.94}$$

$$= J + K \tag{3.95}$$

where J is the *Coulomb Integral*, and K is the *Exchange Integral*. From this expression it can be seen that the Exchange Interaction raises the expectation value associated with the electron-electron repulsion in the singlet states, and therefore increases the energy of the singlet states.

The Coulomb Integral, J, represents the repulsion between between the two electron clouds. The Exchange Integral, K, corresponds to the energy

shift arising from the restrictions imposed on the wavefunctions by the Pauli principle. Because of the positive signs of the two functions in Equation 3.94, J and K are both repulsive electron-electron interactions for the singlet states and increase their energies.

3.6 Electronic configurations

The electronic *configuration* of a many-electron atom specifies the occupancy of the atomic orbitals. For example:

Atomic number	Symbol	Electronic configuration
1	H	$1s^1$
2	He	$1s^2$
3	Li	$1s^2\,2s^1$
4	Be	$1s^2\,2s^2$
5	B	$1s^2\,2s^2\,2p^1$
6	C	$1s^2\,2s^2\,2p^2$
...	...	...

In each configuration,

- n; the principal quantum number is give by an integer number
- ℓ; the orbital angular momentum quantum number is give by a letter; s, p, d, f,...
- The number of electrons occupying each orbital is indicated by the superscripts

Since there are $2\ell + 1$ values of m_ℓ for each value of ℓ, and two values of m_s, following from the Pauli principle each $n\ell$ orbital can hold up to $2(2\ell + 1)$ electrons.

3.6.1 Nomenclature

The following nomenclature is used to describe an electronic configuration.

- Electrons with the equal values of n are said to be in the same *shell*

- Electrons with the equal values of n and ℓ are said to be in the same *sub-shell*
- Electrons with equal values of n and ℓ are said to be *equivalent*
- Each shell can hold up to $2n^2$ electrons, i.e. $2\sum_{\ell=0}^{n-1}(2\ell+1)$ electrons
- Shells containing $2n^2$ electrons are said to be *closed* (or *full*, or *complete*)
- Shells containing $< 2n^2$ electrons are said to be *open* (or *incomplete*, or *incompletely filled*)
- Electrons in open shells are said to be *optically active*

For example, a sub-shell with $\ell = 0$ can contain up to two electrons with the quantum numbers:

$$\ell = 0,\ m_\ell = 0, \text{ and } m_s = \underbrace{\pm 1/2}_{\times 2}.$$

On the other hand a sub-shell with $\ell = 2$ can contain up to 10 electrons with the quantum numbers:

$$\ell = 2,\ m_\ell = \underbrace{-2, -1, 0, +1, +2}_{\times 5}, \text{ and } m_s = \underbrace{\pm 1/2}_{\times 2}.$$

3.6.2 Periodic table of the elements

In the periodic table of the elements, elements with the same valence structure are listed in the columns known as *groups*, while across each row, called a *period*, the number of electrons increases by one at a time.

The chemical properties of the elements are governed by their outer valence electrons therefore the elements in each group have similar characteristics.

Group I: The group I elements are known as the *alkali metals* and in their ground states all have one electron in an outer ns sub-shell (see table below). This optically active outer electron is easily removed to form a positively charged ion (cation), or in the formation of a molecule where it is donated to the molecular bond.

Element	Electronic configuration
H	$1s^1$
Li	$1s^2\,2s^1$
Na	$1s^2\,2s^2\,2p^6\,3s^1$
K	$1s^2\,2s^2\,2p^6\,3s^2\,3p^6\,4s^1$
...	...

Group VII: The group VII elements are known as the *halogens* and in their ground states are missing one electron from their outer np sub-shell (see table below). This incomplete sub-shell makes them extremely chemically reactive and they easily gain an electron to form a negatively charged ion (anion), or in the formation of a molecule where they readily accept an electron to form the molecular bond.

Element	Electronic configuration
F	$1s^2\,2s^2\,2p^5$
Cl	$1s^2\,2s^2\,2p^6\,3s^2\,3p^5$
Br	$1s^2\,2s^2\,2p^6\,3s^2\,3p^6\,4s^2\,3d^{10}\,4p^5$
...	...

Group VIII: The group VIII elements are known as the *nobel gases* and in their ground states contain fully closed shells (see table below). These closed shells make them chemically inert.

Element	Electronic configuration
He	$1s^2$
Ne	$1s^2\,2s^2\,2p^6$
Ar	$1s^2\,2s^2\,2p^6\,3s^2\,3p^6$
Kr	$1s^2\,2s^2\,2p^6\,3s^2\,3p^6\,4s^2\,3d^{10}\,4p^6$
...	...

3.6.3 Terms

Beyond the central-field approximation, which is valid for atoms with one isolated outer electron, the complete many-electron Hamiltonian, $\hat{H}$, does

not commute with the angular momentum operators associated with the individual electrons, i.e.,

$$\left[\hat{H}, \hat{\vec{\ell}}_i\right] \neq 0. \tag{3.96}$$

This indicates that ℓ_i is not a good quantum number in the description of the many-electron structure. Instead of considering the angular momentum of the individual electrons separately, it is instead necessary to consider the combined *total angular momentum*, $\vec{L}$, of all of the electrons together. In a many-electron system $\hat{H}$ does commute with $\hat{\vec{L}}^2$, and the square of the total electron spin, $\hat{\vec{S}}^2$, i.e.,

$$\left[\hat{H}, \hat{\vec{L}}^2\right] = 0 \tag{3.97}$$

$$\left[\hat{H}, \hat{\vec{S}}^2\right] = 0. \tag{3.98}$$

To account for these effects in the description of the atomic structure, electronic configurations are separated into *terms* that are labelled with the total angular momentum quantum number, L, and the total electron spin qantum number, S.

For each configuration the total angular momentum

$$\hat{\vec{L}} = \sum_i \hat{\vec{\ell}}_i, \tag{3.99}$$

and the total spin

$$\hat{\vec{S}} = \sum_i \hat{\vec{s}}_i. \tag{3.100}$$

The values of L and S are therefore determined by adding the angular momenta of the individual electrons, rejecting combinations of L and S forbidden by the Pauli principle.

The symbol describing the value of L and S for a given configuration in known as a *term*. In this nomenclature the total angular momentum quantum number is represented by a capital letter, i.e,

L	=	0	1	2	3	4	...
		S	P	D	F	G	...

The term symbol is then

$$^{2S+1}L \tag{3.101}$$

For example,

The ground state of Fe^+ is ^{6}D; so $L = 2$ and $2S + 1 = 6 \Rightarrow S = 5/2$

The ground state of the He atom is ^{1}S; so $L = 0$ and $2S + 1 = 1 \Rightarrow S = 0$

An excited state of the He atom is ^{3}S; so $L = 0$ and $2S + 1 = 3 \Rightarrow S = 1$

The ground of the H atom is ^{2}S; so $L = 0$ and $2S + 1 = 2 \Rightarrow S = 1/2$

In determining the allowed terms for a given electronic configuration the sum over the orbital angular momenta and spins of the electrons in closed sub-shells is zero, i.e., for a closed sub-shell

$$\hat{\vec{L}} = \sum_i \hat{\vec{\ell}}_i = 0 \tag{3.102}$$

and

$$\hat{\vec{S}} = \sum_i \hat{\vec{s}}_i = 0. \tag{3.103}$$

Therefore for a given configuration the possible values of L and S are determined by the electrons open sub-shells.

3.6.4 Terms for two-electron atoms

Non-equivalent electrons

Consider to non-equivalent electrons, e.g., one in the orbital $n\ell$ and the other in the orbital $n'\ell$ where $n \neq n'$. Because these electrons are in different spin-orbitals the Pauli principle will be satisfied for all possible terms.

For these two electrons their total orbital angular momentum, $\hat{\vec{L}}$, is

$$\hat{\vec{L}} = \hat{\vec{\ell}}_1 + \hat{\vec{\ell}}_2 \tag{3.104}$$

therefore the possible values of the total orbital angular momentum quantum number, L, are

$$L = |\ell_1 - \ell_2|, \ldots, |\ell_1 + \ell_2| \quad \text{in steps of 1} \tag{3.105}$$

In a similar way, the total spin of the two electrons, $\hat{\vec{S}}$, is

$$\hat{\vec{S}} = \hat{\vec{s}}_1 + \hat{\vec{s}}_2 \tag{3.106}$$

and as a result the possible values of the total spin quantum number, S, are

$$S = |s_1 - s_2|, \ldots, |s_1 + s_2| \quad \text{in steps of 1} \tag{3.107}$$

As an example, consider the configuration 2p3p. Here $n \neq n'$ so the Pauli principle will be satisfied. For this configuration

$$\begin{aligned} \ell_1 &= 1 \\ s_1 &= 1/2 \\ \ell_2 &= 1 \\ s_2 &= 1/2 \end{aligned}$$

and therefore

$$\begin{aligned} L &= |\ell_1 - \ell_2|, \ldots, |\ell_1 + \ell_2| \\ &= 0, 1, \text{ and } 2 \\ &\equiv \text{S, P, and D} \end{aligned}$$

and

$$\begin{aligned} S &= |s_1 - s_2|, \ldots, |s_1 + s_2| \\ &= 0 \text{ and } 1 \end{aligned}$$

so $(2S + 1) = 1$ or 3 and the possible allowed terms are

$$\begin{array}{ccc} {}^1\text{S} & {}^1\text{P} & {}^1\text{D} \\ {}^3\text{S} & {}^3\text{P} & {}^3\text{D} \end{array}$$

The number of states associated with each term, i.e., combinations of M_L and M_S, is $(2S + 1)(2L + 1)$ and so here the total number of electronic states associated with this set of six terms is 36. For the configuration 2p3p each p-orbital has six states, i.e., three possible values of m_ℓ combined with two possible values of m_s. Therefore with the two electrons in p-orbitals the total number of states is $6 \times 6 = 36$, in agreement with that given by the set of terms.

Equivalent electrons

Consider two equivalent electrons, i.e., electrons with the same values of n and ℓ. From the Pauli principle if n and ℓ are the same for both electrons, they must have different values of m_ℓ or m_s.

Example 1: In an ns^2 configuration in He,

Both electrons have the same value of n

Both electrons have the same value of ℓ, i.e., $\ell_1 = \ell_2 = 0$

Both electrons have the same value of m_ℓ, i.e., $m_{\ell_1} = m_{\ell_2} = 0$

Therefore the two electrons must have opposite spin, i.e., $m_{s_1} = +1/2$ and $m_{s_2} = -1/2$. Because $s_1 = s_2 = 1/2$, for this configuration $S = 0$, and therefore the corresponding term is ^{1}S.

Example 2: In an np^2 configuration in He (e.g., $2p^2$),

$$\begin{aligned} \ell_1 &= 1 \\ s_1 &= 1/2 \\ \ell_2 &= 1 \\ s_2 &= 1/2 \end{aligned}$$

In this case the possible values of L are

$$\begin{aligned} L &= |\ell_1 - \ell_2|, \ldots, |\ell_1 + \ell_2| \\ &= 0, 1 \text{ and } 2 \\ &= \text{S, P and D} \end{aligned}$$

and the possible values of S are

$$\begin{aligned} S &= |s_1 - s_2|, \ldots, |s_1 + s_2| \\ &= 0 \text{ and } 1 \end{aligned}$$

To determine which combinations of L and S are allowed by the Pauli principle we must consider the form of the total electronic wavefunction of the atom

$$\Psi = \underbrace{\Phi(\vec{r}_1, \vec{r}_2)}_{\text{Space}} \underbrace{\chi(\sigma_1, \sigma_2)}_{\text{Spin}}. \tag{3.108}$$

Since this total wavefunction must be antisymmetric with respect to exchange of the two electrons, when the space part is symmetric, the spin part must be antisymmetric and vice-versa.

The symmetry of the space part of the total wavefunction is determined by the symmetry (parity) of the spherical harmonic functions, $Y_{L,M_L}(\theta, \phi)$ and given by $(-1)^L$. If $(-1)^L = +1$, the function is symmetric while if $(-1)^L = -1$ the function is antisymmetric.

For the three possible values of L above we can then conclude that

$$\begin{aligned} L = 0 &\Rightarrow \text{symmetric} \\ L = 1 &\Rightarrow \text{antisymmetric} \\ L = 2 &\Rightarrow \text{symmetric.} \end{aligned}$$

Therefore when:

$L = 0$; $\chi(\sigma_1, \sigma_2)$ must be antisymmetric, i.e., $S = 0$;

$L = 1$; $\chi(\sigma_1, \sigma_2)$ must be symmetric, i.e., $S = 1$;

$L = 2$; $\chi(\sigma_1, \sigma_2)$ must be antisymmetric, i.e., $S = 0$;

and the terms allowed by the Pauli principle are

$$^1\text{S}, ^3\text{P and } ^1\text{D}.$$

3.6.5 Hund's rules

For a given electronic configuration the set of allowed terms can be ordered in energy following *Hund's rules*. These are a set of three rules, which, although they are empirical, apply rigorously to all ground state electronic configurations.

1. **For a given electronic configuration the term with the highest spin multiplicity, i.e., largest value of S, is lowest in energy.**

   This rule is a consequence of the effect of spin-spin interactions on the energy of a term. Terms with high spin multiplicity are those for which the electron spins are aligned parallel to each other. As discussed above in the case of the exchange interaction (Section 3.5), electrons with parallel spins tend to avoid each other and cannot be located in the same place. Because of this they are spatially separated from each other and the Coulomb repulsion between them is reduced. As a result they are more tightly bound (lower in energy).

2. **For a particular value of S in a given electronic configuration, the term with the highest total orbital angular momentum, i.e., largest value of L, is lowest in energy.**

   When the total orbital angular momentum of a term is lagest, the angular momentum vectors of the individual electrons in the configuration must be aligned parallel to each other, and in a classical description the electrons must be orbiting in the same direction about the nucleus. When orbiting in the same direction as each other, two electrons encounter each other less often than when orbiting in opposite directions. They are therefore on average further apart from each other reducing the Coulomb repulsion between them and lowering the term energy.

Example: In the $1s^2\,2s^2\,2p^1\,3p^1$ excited configuration of C:

$$S = 0 \text{ and } 1 \quad [\text{i.e., } (2S+1) = 1 \text{ and } 3\,] \tag{3.109}$$

$$L = 0, 1 \text{ and } 2 \tag{3.110}$$

Because the two outer electrons are in different orbitals they are non-equivalent and the Pauli principle will be satisfied for all possible terms, which are

$$^1\text{S} \quad ^1\text{P} \quad ^1\text{D}$$
$$^3\text{S} \quad ^3\text{P} \quad ^3\text{D}$$

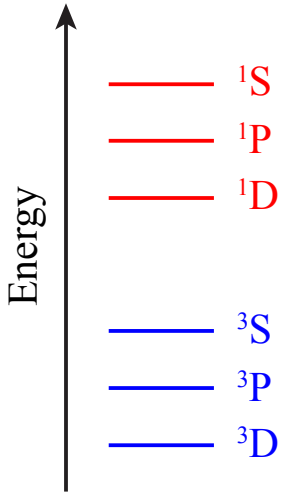

Figure 3.4: Example of the ordering of term energies in increasing energy according to Hund's rules.

Following Hund's rules the set of triplet terms will be lower in energy than the set of singlet terms, and for each set the *D*-term will be lowest in energy, followed by the *P*- and *S*-terms as indicated in Figure 3.4

3.7 Spin-orbit interaction

We have seen above that electronic *configurations* can be separated into *terms* which arise as a result of electron-electron interactions. However, this does not give a complete description of the energy level structure of a many-electron atom.

Further energy splittings of individual terms can arise as a result of relativistic *spin-orbit* interactions, leading to a total Hamiltonian, $\hat{H}$, which takes the general form

$$\hat{H} = \hat{H}_0 + \hat{H}_{SO}, \tag{3.111}$$

where $\hat{H}_0$ is the Hamiltonian obtained before including the effects of spin-orbit interactions, and $\hat{H}_{SO} \propto \hat{\vec{L}} \cdot \hat{\vec{S}}$ is the Hamiltonian operator associated with the spin-orbit interaction which is proportional to the scalar product

of the total electronic orbital angular momentum operator, $\hat{\vec{L}}$, and the total electron spin operator, $\hat{\vec{S}}$.

Since the electron is charged, and a dipolar magnetic field distribution (or magnetic dipole moment) can be associated with a rotating charge, two types of magnetic dipole moment can be associated with an electron bound within an atom. These are (1) the magnetic moment associated with the orbital motion of the electron, and (2) the magnetic moment associated with the spin of the electron. The interaction of these two magnetic moments is known as the spin-orbit interaction and the resulting shifts or splittings of the atomic energy levels are known as *fine structure*.

3.7.1 Orbital magnetic moment

To investigate the origin of the spin-orbit interaction in atoms we first consider a simple classical picture of an electron with charge $-e$ undergoing circular motion in an orbit with a constant radius, $|\vec{r}| = r$, and a constant tangential velocity, $|\vec{v}| = v$ (see Figure 3.5).

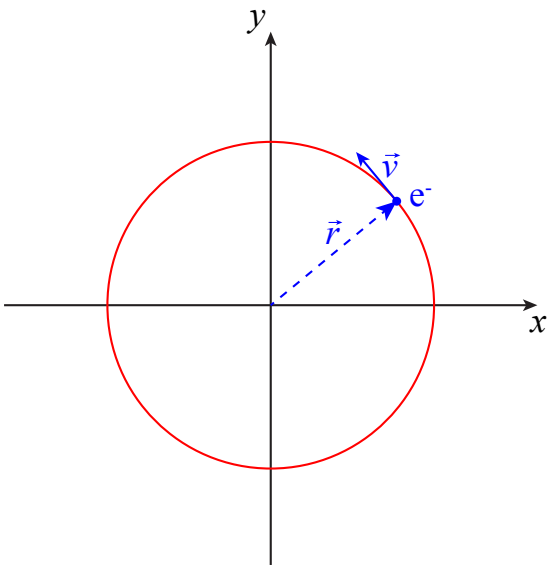

Figure 3.5: Electron undergoing circular motion in an orbit with a constant radius, $|\vec{r}| = r$, and a constant tangential velocity, $|\vec{v}| = v$.

The current, I, associated with the orbit of this electron is

$$I = -\frac{ev}{2\pi r}. \tag{3.112}$$

For an orbit of area, $A = \pi r^2$, this current gives rise to a dipolar magnetic field distribution with a component, μ_z, in the z-dimension

$$\mu_z = IA \tag{3.113}$$

$$= -\frac{ev\pi r^2}{2\pi r} \tag{3.114}$$

$$= -\frac{evr}{2}. \tag{3.115}$$

From Figure 3.5 the orbital angular momentum vector associated with the electron, $\vec{\ell} = (0, 0, \ell_z)$, acts in the z-dimension (i.e., into the page), and

$$\ell_z = m_e v r, \tag{3.116}$$

therefore writing the z-component of the magnetic dipole moment arising from the orbital motion of the electron as, μ_{ℓ_z},

$$\mu_{\ell_z} = -\frac{e}{2m_e}\ell_z. \tag{3.117}$$

Since the same approach can be applied to the calculation of magnetic moments associated with orbital motion in other planes, more generally

$$\vec{\mu}_\ell = -\frac{e}{2m_e}\vec{\ell}. \tag{3.118}$$

Note: This orbital magnetic moment is often expressed in terms of the gyromagnetic ratio of the electron, γ_e, where

$$\gamma_e = -\frac{e}{2m_e} \tag{3.119}$$

such that

$$\vec{\mu}_\ell = \gamma_e\vec{\ell}. \tag{3.120}$$

In the case depicted in Figure 3.5 where the orbital angular momentum vector acts in the z-dimension, since (in SI units)

$$\ell_z = m_\ell\hbar = 0, \pm 1\hbar, \pm 2\hbar, \ldots, \pm\ell\hbar, \tag{3.121}$$

$$\mu_{\ell_z} = -\frac{e}{2m_e}m_\ell\hbar \tag{3.122}$$

$$= -\mu_B m_\ell, \tag{3.123}$$

where

$$\mu_{\mathrm{B}} = \frac{e\hbar}{2m_{\mathrm{e}}} \tag{3.124}$$

$$= 9.274\,009\,994 \times 10^{-24}\ \mathrm{J\,T^{-1}} \tag{3.125}$$

is the Bohr magneton[2].

3.7.2 Spin magnetic moment

A similar procedure to that outlined above (Section 3.7.1) can be followed to obtain a classical approximation for the magnetic moment, μ_s, associated with the electron spin, i.e.,

$$\vec{\mu}_s^{\,\mathrm{Class}} = -\frac{e}{2m_{\mathrm{e}}}\vec{s}. \tag{3.126}$$

However, because the electron spin is a consequence of relativistic quantum mechanics, the above simple classical picture does not give exactly the correct magnitude for the $\vec{\mu}_s$. The connection between the intrinsic spin of an electron and its magnetic moment derived from the relativistic Dirac equation is

$$\vec{\mu}_s^{\,\mathrm{Dirac}} = -2\frac{e}{2m_{\mathrm{e}}}\vec{s}, \tag{3.127}$$

exactly twice the classical result in Equation 3.126. This additional factor of 2 is known as the *electron spin g-factor* and denoted g_{e}. However, experimental measurements[3] of the electron magnetic moment lead to a value for g_{e} which is slightly different from 2,

$$g_{\mathrm{e}} = 2.002\,319\,304\,362 \tag{3.128}$$

This small difference of 0.002 319 304 362 arises from quantum electrodynamic contributions. Formally,

$$\mu_{s_z} = -g_{\mathrm{e}}\mu_{\mathrm{B}}m_s, \tag{3.129}$$

where $m_s = \pm 1/2$.

[2]CODATA Internationally recommended 2014 values of the fundamental physical constants (http://physics.nist.gov/cuu/Constants)

[3]D. Hanneke, S. Fogwell, and G. Gabrielse, New Measurement of the Electron Magnetic Moment and the Fine Structure Constant, *Phys. Rev. Lett.* **100**, 120801 (2008)

3.7.3 The spin-orbit interaction

The above treatment provides a classical description of how magnetic moments can be associated with an electron undergoing circular motion. This motion can correspond to the electrons orbital motion when bound in an atom, or its spin.

To treat the spin-orbit interaction within an atom the most appropriate approach is to first determine the magnetic field arising from the orbital motion of the electron, and to then consider the interaction of the magnetic moment associated with the electron spin with this magnetic field.

Again we begin by considering a classical electron of mass m_e, moving with a velocity $\vec{v}$ in an electric field $\vec{E}$. Such a charged particle moving in an electric field experiences an effective magnetic field $\vec{B}$, where

$$\vec{B} = \frac{\vec{E}\times\vec{v}}{c^2}. \tag{3.130}$$

If the electric field arises from the gradient of an isotropic electric potential, $\phi(r)$ then

$$\vec{E} = -\frac{\vec{r}}{r}\frac{\mathrm{d}\phi}{\mathrm{d}r}, \tag{3.131}$$

where $\vec{r}/r$ represents the radial unit vector, and hence

$$\vec{B} = -\frac{1}{r\,c^2}\frac{\mathrm{d}\phi}{\mathrm{d}r}\,\vec{r}\times\vec{v}. \tag{3.132}$$

However, since

$$\vec{\ell} = \vec{r}\times\vec{p} = m_e\,\vec{r}\times\vec{v}, \tag{3.133}$$

$$\vec{B}_\ell = -\frac{1}{m_e r\,c^2}\frac{\mathrm{d}\phi}{\mathrm{d}r}\,\vec{\ell} \tag{3.134}$$

is then the magnetic field associated with the electron orbiting with angular momentum $\vec{\ell}$.

The interaction energy, V_{mag}, of a magnetic dipole, $\vec{\mu}_{\mathrm{mag}}$, with a magnetic field, $\vec{B}$, can be expressed in a general form as

$$V_{\mathrm{mag}} = -\vec{\mu}_{\mathrm{mag}}\cdot\vec{B}. \tag{3.135}$$

Therefore in the case of the magnetic moment, $\vec{\mu}_s$, associated with the spin of the electron the spin-orbit interaction becomes (in SI units)

$$H_{\mathrm{SO}} = -\vec{\mu}_s \cdot \vec{B} \tag{3.136}$$

$$= \frac{1}{m_e r c^2} \frac{\mathrm{d}\phi}{\mathrm{d}r} \vec{\mu}_s \cdot \vec{\ell} \tag{3.137}$$

$$= -\frac{e}{m_e^2 c^2 r} \frac{\mathrm{d}\phi}{\mathrm{d}r} \vec{s} \cdot \vec{\ell}, \tag{3.138}$$

$$= -\frac{e}{m_e^2 c^2 r} \frac{\mathrm{d}\phi}{\mathrm{d}r} \vec{\ell} \cdot \vec{s}, \tag{3.139}$$

using Equation 3.129 and the properties of the scalar product.

However, this is exactly *twice* the result obtained by solving the relativistic Dirac equation. This deviation by a factor of two arises as result of the assumption that the nucleus in the atom is stationary and the electron is orbiting classically around it. To account for this interaction correctly it is necessary to carry out a relativistic treatment of the electron motion. When this is carried out, the expression for H_{SO} given in Equation 3.139 is modified by a factor of 1/2 because of an effect known as *Thomas Precession* which occurs for an electron moving at speeds close to the speed of light.

In a relativistic treatment, the coordinate system as seen from the nucleus appears to rotate in the plane of the electron motion with a rotation by 180° when the electron has made one complete orbit. Therefore the electron appears to be spinning in its own frame of reference at only half of the rate it would if this reference-frame was stationary, thus reducing the apparent motion by a factor of 1/2.

The complete spin-orbit Hamiltonian is therefore

$$H_{\mathrm{SO}} = -\frac{e}{2m_e^2 c^2 r} \frac{\mathrm{d}\phi}{\mathrm{d}r} \vec{\ell} \cdot \vec{s}, \tag{3.140}$$

which if simplified by defining the spin-orbit coupling constant, $A(L,S)$, as

$$hcA(L,S) = -\frac{e}{2m_e^2 c^2 r} \frac{\mathrm{d}\phi}{\mathrm{d}r} \tag{3.141}$$

so that

$$\frac{H_{\mathrm{SO}}}{hc} = A(L,S)\, \vec{\ell} \cdot \vec{s}. \tag{3.142}$$

To investigate the dependence of the spin-orbit interaction potential on the nuclear charge $+Ze$ and the principal quantum number, n, we must consider that when bound within an atom the electron experiences a Coulomb potential, i.e.,

$$\phi = -\frac{Ze}{4\pi\epsilon_0 r} \tag{3.143}$$

and so

$$\frac{\mathrm{d}\phi}{\mathrm{d}r} = \frac{Ze}{4\pi\epsilon_0 r^2}, \tag{3.144}$$

with the result that the Hamiltonian

$$H_{\mathrm{SO}} = -\frac{e}{2m_{\mathrm{e}}^2 c^2 r}\frac{Ze}{4\pi\epsilon_0 r^2}\,\vec{\ell}\cdot\vec{s}, \tag{3.145}$$

$$\propto \frac{Z}{r^3}. \tag{3.146}$$

The dependence on n can therefore be determined by finding the expectation value of r^{-3}, i.e.,

$$\left\langle\frac{1}{r^3}\right\rangle = \int \Psi^*_{n\ell m_\ell}\frac{1}{r^3}\,\Psi_{n\ell m_\ell}\,\mathrm{d}\tau \tag{3.147}$$

$$= \frac{Z^3}{n^3\,a_0^3\,\ell(\ell+\frac{1}{2})(\ell+1)}, \tag{3.148}$$

where a_0 is the Bohr radius. Therefore

$$H_{\mathrm{SO}} \propto \frac{Z^4}{n^3} \tag{3.149}$$

and for a given value of n rapidly increases with increasing nuclear charge, while as the charge distribution of the electron becomes more extended at high n it reduces.

For Example: In the $2p^1$ configuration in the H atom:

$$s = 1/2 \tag{3.150}$$

$$\ell = 1 \tag{3.151}$$

Therefore

$$\left\langle \frac{1}{r^3} \right\rangle = \frac{1}{8\,a_0^3\,1\,(3/2)\,2} \tag{3.152}$$

$$= \frac{1}{24\,a_0^3} \tag{3.153}$$

and hence

$$A_{2p}(L,S) = 2.22 \times 10^{-6} R_H \tag{3.154}$$

$$\simeq 0.2\ \mathrm{cm}^{-1}. \tag{3.155}$$

This therefore sets the energy scale of the spin-orbit splitting in the $2\,^2P$ term. The resulting split energy level structure is known as *fine structure*.

3.7.4 Spin-orbit operator

The Hamiltonian associated with the spin-orbit interaction can be expressed in terms of the total orbital angular momentum and total spin operators as

$$H_{SO} = -\frac{e}{2m_e^2c^2}\frac{1}{r}\frac{\mathrm{d}\phi}{\mathrm{d}r}\,\vec{L}\cdot\vec{S}. \tag{3.156}$$

The form of this operator indicates that the spin-orbit interaction couples $\vec{L}$ and $\vec{S}$ so that they no longer have fixed z components, i.e., M_L and M_S are not good quantum numbers in the presence of spin-orbit coupling.

However, $\hat{\vec{J}} = \hat{\vec{L}} + \hat{\vec{S}}$ does have a fixed z component M_J. Consequently, the spin-orbit interaction splits terms into *levels* the energies of which depend on the total angular momentum quantum number J and are eigenstates of the $\hat{J}^2$, $\hat{J}_z$, $\hat{L}^2$ and $\hat{S}^2$ operators. The resulting good quantum numbers are therefore J, M_J, L, and S.

When expressed in terms of the spin-orbit coupling constant $A(L,S)$,

$$H_{\rm SO} = hc\,A(L,S)\,\vec{L}\cdot\vec{S}. \tag{3.157}$$

However, since

$$\hat{\vec{J}} = \hat{\vec{L}} + \hat{\vec{S}} \tag{3.158}$$

$$\hat{\vec{J}}^2 = \left(\hat{\vec{L}} + \hat{\vec{S}}\right)^2 \tag{3.159}$$

$$= \hat{\vec{L}}^2 + \hat{\vec{S}}^2 + 2\,\hat{\vec{L}}\cdot\hat{\vec{S}}, \tag{3.160}$$

the scalar product of the total orbital angular momentum and total spin is

$$\hat{\vec{L}}\cdot\hat{\vec{S}} = \frac{1}{2}\left[\hat{\vec{J}}^2 - \hat{\vec{L}}^2 - \hat{\vec{S}}^2\right]. \tag{3.161}$$

Because the spin-orbit interaction is weak compared to the gross energy level structure of the atom, i.e., the energy separation between levels with different values of n, first order perturbation theory can be applied to evaluate its effect on the atomic structure. This requires the expectation value of the operator $\hat{H}_{\rm SO}$ to be determined to give the first order energy shift, $\Delta E^{(1)}$ arising form the interaction,

$$\Delta E^{(1)}_{\rm SO} = \left\langle \hat{H}_{\rm SO} \right\rangle \tag{3.162}$$

$$= \int \Psi^*_{J,L,S,M_J}\,\hat{H}_{\rm SO}\,\Psi_{J,L,S,M_J}\,{\rm d}\tau, \tag{3.163}$$

where Ψ_{J,L,S,M_J} are the wavefunctions of the unperturbed system.

In general the first order energy shift, $\Delta E^{(1)}$, associated with a weak perturbing potential, $V_{\rm perturb}$, is given by first order perturbation theory as

$$\Delta E^{(1)} = \left\langle V_{\rm perturb} \right\rangle = \int \Psi^*_0\,V_{\rm perturb}\,\Psi_0\,{\rm d}\tau, \tag{3.164}$$

where Ψ_0 are the wavefunctions of the unperturbed system.

So since

$$\hat{H}_{\rm SO} = \frac{hc\,A(L,S)}{2}\left[\hat{\vec{J}}^2 - \hat{\vec{L}}^2 - \hat{\vec{S}}^2\right], \tag{3.165}$$

the first order correction to the energy is given by

$$\frac{\Delta E^{(1)}_{\rm SO}}{hc} = \frac{A(L,S)}{2}\left\{\int \Psi^*\,\hat{\vec{J}}^2\,\Psi\,{\rm d}\tau - \int \Psi^*\hat{\vec{L}}^2\,\Psi\,{\rm d}\tau - \int \Psi^*\hat{\vec{S}}^2\,\Psi\,{\rm d}\tau\right\} \tag{3.166}$$

But because, e.g.,

$$\hat{\vec{J}}^2\,\Psi = J(J+1)\,\Psi \tag{3.167}$$

which is equal to

$$\Psi^*\hat{\vec{J}}^2\,\Psi = \Psi^* J(J+1)\,\Psi \tag{3.168}$$

$$= J(J+1)\Psi^*\,\Psi \tag{3.169}$$

because $J(J+1)$ is a constant,

$$\int \Psi^*\hat{\vec{J}}^2\,\Psi\,\mathrm{d}\tau = J(J+1)\underbrace{\int \Psi^*\,\Psi\,\mathrm{d}\tau}_{=1} \tag{3.170}$$

$$= J(J+1). \tag{3.171}$$

A similar procedure can be followed to obtain the expectation values of $\hat{\vec{L}}^2$ and $\hat{\vec{S}}^2$ with the result that

$$\frac{\Delta E_{\mathrm{SO}}}{hc} = \frac{A(L,S)}{2}\left[J(J+1) - L(L+1) - S(S+1)\right]. \tag{3.172}$$

For a given term, i.e., for given values of L and S, the total angular momentum quantum number, J, takes the values

$$J = |L-S|, \ldots, |L+S| \text{ in steps of 1}, \tag{3.173}$$

and the projection of the total angular momentum vector on the z axis, M_J is

$$M_J = 0, \pm 1, \pm 2, \ldots, \pm J. \tag{3.174}$$

Therefore the spin-orbit interaction results in sets of levels associated with each term, the energies of which depend on L, S and J. These levels are labelled in spectroscopic notation as

$$^{2S+1}L_J \tag{3.175}$$

For Example: In the $2p^1$ configuration in the H atom:

$$L = \ell = 1 \tag{3.176}$$

$$S = s = \frac{1}{2} \tag{3.177}$$

Therefore

$$J = \left|1 - \frac{1}{2}\right|, \ldots, \left|1 + \frac{1}{2}\right| \tag{3.178}$$

$$= \frac{1}{2} \text{ and } \frac{3}{2}. \tag{3.179}$$

leading to two levels

$$^2P_{1/2} \text{ and } ^2P_{3/2}. \tag{3.180}$$

If the spin-orbit coupling constant $A_{2p}(L,S) = 0.243 \text{ cm}^{-1}$,

$$\frac{\Delta E_{SO}(J = 1/2)}{hc} = -A_{2p}(L,S) = 0.243 \text{ cm}^{-1} \tag{3.181}$$

and

$$\frac{\Delta E_{SO}(J = 3/2)}{hc} = +\frac{1}{2}A_{2p}(L,S) = 0.121 \text{ cm}^{-1} \tag{3.182}$$

and the spin-orbit splitting between the two levels is

$$\frac{3}{2}A_{2p}(L,S) = 0.364 \text{ cm}^{-1} \tag{3.183}$$

From the above it can be seen that in general the energy difference between level J and level $J-1$ is

$$\Delta E_{SO}(J) - \Delta E_{SO}(J-1) = hc\, A(L,S)\, J. \tag{3.184}$$

This is known as the *Landé interval rule*.

3.7.5 *LS* coupling (Russell-Saunders coupling)

In the above discussion of the spin-orbit interaction in atoms the most appropriate description is provided by considering that the total orbital angular momentum, $\hat{\vec{L}}$, of all of the electrons is coupled to the total spin, $\hat{\vec{S}}$, of all the electrons to give the total orbital angular momentum, $\hat{\vec{J}}$, i.e,

$$\hat{\vec{S}} = \sum_i \hat{\vec{s}}_i \tag{3.185}$$

and

$$\hat{\vec{L}} = \sum_i \hat{\vec{\ell}}_i \tag{3.186}$$

combine to give

$$\hat{\vec{J}} = \hat{\vec{L}} + \hat{\vec{S}}. \tag{3.187}$$

This regime, in which the total orbital angular momentum and total spin couple, is known as *LS coupling* or *Russell-Saunders coupling* and is most appropriate for atoms with low nuclear charge, Z, (i.e., low-Z atoms) in which the spin-orbit interaction is weaker than the electron-electron interactions.

In this case, Hund's third rule can be applied to arrange the resulting levels in order of increasing energy. This rule has three cases.

3a. Normal case: For a particular term in a given electronic configuration, if the outer subshell of the configuration is less than half full the level with the smallest value of J is lowest in energy.

3b. Inverted case: For a particular term in a given electronic configuration, if the outer subshell of the configuration is more than half full the level with the largest value of J is lowest in energy.

3c. For a particular term in a given electronic configuration, if the outer subshell is half full there is no multiplet energy splitting.

Therefore the energy degeneracy of terms with different values of J is lifted by the spin-orbit interaction. However, the energy degeneracy of sublevels with different values M_J remains.

3.7.6 jj-coupling

In contrast to the above description of angular momentum coupling in low-Z atoms in terms of LS coupling, in high-Z atoms, because the spin-orbit coupling constant $A(L,S)$ depends strongly on Z, i.e,

$$A(L,S) \quad \propto \quad Z^4, \tag{3.188}$$

the spin-orbit interaction between $\hat{\vec{\ell}}_i$ and $\hat{\vec{s}}_i$ for each individual electron can be very strong and combining them gives each individual electron its own value of $\hat{\vec{j}}_i$. In such cases, it the most appropriate description of the angular momentum coupling is given by combining these total angular momenta of the individual electrons to obtain $\hat{\vec{J}}$, i.e.,

$$\hat{\vec{j}}_i = \hat{\vec{\ell}}_i + \hat{\vec{s}}_i \tag{3.189}$$

and

$$\hat{\vec{J}} \quad = \quad \sum_i \hat{\vec{j}}_i \tag{3.190}$$

such that in this case

$$J \quad = \quad |j_1 - j_2|, \ldots, |j_1 + j_2| \text{ in steps of 1.} \tag{3.191}$$

These coupling schemes represent a way in which to classify the energy level structure in many electron atoms, but neither the LS- nor the jj-coupling scheme give a complete description of the structure. The changes in the groupings of levels from the LS coupling regime for low-Z atoms to the jj coupling regime for high-Z atoms in the ground state configurations of the group IV elements of the periodic table can be seen in Figure 3.6. In all cases the total number of levels is the same. However, when Z is low, i.e., for C and Si, the grouping of 3+1 energy levels follows more closely the LS-coupling description, while when Z is high, i.e., for Sn and Pb, the grouping of 2+2 energy levels is better described by the jj-coupling scheme.

3.7.7 Parity of terms in many-electron atoms

As discussed in Section 2.3.3 the parity of a one-electron wavefunction is given by $(-1)^\ell$, i.e., the parity of $Y_{\ell m_\ell}(\theta,\phi)$.

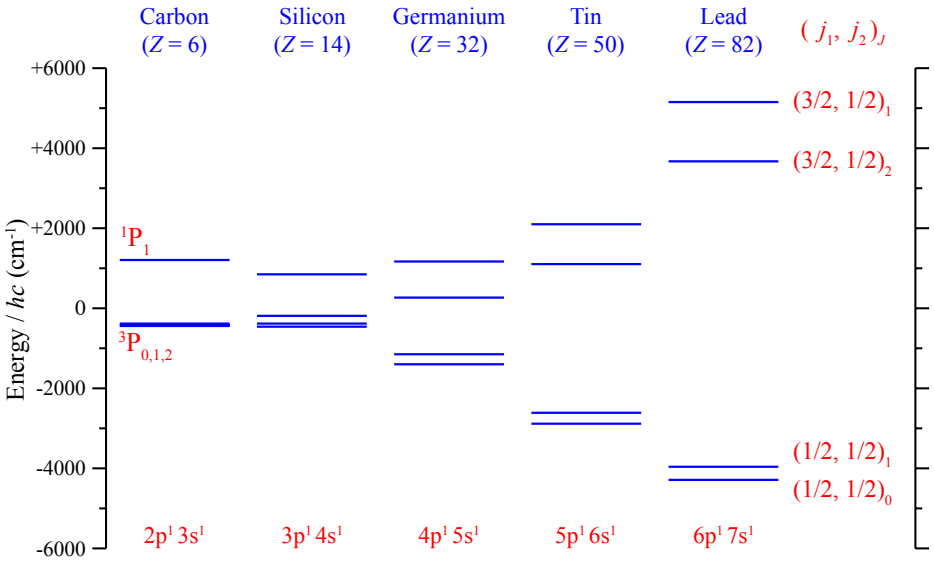

Figure 3.6: Energy level structure of the ground sate configurations of the group IV elements.

In the case of a many-electron atom, the parity of a particular term is given by

$$(-1)^{\ell_1}(-1)^{\ell_2}(-1)^{\ell_3}\times\cdots\times(-1)^{\ell_i} \quad = \quad (-1)^{\sum_i \ell_i}, \tag{3.192}$$

where ℓ_i are the orbital angular momentum quantum numbers of the individual electrons. It is important to note that this is not equivalent to $(-1)^L$.

If a term has odd parity this is indicated by a superscript 'o'after the term symbol, i.e.,

$$^2\mathrm{P}^{\mathrm{o}} \tag{3.193}$$

If a term has even parity this is indicated by omitting this superscript, i.e.,

$$^2\mathrm{P}. \tag{3.194}$$

For example the ground state electronic configuration of the C atom is $1s^2\,2s^2\,2p^2$ so

$$\sum_i \ell_i \quad = \quad 2 \quad \Rightarrow \quad \text{even parity} \tag{3.195}$$

and the ground level is then simply

$$^2\mathrm{P}_0 \tag{3.196}$$

However, since the ground state configuration of the B atom is $1s^2\,2s^2\,2p^1$,

$$\sum_i \ell_i \;=\; 1 \quad\Rightarrow\quad \text{odd parity} \tag{3.197}$$

and the ground level is

$$^2\mathrm{P}^{\mathrm{o}}_{1/2} \tag{3.198}$$

Chapter 4

Atomic spectra

The transitions that can occur between atomic energy levels are governed by sets of *selection rules*. These selection rules impose restrictions on the transitions that are allowed.

4.1 Selection rules for electric dipole transitions

Consider an atom in the presence of an electromagnetic field. The oscillating electric component of this field interacts most strongly with the atom so we therefore neglect the much weaker interaction of the oscillating magnetic component of the field. The oscillating electric field takes the form

$$\vec{E} = \vec{E}_0 \, e^{i\omega t}, \tag{4.1}$$

where $\vec{E}_0 = (E_{0_x}, E_{0_y}, E_{0_z})$ is the amplitude of the field, and $\omega = 2\pi\nu$ is the angular oscillation frequency.

The interaction of the atom with the oscillating electric field occurs via its electric dipole moment, $\vec{\mu} = e\vec{r}$ such that

$$V_{\text{dip}} = -\vec{\mu} \cdot \vec{E}, \tag{4.2}$$

so that in the Hamiltonian in the presence of the field is

$$\hat{H} = \hat{H}_0 - \vec{\mu} \cdot \vec{E}, \tag{4.3}$$

where $\hat{H}_0$ is the field-free Hamiltonian.

When the time-dependent perturbation resulting from the oscillating electric field is small compared to $\hat{H}_0$, first-order time-dependent perturbation theory can be applied. This leads to *Fermi's golden rule* by which the transition probability, T_{if}, between an initial state, i, and final state, f, can be determined

$$T_{\text{if}} = \left| \int \Psi_{\text{f}}^{*} V_{\text{dip}} \Psi_{\text{i}} \, \mathrm{d}\tau \right|^2 . \tag{4.4}$$

For each pair of initial and final states if $T_{\text{if}} = 0$ the transition in *forbidden*, while if $T_{\text{if}} \neq 0$ the transition is *allowed*.

To obtain further insight into the probability of a a transition occurring, consider the interaction of the atom with the x, y and z components of the oscillating electric field separately. In spherical polar coordinates,

$$\vec{\mu} = e\vec{r} = e\,(r\sin\theta\cos\phi, r\sin\theta\sin\phi, r\cos\theta). \tag{4.5}$$

The z component of the interaction potential is therefore

$$V_{\text{dip}_z} = e\,r\cos\theta\,E_{0_z}\,\mathrm{e}^{i\omega t}. \tag{4.6}$$

For a one-electron atom, the total electronic wavefunction excluding spin takes the form

$$\Psi_{n\ell m_\ell} = R_{n\ell}(r)\,Y_{\ell m_\ell}(\theta,\phi). \tag{4.7}$$

Therefore following Fermi's golden rule, the probability for a transition between an initial state $\Psi_{n\ell m_\ell}$ and a final state $\Psi_{n'\ell' m'_\ell}$ to occur is

$$\begin{aligned} T_{n'\ell' m'_\ell, n\ell m_\ell} = {} & E_{0_z}^2 \left| \int_0^\infty R^{*}_{n'\ell'}(r)\, r\, R_{n\ell}(r)\, r^2 \, \mathrm{d}r \;\times \right. \\ & \left. \times \int_0^{2\pi}\int_0^{\pi} Y^{*}_{\ell' m'_\ell}(\theta,\phi)\,\cos\theta\, Y_{\ell m_\ell}(\theta,\phi)\sin\theta\,\mathrm{d}\theta\,\mathrm{d}\phi \right|^2 \end{aligned} \tag{4.8}$$

The radial part of this integral imposes no restrictions on the values of $n\ell$ and $n'\ell'$. However, for any give values of n and ℓ, the angular part of the integral does limit the values of n' and ℓ' for which the transition probability is non-zero.

The angular part of Equation 4.8 can be expressed completely in terms of spherical harmonic functions by considering that

$$Y_{1,0}(\theta,\phi) = \sqrt{\frac{3}{4\pi}}\cos\theta \tag{4.9}$$

and therefore

$$\cos\theta \;=\; \sqrt{\frac{4\pi}{3}}Y_{1,0}(\theta,\phi), \tag{4.10}$$

and

$$Y^{*}_{\ell,m_\ell}(\theta,\phi) \;=\; (-1)^{m_\ell}\,Y_{\ell,-m_\ell}(\theta,\phi), \tag{4.11}$$

leading to the integral

$$(-1)^{m_\ell}\sqrt{\frac{4\pi}{3}}\int_0^{2\pi}\!\!\int_0^{\pi} Y_{\ell,-m_\ell}(\theta,\phi)\,Y_{1,0}(\theta,\phi)\,Y_{\ell,m_\ell}(\theta,\phi)\sin\theta\,\mathrm{d}\theta\,\mathrm{d}\phi \tag{4.12}$$

which, from the properties of the spherical harmonic functions, is equal to zero unless

$$\ell' \;=\; \ell\pm 1 \quad\Rightarrow\quad \Delta\ell = \pm 1 \tag{4.13}$$

$$m'_\ell \;=\; m_\ell \quad\Rightarrow\quad \Delta m_\ell = 0. \tag{4.14}$$

For the x and y components of the oscillating electric field $\Delta\ell = \pm 1$ and $\Delta m_\ell = \pm 1$.

Because the electric dipole interaction potential, V_{dip}, does not depend on $\vec{s}$ the electron spin cannot change in a one-electron electric dipole transition, i.e.,

$$\Delta s \;=\; 0. \tag{4.15}$$

In addition, since the corresponding operator

$$V_{\mathrm{dip}} \;=\; -e\,\vec{r}\cdot\vec{E} \tag{4.16}$$

has odd parity (because $\vec{r}$ has odd parity), and the integrand

$$\Psi^{*}_{\mathrm{f}}\,V_{\mathrm{dip}}\,\Psi_{\mathrm{i}} \tag{4.17}$$

must be even for $T_{\mathrm{if}} \neq 0$, therefore

$$\Psi^{*}_{\mathrm{f}}\,\Psi_{\mathrm{i}} \tag{4.18}$$

must be odd. For this to be the case the initial and final states must have opposite parity, i.e., one must be odd and one must be even. This is the

origin of the selection rule that parity must change in an electric dipole transition.

The complete set of selection rules for electric dipole transitions in one-electron atoms is therfore:

Electric dipole selection rules for one-electron atoms:

$\Delta\ell = \pm 1$

$\Delta m_\ell = 0, \pm 1$

$\Delta s = 0$

Parity must change

If there is a strong spin-orbit interaction:

$$\Delta j = 0, \pm 1 \quad \text{but} \quad j = 0 \nrightarrow j' = 0$$

Along with these *electric dipole allowed transitions* other transitions can occur (e.g., magnetic dipole transitions, electric quadrupole transitions), but with probabilities that are considerable smaller.

Examples of allowed and forbidden electric dipole transitions in the H atom are:

Allowed transitions:	1s	$\rightarrow$	2p
	1s	$\rightarrow$	3p
	2p	$\rightarrow$	5d
Not allowed:	1s	$\nrightarrow$	2s
	1s	$\nrightarrow$	3d

In many-electron atoms a similar set of selection rules hold for electric dipole transitions. These include a subset of *rigorous* selection rules which must hold for a transition to occur at all, and a additional subset of selection

rules which if they are also fulfilled give rise to strong transitions.

Electric dipole selection rules for many-electron atoms:

Rigorous selection rules:

$\Delta J = 0, \pm 1 \quad$ but $\quad J = 0 \nrightarrow J' = 0$

$\Delta M_J = 0, \pm 1$

Parity must change

In addition transitions are weak unless:

$\Delta S = 0$

$\Delta L = 0, \pm 1 \quad$ but $\quad L = 0 \nrightarrow L' = 0$

For example, the C atom has an excited electronic configuration $1s^2\ 2s^2\ 2p^1\ 4d^1$ with an associated level

$$^3F_2^o \tag{4.19}$$

for which

$$(2S+1) = 3 \quad \Rightarrow S = 1, \tag{4.20}$$

$$L = 3 \tag{4.21}$$

$$J = 2 \tag{4.22}$$

$$\text{'o'} \quad \Rightarrow \quad \text{odd parity} \tag{4.23}$$

The following transitions from this level can be classified as:

$^3F_2^o \rightarrow {}^3P_1$ Weak because $\Delta L \neq \pm 1$

$^3F_2^o \rightarrow {}^3P_1^o$ Forbidden because parity does not change

$^3F_2^o \rightarrow {}^1D_2$ Weak because $\Delta S \neq 0$, (*intercombination line*)
generally stronger than first transition above

$^3F_2^o \rightarrow {}^3D_2$ Strong allowed transition

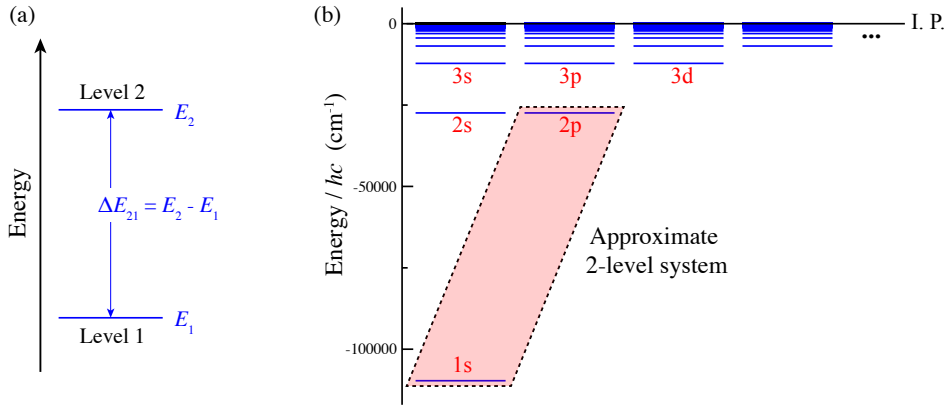

Figure 4.1: Two-level systems. (a) An ideal two-level system with the energy difference, ΔE_{21}, between the two levels, 1 and 2, indicated. (b) Example of an approximate two-level system in the H atom. In this case the two relevant levels are the 1s and 2p levels. This can be considered a two-level system because after excitation from level 1 (1s) to level 2 (2p) the system can only decay back to level 1.

4.2 Rates of photon emission and absorption

To treat the absorption and emission of photons by atoms we first consider a simple two-level system as depicted in Figure 4.1(a). An example of such as system is that associated with the 2s and 2p states in the H atom [see Figure 4.1(b)].

If a two-level system is exposed to an electromagnetic field of frequency, $\nu_{21} = \Delta E_{21}/h$, corresponding to the energy interval between the two levels, three processes must be considered: *Absorption*, *spontaneous emission*, and *stimulated emission*.

Absorption: This involves the system, initially in level 1, absorbing a photon from the electromagnetic field and being excited to level 2.

The rate of absorption, Γ_{abs}, is proportional to (i) the number of atoms (population) in level 1, N_1, and (ii) the energy density, $U(\nu_{21})$, of the electromagnetic field, i.e.,

$$\Gamma_{\text{abs}} \propto N_1 \, U(\nu_{21}). \tag{4.24}$$

Spontaneous emission: This involves the system, initially in level 2, decaying spontaneously to level 1 with the emission of a photon of frequency, ν_{21}.

The rate of spontaneous emission, Γ_{spon}, is proportional to the number of atoms (population) in level 2, N_2, i.e.,

$$\Gamma_{\text{spon}} \propto N_2. \tag{4.25}$$

Stimulated emission: This involves a photon from the electromagnetic field 'stimulating', the system, initially in level 2, to decay to level 1 with the emission of another photon.

The rate of stimulated emission, Γ_{stim}, is proportional to (i) the number of atoms (population) of level 2, N_2, and (ii) the energy density, $U(\nu_{21})$, of the electromagnetic field, i.e.,

$$\Gamma_{\text{stim}} \propto N_2\, U(\nu_{21}). \tag{4.26}$$

The photon emitted by the system following stimulated emission has the same frequency, is coherent with, i.e., its electromagnetic field is oscillating in phase with, and propagates in the same direction as the photon that stimulated the emission. This process of simulated emission, in which one photon incident on an excited system causes the emission of a second photon with identical properties, is the basis on which the LASER (Light Amplification by Stimulated Emission of Radiation) operates.

4.2.1 Two-level rate equations

Consider an ensemble of two-level atoms with N_1, the number of atoms in energy level 1, with energy E_1, and N_2 the number in energy level 2 with energy E_2. If this ensemble is exposed to a thermal electromagnetic field, i.e., a field in which the photons are propagating in random directions with random polarisations, with a spectral energy density $U(\nu_{12}) \equiv U(\nu_{21})$. The time-dependence of the population of levels 1 and 2 in this system can be

expressed as

$$\frac{\mathrm{d}N_1}{\mathrm{d}t} = \overbrace{-C\,U(\nu_{12})\,N_1}^{\text{Absorption}} + \overbrace{A\,N_2}^{\text{Spon. decay}} + \overbrace{B\,U(\nu_{12})\,N_2}^{\text{Stim. emiss.}} \tag{4.27}$$

$$\frac{\mathrm{d}N_2}{\mathrm{d}t} = \overbrace{+C\,U(\nu_{12})\,N_1}^{\text{Absorption}} - \overbrace{A\,N_2}^{\text{Spon. decay}} - \overbrace{B\,U(\nu_{12})\,N_2}^{\text{Stim. emiss.}}, \tag{4.28}$$

where A, B, and C are constants.

When the ensemble of two-level atoms is in equilibrium with the thermal electromagnetic field

$$\frac{\mathrm{d}N_1}{\mathrm{d}t} = \frac{\mathrm{d}N_2}{\mathrm{d}t} = 0, \tag{4.29}$$

i.e., in the steady state there is no change in the average population of either level 1 or level 2. Therefore

$$C\,U(\nu_{12})\,N_1 = A\,N_2 + B\,U(\nu_{12})\,N_2, \tag{4.30}$$

or

$$\frac{N_1}{N_2} = \frac{A + B\,U(\nu_{12})}{C\,U(\nu_{12})}. \tag{4.31}$$

When the system is in thermal equilibrium, the ratio of the population in level 1, to the population in level 2 follows a Maxwell-Boltzmann distribution, i.e,

$$\frac{N_1}{N_2} = \frac{\mathrm{e}^{(-E_1/k_\mathrm{B}T)}}{\mathrm{e}^{(-E_2/k_\mathrm{B}T)}} \tag{4.32}$$

$$= \mathrm{e}^{(h\nu_{12}/k_\mathrm{B}T)}, \tag{4.33}$$

where $h\nu_{12} = E_2 - E_1$, and k_B is the Boltzmann constant.

Substituting Equation 4.33 into Equation 4.31 and rearranging the resulting equation leads to

$$C\,U(\nu_{12})\,\mathrm{e}^{(h\nu_{12}/k_\mathrm{B}T)} = A + B\,U(\nu_{12}) \tag{4.34}$$

and so

$$U(\nu_{12}) = \frac{A}{C\,\mathrm{e}^{(h\nu_{12}/k_\mathrm{B}T)} - B} \tag{4.35}$$

$$= \frac{(A/B)}{(C/B)\,\mathrm{e}^{(h\nu_{12}/k_\mathrm{B}T)} - 1} \tag{4.36}$$

However, the spectral energy density of the electromagnetic field associated with a radiating blackbody can be expressed, following the Plank formula, as

$$U(\nu_{12}) = \frac{8\pi\,\nu_{12}^2}{c^3}\,\frac{h\nu_{12}}{\mathrm{e}^{(h\nu_{12}/k_\mathrm{B}T)} - 1} \tag{4.37}$$

$$= \frac{8\pi\,h\,\nu_{12}^3}{c^3}\,\frac{1}{\mathrm{e}^{(h\nu_{12}/k_\mathrm{B}T)} - 1}. \tag{4.38}$$

Therefore comparison of Equation 4.38 with Equation 4.36 leads to the conclusion that

$$C = B \tag{4.39}$$

and

$$A = \frac{8\pi\,h\,\nu_{12}^3}{c^3}\,B. \tag{4.40}$$

The variables A and B are known as the Einstein coefficients for spontaneous and stimulated emission, respectively.

$A \equiv$ Einstein A-coefficient for spontaneous emission

$B \equiv$ Einstein B-coefficient for stimulated emission

The Einstein B-coefficient can be expressed in terms of the transition probability given by Fermi's Golden Rule as

$$B = \frac{2\pi}{3\,\hbar^2}\left(\frac{1}{4\pi\epsilon_0}\right)\left|\int \Psi_2^*\,\hat{\vec{\mu}}\,\Psi_1\,\mathrm{d}\tau\right|^2, \tag{4.41}$$

where, for electromagnetic radiation linearly polarised in the z dimension, $\vec{\mu} = e\,z$.

4.2.2 Excited state lifetimes

Two-level system

In the absence of an electromagnetic field to stimulate emission an isolated two-level atom in its excited state (level 2) will decay spontaneously. The rate, Γ_{spon}, at which this spontaneous decay occurs is equal to the Einstein A-coefficient for the transition from the excited state (level 2) to the ground state (level 1), i.e.,

$$\Gamma_{\text{spon}} \quad = \quad A_{12}. \tag{4.42}$$

The lifetime of the excited state, τ_{spon}, is equal to the inverse of this decay rate

$$\tau_{\text{spon}} \quad = \quad \frac{1}{\Gamma_{\text{spon}}}. \tag{4.43}$$

For example:

Consider a H atom in the 2p state with $m_\ell = 0$, i.e.,

$$\Psi_{n\,\ell\,m_\ell} \quad = \quad \Psi_{2\,1\,0}. \tag{4.44}$$

From this state the atom can only decay to the 1s ground state with $m_\ell = 0$, i.e.,

$$\Psi_{n'\,\ell'\,m'_\ell} \quad = \quad \Psi_{1\,0\,0}. \tag{4.45}$$

Because of this single decay channel this can be considered a two-level system so to determine the lifetime of the excited state using Equation 4.40 and Equation 4.41

$$A_{12} \quad = \quad \frac{8\pi^2\,\nu_{12}^3}{3\epsilon_0\,\hbar\,c^3}\left|\int \Psi_{1\,0\,0}^*\;\hat{\vec{\mu}}\;\Psi_{2\,1\,0}\,\mathrm{d}\tau\right|^2. \tag{4.46}$$

Note: this expression for the Einstein A-coefficient is sometimes also written in an equivalent form in terms of the angular frequency, $\omega_{12} = 2\pi\,\nu_{12}$, and $h = 2\pi\,\hbar$ as

$$A_{12} \quad = \quad \frac{2\,\omega_{12}^3}{3\epsilon_0\,h\,c^3}\left|\int \Psi_{1\,0\,0}^*\;\hat{\vec{\mu}}\;\Psi_{2\,1\,0}\,\mathrm{d}\tau\right|^2. \tag{4.47}$$

For the $\Delta m_\ell = 0$ transition between the states Ψ_{210} and Ψ_{100} the electric dipole transition operator, $\hat{\vec{\mu}}$, is

$$\hat{\vec{\mu}} = e\hat{z} = er\cos\theta. \tag{4.48}$$

and since

$$\Psi_{n\ell m_\ell} = R_{n\ell}(r)\,Y_{\ell m_\ell}(\theta,\phi) \tag{4.49}$$

The A-coefficient for the transition is

$$A_{12} = \frac{8\pi^2\nu_{12}^3}{3\epsilon_0\hbar c^3}\left|\int_0^\infty R_{10}^*(r)\,er\,R_{21}(r)\,r^2\mathrm{d}r\times\ldots \right.$$
$$\left.\times\int_0^{2\pi}\int_0^\pi Y_{00}^*(\theta,\phi)\,\cos\theta\,Y_{10}(\theta,\phi)\,\sin\theta\,\mathrm{d}\theta\mathrm{d}\phi\right|^2. \tag{4.50}$$

Using the radial wavefunctions for the H atom in Equation 2.65 and in Table 2.2, together with the spherical harmonic functions in Equation 2.62 and in Table 2.1, Equation 4.50 becomes

$$A_{12} = \frac{8\pi^2\nu_{12}^3}{3\epsilon_0\hbar c^3}\left|\sqrt{\frac{1}{3}}\,1.29\,ea_0\right|^2. \tag{4.51}$$

Since in the H atom the energy difference between the 1s and 2p states is given by the Rydberg formula as

$$\frac{\Delta E_{12}}{hc} = R_\mathrm{H}\left[\frac{1}{1^2}-\frac{1}{2^2}\right] \tag{4.52}$$
$$= 82258\ \mathrm{cm}^{-1} \tag{4.53}$$
$$\equiv 121.568\ \mathrm{nm}, \tag{4.54}$$
$$\nu_{12} = 2.466\times10^{15}\ \mathrm{Hz}, \tag{4.55}$$

and

$$A_{12} = 6.25\times10^8\ \mathrm{s}^{-1}\quad(\text{or}\quad 6.25\times10^8\ \mathrm{Hz}). \tag{4.56}$$

Therefore the lifetime, $\tau_{2\mathrm{p}}$, of the 2p state is

$$\tau_{2\mathrm{p}} = \frac{1}{A_{12}} \tag{4.57}$$
$$= 1.60\times10^9\ \mathrm{s} \tag{4.58}$$
$$= 1.60\ \mathrm{ns}. \tag{4.59}$$

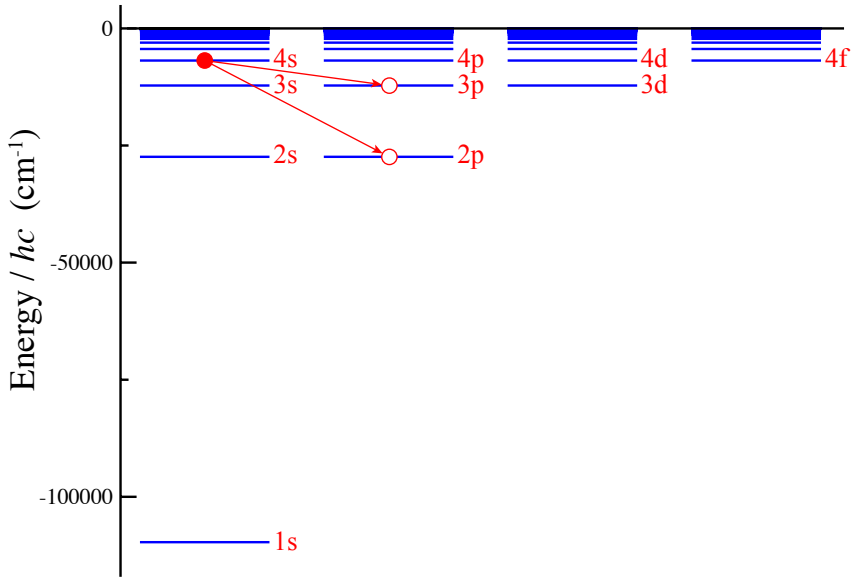

Figure 4.2: Spontaneous decay pathways from the 4s state in the H atom.

Multi-level system

In a multi-level system the rate of spontaneous decay, Γ_i, of an excited state, i, is obtained by summing the Einstein A-coefficients for all possible decay pathways, A_{if} to all allowed final states f, i.e., the total decay rate is the sum of the rates of decay via each decay pathway,

$$\Gamma_i = \sum_f A_{if}. \tag{4.60}$$

Consequently, the lifetime, τ_i, of an excited state in a multi-level system is

$$\tau_i = \frac{1}{\Gamma_i} \tag{4.61}$$

$$= \left[\sum_f A_{if}\right]^{-1} \tag{4.62}$$

For example:

Under the selection rules for electric dipole transition, a H atom in the 4s state can decay to the 3p or 2p states (see Figure 4.2)

Following a similar procedure to that outlined above the Einstein A-coefficients for the 4s→3p and 4s→2p transitions can be determined to be

$$A_{4s\,3p} = 1.83 \times 10^6 \text{ s}^{-1} \quad (4.63)$$

$$A_{4s\,2p} = 2.58 \times 10^6 \text{ s}^{-1}. \quad (4.64)$$

From Equation 4.60, the total rate of spontaneous decay of the 4s state, Γ_{4s}, is therefore

$$\Gamma_{4s} = A_{4s\,3p} + A_{4s\,2p} \quad (4.65)$$

$$= 4.41 \times 10^6 \text{ s}^{-1}. \quad (4.66)$$

The lifetime of the 4s state, τ_{4s}, can then be determined to be

$$\tau_{4s} = \frac{1}{\Gamma_{4s}} \quad (4.67)$$

$$= 227 \text{ ns}. \quad (4.68)$$

4.2.3 Effects of finite excited state lifetimes

The finite lifetimes of excited states of atoms impose limits on the precision with which the frequency (energy difference) associated with transitions to, or from, these states can be determined. This follows from Heisenberg's time-energy uncertainty relation

$$\Delta E \, \Delta t \geq \frac{\hbar}{2}, \quad (4.69)$$

where ΔE is the uncertainty in the energy, and Δt is the uncertainty in the time.

As a consequence of this, transitions involving excited states with short lifetimes have large spectral widths, i.e., after excitation the short excited state lifetime means that the time when the atom will spontaneously decay can be determined precisely, but the frequency of the photons emitted when the decay occurs will not be very precisely defined.

On the other hand, transitions to states with long lifetimes have narrow spectral widths, i.e., after excitation the long excited state lifetime means that the time when the atom will spontaneously decay cannot be precisely

determined, but the frequency of the emitted photons will be very precisely defined.

4.2.4 Metastable states

If the spontaneous decay of an excited state in an atom is forbidden by the selection rules for electric dipole transitions (see Section 4.1), i.e., if $A_{fi} = 0$ for all final states, then the excited state is said to be *metastable*.
For example:
In the H atom the 2s state is a metastable state as it is forbidden to decay to the 1s ground state by the selection rule that $\Delta\ell = \pm 1$ (see Figure 4.3).

In the 1s2s configuration of the He atom the $^1S_0$ and $^3S_1$ levels are both metastable (see Figure 4.3).

The 1s2s $^1S_0$ level cannot decay to the $1s^2\ ^1S_0$ ground state because the $\Delta L = 0, \pm 1$ but $L = 0 \nrightarrow L' = 0$ selection rule is not fulfilled.

The 1s2s $^3S_1$ level cannot decay to the $1s^2\ ^1S_0$ ground state because the $\Delta L = 0, \pm 1$ but $L = 0 \nrightarrow L' = 0$ selection rule, and the $\Delta S = 0$ selection rule are both not fulfilled.

Each of these metastable states can decay by higher order processes, i.e, magnetic dipole transitions, or electric quadrupole transitions, but these are very slow. Consequently the 1s2s $^3S_1$ level in He, the decay of which is doubly forbidden by the selection rules for electric dipole transitions lives for 7870 s and is the longest lived excited state of an atom[1].

[1] S. S. Hodgman, R. G. Dall, L. J. Byron, K. G. H. Baldwin, S. J. Buckman and A. G. Truscott, Metastable Helium: A New Determination of the Longest Atomic Excited-State Lifetime, *Phys. Rev. Lett.* **103**, 053002 (2009)

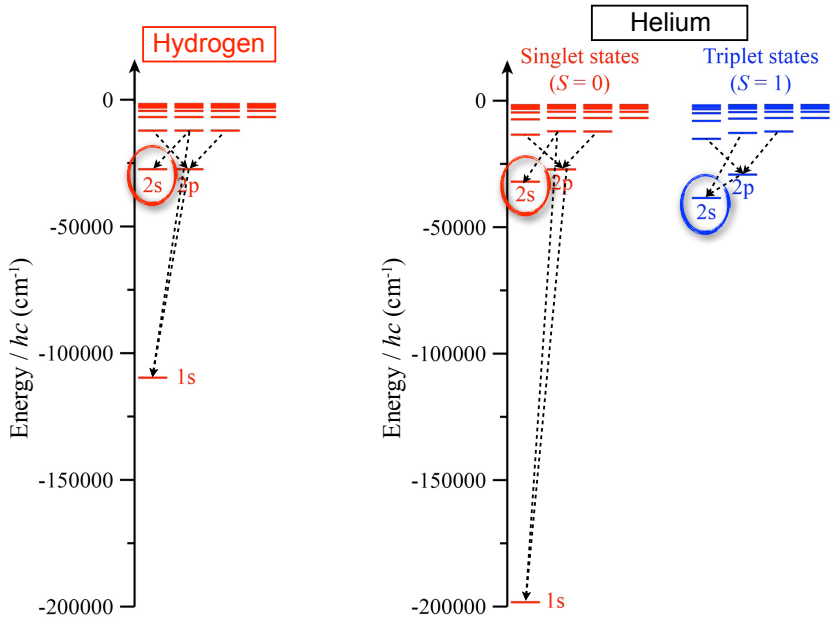

Figure 4.3: The metastable 2s state in the H atom, and the metastable 1s2s $^1S_0$ and 1s2s $^3S_1$ levels in the He atom (circled). Electric dipole allowed transitions to these levels from more highly excited states, and allowed decay pathways to the ground states are indicated.

4.3 Lasers

When a samples of two-level atomic systems are in thermal equilibrium with their environment the ratio of the population of level 1, N_1, to the population of level 2, N_2, follows a Maxwell-Boltzmann distribution, i.e.,

$$\frac{N_1}{N_2} = e^{(h\nu_{12}/k_B T)}. \tag{4.70}$$

As a result, $N_1 > N_2$, and there are always many more atoms in level 1 than in level 2. Therefore if a photon of frequency ν_{12} passes through this sample of atoms it is more likely to be absorbed that to stimulate emission.

To ensure that stimulated emission is more probable than absorption it is therefore necessary to have more atoms in the sample in level 2 than in level 1, i.e., $N_2 > N_1$. This situation is known as a *population inversion*.

If a population inversion is achieved, and the rate of stimulated emission (the Einstein B-coefficient) is greater that the rate of spontaneous emission

(the Einstein A-coefficient), incoming photons can cause stimulated emission, and the resulting photons can stimulate further emission leading to an intense, coherent beam of monochromatic photons all travelling in the same direction - a laser beam.

However, it is in general not possible to generate a population inversion in a pure two-level system. This is because:

- If the population is initially in level 1 (i.e., $N_1 \gg N_2$) absorption is most likely

- This leads to an increase in the population of level 2 until $N_1 = N_2$ at which time further absorption and stimulated emission are both equally likely to occur

Therefore a population inversion cannot be achieved and stimulated emission cannot become the dominant excited state decay process.

To achieve a population inversion a system with at least three levels is required.

4.3.1 Three-level lasers

A schematic diagram of a three-level system that can be exploited in the operation of a laser is presented in Figure 4.4.

The process of generating a population inversion in this system begins with the sample of atoms all in level 1.

A: The first step of the process of generating the population inversion involves exciting, 'pumping', atoms from level 1 to level 2 using photons at frequency, ν_{12}.

B: This is then followed by fast spontaneous decay (*internal conversion*) to level 3 which is metastable leading to a population inversion between level 3 and level 1.

C: Lasing can then occur on the transition from level 3 to level 1 at frequency ν_{31}. Because level 3 is long-lived (metastable) it is possible to ensure that stimulated emission from level 3 to level 1 is faster than spontaneous emission.

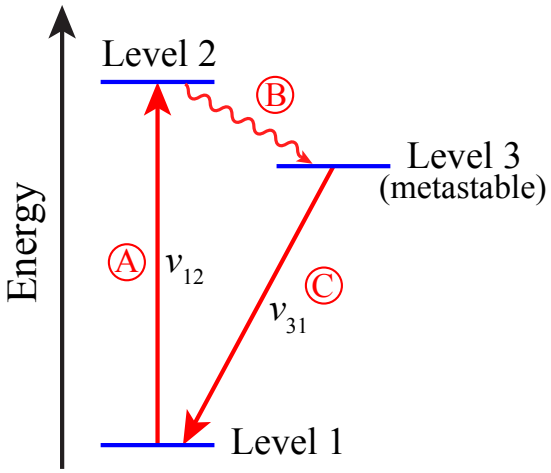

Figure 4.4: Schematic diagram of a three-level system in which a population inversion can be achieved between level 3 and level 1 and exploited as a laser.

In this system, because the frequency of the electromagnetic radiation used to prepare the population inversion, ν_{12}, is different to the frequency at which the stimulated emission occurs, ν_{31}, a population inversion can be readily achieved.

Having prepared a system with a population inversion, to ensure the successful operation of a laser the rate of stimulated emission must be grater than the rate of spontaneous emission (Einstein A-coefficient). Because the Einstein A-coefficient is proportional to the cube of the transition frequency, i.e.,

$$A_{if} \quad \propto \quad \nu_{if}^3, \tag{4.71}$$

this is more easily achieved at lower transition frequencies. For this reason the first laser operated at microwave frequencies using a transition in the ammonia molecule (NH_3) and was known as a MASER – Microwave Amplification by Stimulated Emission of Radiation[2] (see also [3]). However, as

[2]J. P. Gordon, H. J. Zeiger and C. H. Townes, The Maser – New Type of Microwave Amplifier, Frequency Standard, and Spectrometer, *Phys. Rev.* **99**, 1264 (1955)

[3]C. H. Townes, *How the Laser Happened: Adventures of a Scientist*, Oxford University Press (2002)

in Figure 4.4 this problem can also be overcome by selecting a system in which level 3 is long-lived (metastable).

Following the development of the MASER the first LASER to operate in the visible region of the electromagnetic spectrum employed ruby as the lasing medium[4]. The ruby laser is an example of a three-level system with an energy level structure of the kind depicted in Figure 4.4.

Ruby is an aluminium oxide (Al_2O^3) crystal which contains chromium, Cr^{3+} impurities. It has strong absorption bands at wavelengths of ~ 400 nm and ~ 550 nm (corresponding to ν_{12} in Figure 4.4). Excitation at these wavelengths is followed by rapid non-radiative decay to a metastable level 3 which has a lifetimes of ~ 3 ms. The lasing transition from level 3 to level 1 lies at a wavelength of 694 nm in the red region of the electromagnetic spectrum.

However, three-level lasers of the kind outlined in Figure 4.4 such as the ruby laser are not so efficient because after being stimulated to decay from level 3 to level 1, the photons generated in the stimulated emission process can be reabsorbed if generated in sufficient quantities.

4.3.2 Four-level lasers

To overcome the problem of absorption of amplified photons by the lasing medium, and therefore obtain improved operation efficiency, lasers based upon four-level systems can also be implemented. An example of such a laser is the helium-neon (He-Ne) laser, the energy level structure of which is displayed schematically in Figure 4.5.

In the case of the He-Ne laser, level 1 is the overall ground state of the He and Ne system, i.e., the He atom in the $1s^2\,{}^1S_0$ level and the Ne atom in the $1s^2\,2s^2\,2p^6\,{}^1S_0$ level. Level 2 is associated with the ${}^1S_0$ and ${}^3S_1$ levels of the excited 1s 2s configuration of the He atom, and level 3 corresponds to the excited $1s^2\,2s^2\,2p^5\,4s^1$ and $1s^2\,2s^2\,2p^5\,5s^1$ configurations of the Ne atom, while level 4 is associated with the $1s^2\,2s^2\,2p^5\,3p^1$ and $1s^2\,2s^2\,2p^5\,4p^1$ configurations of Ne.

As in the case of the three-level laser the process of generating a popu-

[4]T. Maiman, Stimulated Optical Radiation in Ruby, *Nature* **187**, 493 (1960)

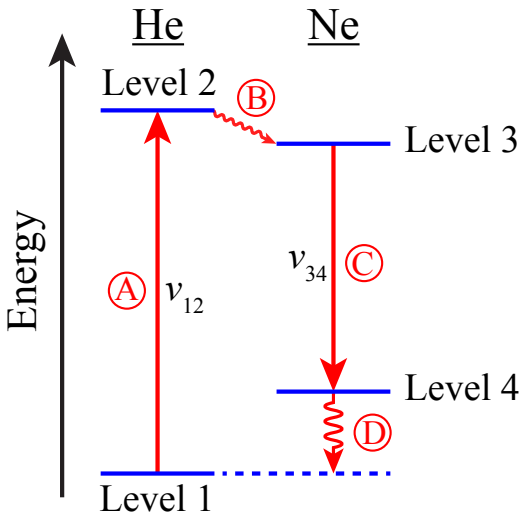

Figure 4.5: Schematic diagram of a four-level system in which a population inversion is achieved between level 3 and level 4 and exploited in a laser.

lation inversion in this four-level system begins with the sample of atoms all in level 1.

A: The first step of the process of generating a population inversion involves exciting, 'pumping', atoms from level 1 to level 2. This is sometimes achieved optically, but in the case of the He-Ne laser involves the generation of an electric discharge in a mixture of He and Ne gas.

B: Excitation of level 2 is then followed by rapid energy transfer to level 3. In the case of the He-Ne laser this is achieved via collisions between the excited He atoms and ground state Ne atoms in the gas mixture.

C: Lasing occurs on the transition from level 3 to level 4 at frequency ν_{34}.

D: Level 4 is selected to rapidly decay by spontaneous emission to the ground state, level 1, such that following stimulated emission from level 3 the atoms in the system do not remain for a long time in level 4. Consequently, reabsorption of amplified radiation cannot occur.

The He-Ne laser is a gas laser operated with a $\sim 10:1$ ratio of He to Ne gas, at pressures on the order of 10 mbar. Such a laser can be operated

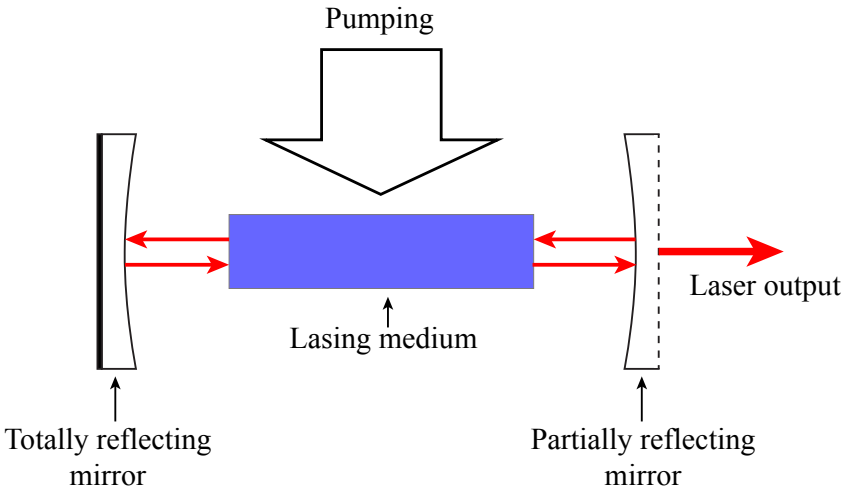

Figure 4.6: Schematic diagram a laser resonator with one totally reflecting mirror and one partially reflecting mirror surrounding the lasing medium. In such a configuration the lasing medium is typically transversely pumped to generate a population inversion.

at several wavelengths in the red or infrared regions of the electromagnetic spectrum, the most common being 633 nm.

4.3.3 Typical laser characteristics

In a typical laser system the lasing medium is enclosed between two mirrors which form an optical cavity, or resonator as depicted in Figure 4.6. One of these mirrors is selected to be very highly (totally) reflecting at the wavelength at which the laser is operated while the other is chosen to be partially reflecting. In such a configuration the laser medium is transversely pumped to generate a population inversion, or in the case of the He-Ne laser, in the region between the two mirrors an electric discharge is generated. In such a resonator, photons that are generated by stimulated emission are fed back into the lasing medium when reflected at the cavity mirrors, to cause further stimulated emission while a small fraction of photons are extracted through the partially reflecting mirror as the laser output.

Lasers can be operated in pulsed or continuous (CW) modes each with different characteristics and potential applications. Since the frequency

	Continuous lasers	Pulsed lasers
Wavelength range	ir – vis	ir – uv
Power (peak)	$\lesssim 100$ W	$> 10^{10}$ W
Bandwidth ($\Delta\nu$)	< 1 MHz	100 MHz – 20 THz
Pulse duration (Δt)	–	10 ns – 50 fs
Examples	Diode lasers	Nd:YAG lasers ($\lambda = 1064$ nm)
	He-Ne lasers	Ti:Sa lasers ($\lambda = 800$ nm)

Table 4.1: Typical parameters of continuous and pulsed lasers.

width (bandwidth), $\Delta\nu$, is limited by the temporal duration (pulse duration), Δt, pulsed lasers have bandwidths that are approximately equal to the inverse of the pulse duration, i.e., $\Delta\nu \simeq (\Delta t)^{-1}$.

4.4 Laser cooling

Precision measurements of transition frequencies in atoms, molecules and ions requires narrow bandwidth (CW) lasers and cold samples so that the interaction times between the quantum system and the laser radiation does not affect the frequency resolution that can be achieved. Frequency measurements at the highest precision are of importance in tests of fundamental physics including, e.g., searches for time-variations of the fundamental constants, the implementation of atomic clocks, quantum computing, and the use of cold atoms and molecules to model 'simulate' complex condensed matter quantum systems. The development of laser cooling as a way to prepare very cold samples of alkali metal atoms, in the 1980s and 1990s, opened up many new possibilities in these areas of reseaerch.

4.4.1 Particle momentum in a gas of hot atoms

Consider a gas of ^{133}Cs atoms at room temperature. Since $M_{^{133}\mathrm{Cs}} = 2.21 \times 10^{-25}$ kg, at $T = 300$ K in one-dimension

$$\frac{1}{2} M_{^{133}\mathrm{Cs}} v_{\mathrm{rms}}^2 = \frac{1}{2} k_{\mathrm{B}} T, \tag{4.72}$$

and so

$$v_{\mathrm{rms}} \simeq 137\,\mathrm{m\,s^{-1}}. \tag{4.73}$$

Moving at this speed the momentum, p_{Cs}, of a single ^{133}Cs atom is therefore

$$p_{\mathrm{Cs}} \simeq M_{^{133}\mathrm{Cs}}\, v_{\mathrm{rms}} \tag{4.74}$$

$$= 3 \times 10^{-23}\,\mathrm{kg\,m\,s^{-1}}. \tag{4.75}$$

4.4.2 Laser cooling Cs

Because alkali metal atoms, e.g., Li, Na, K, Rb, Cs, have one outer optically active electron in a s-orbital they all possess $^2\mathrm{S}_{1/2} \rightarrow {}^2\mathrm{P}_{3/2}$ transitions that approximate two-level systems. In the case of laser cooling this is beneficial because when excited to the upper $^2\mathrm{P}_{3/2}$ level the atoms will always decay directly back to the starting $^2\mathrm{S}_{1/2}$ level.

In the case of Cs this transition involves the electron initially in the 6s orbital and its excitation to the 6p orbital, i.e., the $6\,^2\mathrm{S}_{1/2} \rightarrow 6\,^2\mathrm{P}_{3/2}$ transition. This occurs at a wavelength of $\lambda_{\mathrm{Cs}} = 852$ nm.

Since the momentum, $p_{h\nu}$, associated with a single photon of wavelength, λ, is

$$p_\lambda = \frac{h}{\lambda}, \tag{4.76}$$

In the case of a photon at 852 nm,

$$p_\lambda = 7.8 \times 10^{-28}\,\mathrm{kg\,m\,s^{-1}}. \tag{4.77}$$

When the atom absorbs the photon it experiences a small change in momentum. However, since

$$p_\lambda \ll p_{\mathrm{Cs}} \tag{4.78}$$

the absorption of one single photon has little effect on the atoms momentum.

However, if many photons are scattered (absorbed and spontaneously re-emitted) by an atom the effect of the small individual changes in momentum add up. But because

$$\frac{p_{\mathrm{Cs}}}{p_\lambda} \simeq 38\,461 \tag{4.79}$$

it is necessary that a single thermal Cs atom scatters 38461 photons in order to be brought to rest.

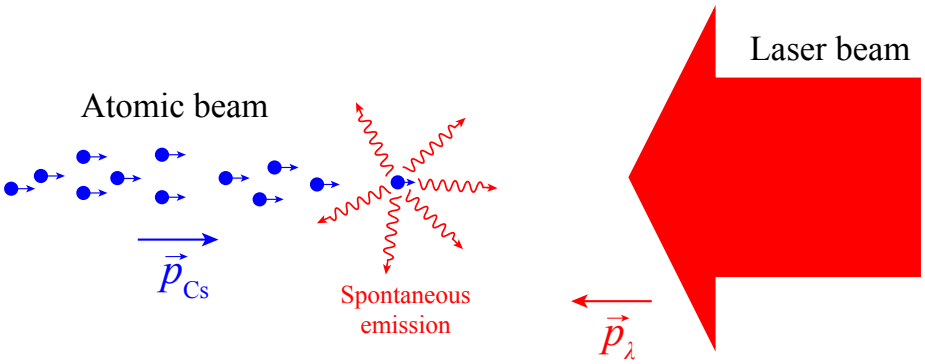

Figure 4.7: Laser deceleration of an atomic beam. The atoms absorb photons from a laser beam counter propagating along the axis of the atomic beam with each photon absorbed the momentum of the atoms in their direction of propagation is slightly reduced. When the atoms subsequently spontaneously decay, the emission can occur in any direction. The effects of the changes in the momentum of the atoms associated with these emitted photons therefore averages to zero in each direction after many absorption-emission cycles.

4.4.3 Laser deceleration

The momentum transfer associated with an atom absorbing a photon can be exploited to decelerate the atom, or a beam of atoms, moving in one particular direction by arranging that a laser beam counter propagates along the axis of the atomic beam as indicated in Figure 4.7. Every time one of the atoms in the atomic beam absorbs a photon it experiences a changes in its momentum of $-p_\lambda$ in its direction of propagation. When the excited atom subsequently decays, the spontaneously emission can occur in any direction. As a result the changes in momentum associated with the spontaneous emission average to zero over many absorption-emission cycles.

Because the atoms are travelling in the direction opposite to the direction of propagation of the laser beam the Doppler shift of the laser radiation must be considered when setting the frequency of the laser radiation to be resonant with the atomic transition. Since the effective frequency of the

laser radiation in the frame-of-reference of the atoms, ν', is

$$\nu' = \nu_{\mathrm{L}} \frac{1}{\left(1 + \frac{v}{c}\right)}, \tag{4.80}$$

where ν_{L} is the frequency at which the laser is operated, v is the speed at which the atoms are travelling in the direction opposite to that in which the laser propagates, and c is the speed of light in vacuum. In order, for the laser radiation to be resonant with the atomic transition frequency, ν_{if}, it is therefore necessary to adjust the frequency at which the laser is operated to

$$\nu_{\mathrm{L}} = \nu_{if} \frac{1}{\left(1 + \frac{v}{c}\right)}. \tag{4.81}$$

It is important to note that in this approach to decelerating a beam of atoms it is necessary to continually adjust the laser frequency to account for the changes in the Doppler shift as the atoms slow down.

The final momentum of an atom decelerated via this laser cooling scheme is limited by the recoil momentum associated with the emission of the last photon. Therefore the minimum speed to which a beam of ^{133}Cs atoms can be decelerated, $v_{\mathrm{Cs}}^{\mathrm{min}}$, is

$$v_{\mathrm{Cs}}^{\mathrm{min}} = \frac{p_\lambda}{M_{^{133}\mathrm{Cs}}} \tag{4.82}$$

$$= \frac{h}{\lambda} \frac{1}{M_{^{133}\mathrm{Cs}}} \tag{4.83}$$

$$\simeq 0.003\ \mathrm{m\,s^{-1}}. \tag{4.84}$$

In this approach to laser deceleration 'cooling' atoms, the maximum deceleration is achieved when the time between the atom absorbing two consecutive photons in minimal. Because the excited state, the $6\,^2\mathrm{P}_{3/2}$ state in the case of Cs, has a finite lifetime $\tau_{\mathrm{Cs}} = 30$ ns, it is necessary to ensure that it has decayed spontaneously before the atom can absorb another photon. If the intensity of the laser beam is not selected to meet this criterion it will cause stimulated emission, canceling the effect of the reduction in the momentum of the atom following the initial absorption of the photon. To achieve the maximum deceleration it is most optimal to set the intensity of the laser beam so that the average time between the absorption of two

consecutive photons, Δt_{abs}, is twice the excited state lifetime, i.e.,

$$\Delta t_{\text{abs}} \simeq 2\,\tau_{\text{Cs}}. \tag{4.85}$$

Hence, for maximum deceleration the absorption rate must be set to be approximately have of the spontaneous emission rate.

To further ensure that stimulated emission does not limit the deceleration (cooling) efficiency, the laser radiation is chosen to be circularly polarised, with one chosen helicity, in which case it will only drive, e.g., $\Delta M_J = +1$ transitions. If the transition

$$\begin{array}{ccc} 6\,^2\text{S}_{1/2} & \longrightarrow & 6\,^2\text{P}_{3/2} \\ (M_J = +1/2) & & (M_J = +3/2) \end{array} \tag{4.86}$$

is driven using circularly polarised light $\Delta M_J = +1$ as indicated, and the excited state with $M_J = +3/2$ cannot be stimulated to emit by a further $\Delta M_J = +1$ transition because the maximum value of M_J of ground level is $1/2$.

In the case of the Cs atom, since $\tau_{\text{Cs}} = 30$ ns, for maximal deceleration the average time between the absorption of two consecutive photons is therefore 60 ns. Therefore for the atom to scatter 38 361 photons to be decelerated from an initial speed $u = 137$ m/s to 0 m/s requires at time, t, of

$$t = \frac{p_{\text{Cs}}}{p_\lambda} 2\tau_{\text{Cs}} \tag{4.87}$$

$$= 2.3 \text{ ms}. \tag{4.88}$$

For a final speed of 0 m/s the corresponding acceleration, a_{Cs}, is therefore

$$a_{\text{Cs}} = -\frac{u}{t} \tag{4.89}$$

$$= -5.9 \times 10^4 \text{ m s}^{-2} \tag{4.90}$$

$$\simeq 6\,000\, g. \tag{4.91}$$

4.4.4 Magnetic trapping and further cooling

When decelerated using the approach described above, the resulting cold atoms can be trapped magnetically. This is achieved by generating a minimum of magnetic field strength in three-dimensions by operating two

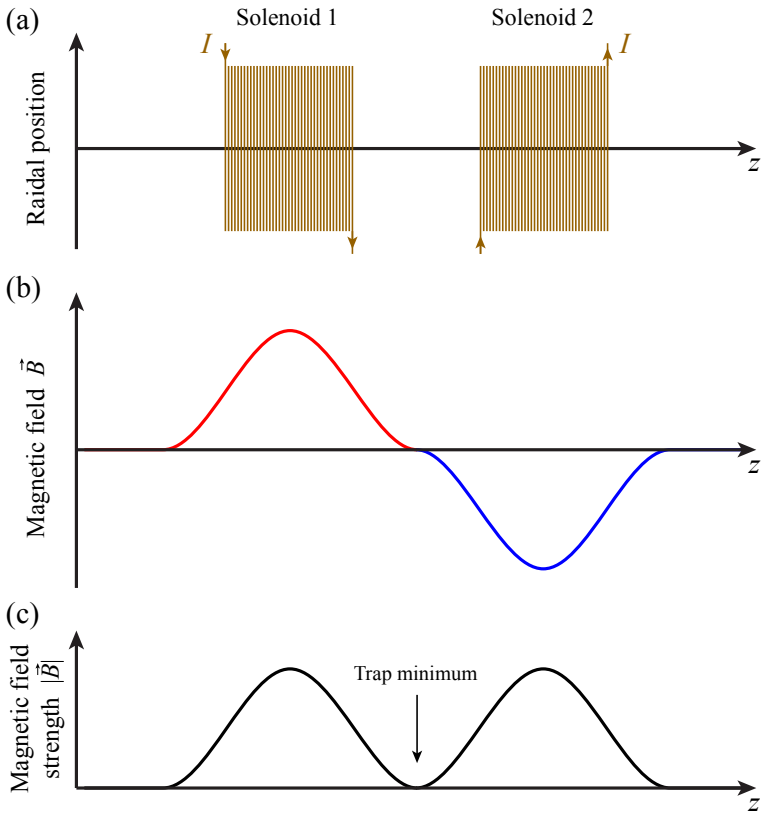

Figure 4.8: (a) Two co-axial solenoids in an anti-Helmholtz configuration with current, I, flowing in the opposite direction in each. (b) Schematic diagram of the the magnetic field on the axis of the two solenoids in (a). (c) The magnitude of the magnetic field in (b) with the three-dimensional trap minimum indicated.

solenoids with electrical current flowing in the opposite direction in each as indicated in Figure 4.8. The resulting magnetic field distribution has a zero-field point mid-way between the two solenoids around which cold atoms can be trapped. Such a configuration of current carrying solenoids is known as a *anti-Helmholtz configuration* and gives rise to a *quadrupole magnetic field distribution*.

When trapped in such a *magnetic quadrupole trap* after deceleration the atoms can continue to be laser cooled using six counterpropagating laser beams. In this way temperatures of the trapped atoms on the order of

$T \sim 1$ μK can be achieved, with approximately 10^8 atoms confined in a volume of ~ 1 mm^3.

From this point it is difficult to cool the atoms further using laser cooling techniques because of the momentum transfer that occurs following the photon recoil upon spontaneous emission. However, they can be further cooled by a technique known as *evaporative cooling*. This involves gradually lowering the depth of the magnetic trap to allow the fastest moving atoms to escape. The remaining atoms can then rethermalise by collisions to a lower temperature. In this way final temperatures in the range from 10^{-7} – 10^{-9} K (100 nK – 1 nK) can be achieved.

At these low temperatures the ultracold atoms can form a *Bose-Einstein Condensate* (BEC) in which, because the de Broglie wavelength of each of the atoms is large, the spatial wavefunctions of the atoms overlap and all atoms collect in the same quantum state of the magnetic trap.

Part II

Molecules

Chapter 5

Diatomic molecules

5.1 Introduction

Atoms rarely remain isolated. At sufficient density they are more likely to bind with each other to form molecules or solids. For example, a gas of H atoms will combine to form molecular hydrogen, H_2, and a gas of atomic nitrogen will combine to form N_2. Because of this, in the laboratory we cannot fill a gas cylinder with H or N atoms. The cylinders of gas that are used only contain H_2 or N_2 molecules. The exceptions to this are the rare gas atoms, He, Ne, Ar, Kr and Xe which are stable and unreactive because of their closed-shell electronic structure. These atoms do not readily form molecules at room temperature.

In molecules, as in atoms, the energy level structure is dominated by Coulomb interactions. However, in molecules the motion (vibrational and rotational) of the nuclei must also be considered. In the following we will treat the covalently bound diatomic molecular hydrogen cation, H_2^+, and the neutral hydrogen molecule, H_2, and its isotopomers, e.g., HD, D_2, HT, etc.... We will also discuss ionically bound diatomic molecules such as NaCl, LiF, HF, etc....

Simple diatomic molecules such as these are important in several areas of research including

i Precision spectroscopic tests of molecular quantum mechanics and fundamental physics

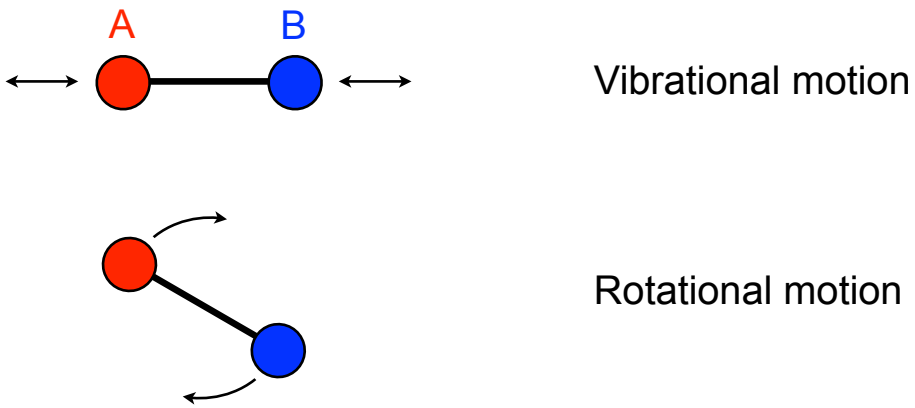

Figure 5.1: Schematic examples of the vibrational and rotational motion of a diatomic molecule AB.

ii Studies of simple chemical processes and dynamics

iii Atmospheric chemistry and sensing

iii Chemistry in the interstellar medium

Molecular spectra are in general more complicated than atomic spectra. This additional complexity arises from the quantised vibrational and rotational motion of the nuclei (see Figure 5.1) which must be considered in addition to the electronic structure.

5.1.1 Molecular Schrödinger equation

In a molecule with N nuclei of charge Z_N and mass M_N located at positions $\vec{R}_N$, and i electrons located at positions $\vec{r}_i$, the time-independent Schrödinger equation takes the form

$$\hat{H}\,\Psi(\vec{R}_1,\vec{R}_2,\ldots,\vec{R}_N;\vec{r}_1,\vec{r}_2,\ldots,\vec{r}_i) \quad = \quad E\,\Psi(\vec{R}_1,\vec{R}_2,\ldots,\vec{R}_N;\vec{r}_1,\vec{r}_2,\ldots,\vec{r}_i), \tag{5.1}$$

where $\Psi(\vec{R}_N;\vec{r}_i)$ is the total wavefunction of the system, and the Hamiltonian operator, $\hat{H}$, accounts for the kinetic energy of the nuclei, the kinetic energy

of the electrons and the total potential energy of the system.

$$\hat{H} = \hat{H}(\vec{R}_1, \vec{R}_2, \ldots, \vec{R}_N; \vec{r}_1, \vec{r}_2, \ldots, \vec{r}_i) \tag{5.2}$$

$$\begin{aligned} = & -\frac{\hbar^2}{2M_1}\nabla_1^2 - \frac{\hbar^2}{2M_2}\nabla_2^2 - \cdots - \frac{\hbar^2}{2M_N}\nabla_N^2 + \ldots \\ & -\frac{\hbar^2}{2m_e}\nabla_1^2 - \frac{\hbar^2}{2m_e}\nabla_2^2 - \cdots - \frac{\hbar^2}{2m_e}\nabla_i^2 + \ldots \\ & + \underbrace{V(\vec{R}_N; \vec{r}_i)}_{\text{Coulomb interactions}} \end{aligned} \tag{5.3}$$

$$= \sum_N \left[-\frac{\hbar^2}{2M_N}\nabla_N^2\right] + \sum_i \left[-\frac{\hbar^2}{2m_e}\nabla_i^2\right] + V(\vec{R}_N; \vec{r}_i). \tag{5.4}$$

The potential energy term is then the sum over the electron-electron Coulomb repulsion, the nucleus-nucleus Coulomb repulsion, and the electron-nucleus Coulomb attraction, i.e,

$$V(\vec{R}_N; \vec{r}_i) = \frac{e^2}{4\pi\epsilon_0}\left[\sum_{i>j}\frac{1}{|\vec{r}_i - \vec{r}_j|} + \sum_{N>M}\frac{Z_N Z_M}{|\vec{R}_N - \vec{R}_M|} - \sum_{N,i}\frac{Z_N}{|\vec{R}_N - \vec{r}_i|}\right]. \tag{5.5}$$

Because of the last term in this expression that represents the interaction between the electrons and the nuclei, it is in general not possible to simplify the molecular Schrödinger equation by separating the nuclear, $\nu(\vec{R}_N)$, and electronic, $\psi(\vec{r}_i)$, parts of the total wavefunction, i.e.,

$$\Psi(\vec{R}_N; \vec{r}_i) \neq \nu(\vec{R}_N)\,\psi(\vec{r}_i). \tag{5.6}$$

However, under certain conditions an approximation known as the *Born-Oppenheimer approximation* can be applied and this does allow a partial separation of nuclear and electronic motion.

5.2 Born-Oppenheimer approximation

The Born-Oppenheimer approximation is based on the notion that in general because the nuclei in a molecule are much heavier than the electrons,

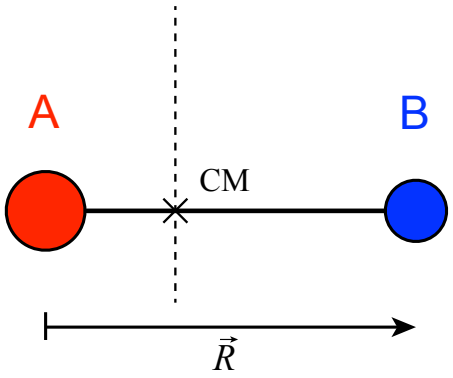

Figure 5.2: A diatomic molecule with the relative positions of nuclei A and B represented by the vector $\vec{R}$. CM is the center of mass of the molecule.

i.e.,

$$\frac{m_e}{M_N} \ll 1 \tag{5.7}$$

they move much more slowly than the electrons. Therefore for every change in the position of the nuclei the electrons can be considered to adjust their positions instantaneously. Taking this into account it is possible to express the total wavefunction of the system as a product of nuclear and electronic parts such that the electronic wavefunction depends on the instantaneous position of the nuclei but not on their motion.

Consider the diatomic molecule AB in Figure 5.2. For this system with a reduced nuclear mass, μ_{AB}, of

$$\mu_{AB} = \frac{M_A M_B}{M_A + M_B} \tag{5.8}$$

the Hamiltonian takes the form

$$\hat{H}(\vec{R};\vec{r}_i) = -\frac{\hbar^2}{2\mu_{AB}}\nabla_R^2 + \sum_i -\frac{\hbar^2}{2m_e}\nabla_i^2 + V(\vec{R};\vec{r}_i). \tag{5.9}$$

To this system the Born-Oppenheimer approximation can by applied in 6 steps.

1. First the nuclei must be fixed in space at a selected internuclear separation, i.e.,

$$\vec{R} = \text{const.} \tag{5.10}$$

In this situation the nuclear kinetic energy term in Equation 5.9,

$$-\frac{\hbar^2}{2\mu_{\mathrm{AB}}}\nabla_R^2 \tag{5.11}$$

can be neglected.

2. The Schrödinger equation can then be solved for the motion of the electrons in the field of the fixed nuclei.

$$\hat{H}_{\mathrm{elec}}\,\Psi(\vec{R};\,\vec{r}_i) \quad = \quad E_{\mathrm{elec}}\,\Psi(\vec{R};\,\vec{r}_i), \tag{5.12}$$

where

$$\hat{H}_{\mathrm{elec}} \quad = \quad \sum_i -\frac{\hbar^2}{2m_{\mathrm{e}}}\nabla_i^2 \quad + \quad V(\vec{R};\,\vec{r}_i), \tag{5.13}$$

is the electronic Hamiltonian, and E_{elec} are the electronic eigenenergies of the system. The solution to Equation 5.12 is then obtained for a range of different values of $\vec{R}$ giving a complete description of the electronic energies and wavefunctions in terms of the the internuclear separation.

3. The solution of the complete Hamiltonian of the molecule including nuclear motion is then assumed to take the form

$$\Psi(\vec{R};\,\vec{r}_i) \quad = \quad \nu(\vec{R})\,\psi(\vec{R};\,\vec{r}_i), \tag{5.14}$$

i.e., the nuclear part of the wavefunction depends only on the internuclear separation, and the electronic part depends on the internuclear separation and the positions of the electrons[1].

4. In this form the total wavefunction $\Psi(\vec{R};\,\vec{r}_i)$ is then inserted into the full Schrödinger equation including the nuclear kinetic energy term in Equation 5.11, i.e.,

$$\left[-\frac{\hbar^2}{2\mu_{\mathrm{AB}}}\nabla_R^2 + \sum_i -\frac{\hbar^2}{2m_{\mathrm{e}}}\nabla_i^2 + V(\vec{R};\,\vec{r}_i)\right]\nu(\vec{R})\,\psi(\vec{R};\,\vec{r}_i) \quad = \quad E\,\nu(\vec{R})\,\psi(\vec{R};\,\vec{r}_i) \tag{5.15}$$

[1]Note: This dependence of the nuclear and electronic parts of the total wavefunction on $\vec{R}$ and $\vec{r}_i$ is different to that in Equation 5.6.

5. Applying the nuclear kinetic energy operator to the total wavefunction in Equation 5.15 leads to

$$-\frac{\hbar^2}{2\mu_{\mathrm{AB}}}\nabla_R^2\,\Psi(\vec{R};\,\vec{r}_i) \;=\; -\frac{\hbar^2}{2\mu_{\mathrm{AB}}}\nabla_R^2\,\nu(\vec{R})\,\psi(\vec{R};\,\vec{r}_i) \tag{5.16}$$

$$\;=\; -\frac{\hbar^2}{2\mu_{\mathrm{AB}}}\left[\psi\nabla_R^2\nu + 2\nabla_R\nu\nabla_R\psi + \nu\nabla_R^2\psi\right], \tag{5.17}$$

where in this case $\nu = \nu(\vec{R})$ and $\psi = \psi(\vec{R};\,\vec{r}_i)$, and for the two functions ν and ψ

$$\begin{aligned}\nabla^2\,\nu\,\psi &= \nabla(\nabla\nu\,\psi)\\ &= \nabla(\psi\,\nabla\nu + \nu\,\nabla\psi)\\ &= \nabla\psi\,\nabla\nu + \psi\,\nabla^2\nu + \nabla\nu\,\nabla\psi + \nu\,\nabla^2\psi\\ &= \nu\,\nabla^2\psi + 2\,\nabla\nu\,\nabla\psi + \psi\,\nabla^2\nu\end{aligned} \tag{5.18}$$

The insight of Born and Oppenheimer[2] was that the electronic wavefunctions are insensitive to changes in the positions of the nuclei, i.e., the terms involving the gradients of ψ with respect to the nuclear coordinates, $\nabla_R\psi$ and $\nabla_R^2\psi$ in Equation 5.17, can be neglected in solving the problem. Therefore

$$-\frac{\hbar^2}{2\mu_{\mathrm{AB}}}\nabla_R^2\,\Psi(\vec{R};\,\vec{r}_i) \;=\; -\frac{\hbar^2}{2\mu_{\mathrm{AB}}}\,\psi(\vec{R};\,\vec{r}_i)\,\nabla_R^2\nu(\vec{R}) \tag{5.19}$$

5. Using this result (Equation 5.19) the total wavefunction given in Equation 5.15 can be simplified leading to

$$\psi(\vec{R};\,\vec{r}_i)\left[-\frac{\hbar^2}{2\mu_{\mathrm{AB}}}\nabla_R^2\,\nu(\vec{R})\right] + \overbrace{\left[\sum_i -\frac{\hbar^2}{2m_{\mathrm{e}}}\nabla_i^2 + V(\vec{R};\,\vec{r}_i)\right]}^{\Rightarrow\,\hat{H}_{\mathrm{elec}}(\vec{R};\vec{r}_i)\,\psi(\vec{R};\vec{r}_i)\;=\;E_{\mathrm{elec}}\,\psi(\vec{R};\vec{r}_i)}\nu(\vec{R})\,\psi(\vec{R};\,\vec{r}_i)$$
$$= E\,\nu(\vec{R})\,\psi(\vec{R};\,\vec{r}_i). \tag{5.20}$$

[2] M. Born and R. Oppenheimer, Zur Quantentheorie der Molekeln (On the quantum theory of molecules), *Annalen der Physik*, **389**, 457, (1927)

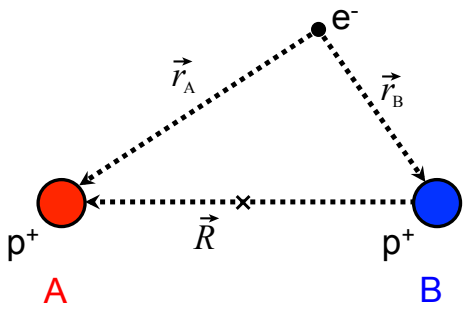

Figure 5.3: Coordinate system describing the molecular hydrogen cation H_2^+.

Since the second term in brackets, operating on the electronic part of the total wavefunction, gives the electronic energy, E_{elec}, of the system Equation 5.20 reduces to

$$\left[-\frac{\hbar^2}{2\mu_{AB}}\nabla_R^2 + E_{\text{elec}}(\vec{R})\right]\nu(\vec{R}) \quad = \quad E\,\nu(\vec{R}), \tag{5.21}$$

the Schrödinger equation for the nuclear motion. Hence, the electronic energies, $E_{\text{elec}}(\vec{R})$, act as the effective potential in which the nuclei move.

5.3 The molecular hydrogen cation H_2^+

To apply the Born-Oppenheimer approximation to a real system, consider the case of the molecular hydrogen cation H_2^+. This simple diatomic molecular ion is composed of two protons and one electron. In using the Born-Oppenheimer approximation it is necessary to solve two separate Schrödinger equations, (1) an electronic Schrödinger equation, and (2) a nuclear Schrödinger equation.

First the positions of the nuclei must be fixed, i.e., a constant value of $\vec{R}$ is selected and the electronic motion is treated. This leads to the electronic Hamiltonian

$$\hat{H}_{\text{elec}} \quad = \quad -\frac{\hbar^2}{2m_e}\nabla_r^2 - \frac{e^2}{4\pi\epsilon_0\, r_A} - \frac{e^2}{4\pi\epsilon_0\, r_B} + \frac{e^2}{4\pi\epsilon_0\, R}, \tag{5.22}$$

in the coordinate system indicated in Figure 5.3. In atomic units, where

$$e \;=\; m_{\rm e} \;=\; \hbar \;=\; 1, \tag{5.23}$$

this can be simplified to the form

$$\hat{H}_{\rm elec} \;=\; -\frac{\nabla_r^2}{2} - \frac{1}{r_{\rm A}} - \frac{1}{r_{\rm B}} + \frac{1}{R}. \tag{5.24}$$

The resulting electronic Schrödinger equation is therefore

$$\left(-\frac{\nabla_r^2}{2} - \frac{1}{r_{\rm A}} - \frac{1}{r_{\rm B}} + \frac{1}{R}\right)\psi(\vec{R};\vec{r}_{\rm A},\vec{r}_{\rm B}) \;=\; E_{\rm elec}\,\psi(\vec{R};\vec{r}_{\rm A},\vec{r}_{\rm B}) \tag{5.25}$$

5.3.1 H_2^+ wavefunctions

When $r_{\rm A}$ is small: the electron is close to proton A. The proton and electron at A appear as a neutral H atom while proton B is an isolated proton. In this case the electronic wavefunction for the ground state of the molecule reduces to that of a 1s orbital, ϕ_{1s}, centred upon proton A, i.e.,

$$\psi(\vec{R};\vec{r}_{\rm A},\vec{r}_{\rm B}) \;\longrightarrow\; \phi_{1s}(\vec{r}_{\rm A}) \;=\; \frac{1}{\sqrt{\pi\,a_0^3}}\,{\rm e}^{-r_{\rm A}/a_0}, \tag{5.26}$$

where a_0 is the Bohr radius (see Table 2.1 and Table 2.2).

When $r_{\rm B}$ is small: the electron is close to proton B and the electronic wavefunction for the ground state of the molecule reduces to that of a 1s orbital, ϕ_{1s}, centred upon proton B, i.e.,

$$\psi(\vec{R};\vec{r}_{\rm A},\vec{r}_{\rm B}) \;\longrightarrow\; \phi_{1s}(\vec{r}_{\rm B}) \;=\; \frac{1}{\sqrt{\pi\,a_0^3}}\,{\rm e}^{-r_{\rm B}/a_0}. \tag{5.27}$$

Between these two cases the total wavefunction is a superposition of the situation in which the electron is at proton A, and that in which the electron is at proton B, i.e.,

$$\psi(\vec{R};\vec{r}_{\rm A},\vec{r}_{\rm B}) \;\simeq\; C_1\,\phi_{1s}(\vec{r}_{\rm A}) + C_2\,\phi_{1s}(\vec{r}_{\rm B}), \tag{5.28}$$

where C_1 and C_2 are constants.

Since H_2^+ is a homonuclear diatomic molecule, i.e., it is composed of two identical nuclei, the probability of finding the electron at proton A has to be always equal to that of finding the electron at proton B. Therefore

$$|C_1|^2 \;=\; |C_2|^2 \;=\; |C|^2 \tag{5.29}$$

and the electronic wavefunction can therefore be symmetric, ψ_+, or anti-symmetric, ψ_-, with respect to exchange of A and B,

$$\psi_+ \;=\; C\left[\phi_{1s}(\vec{r}_A) + \phi_{1s}(\vec{r}_B)\right] \qquad \text{'symmetric'} \tag{5.30}$$

$$\psi_- \;=\; C\left[\phi_{1s}(\vec{r}_A) - \phi_{1s}(\vec{r}_B)\right] \qquad \text{'antisymmetric'} \tag{5.31}$$

The symmetry of molecular electronic wavefunctions of these kinds is labelled using the german words '*gerade*' and '*ungerade*',

$$\begin{aligned} \text{symmetric} &\equiv \text{'gerade'} \\ \text{antisymmetric} &\equiv \text{'ungerade'} \end{aligned}$$

and this approach to constructing molecular orbitals from superpositions of atomic orbitals is known as the LCAO method (LCAO ≡ Linear Combination of Atomic Orbitals).

The value of the constant C in Equation 5.30 and Equation 5.31 can be obtained by normalisation of the functions. This requires that

$$\int \left|\psi_\pm(\vec{r}_A, \vec{r}_B)\right|^2 \, dr_A \, dr_B \;=\; 1 \tag{5.32}$$

and therefore

$$C^2 \int \left[\phi_{1s}(\vec{r}_A) \pm \phi_{1s}(\vec{r}_B)\right]^* \left[\phi_{1s}(\vec{r}_A) \pm \phi_{1s}(\vec{r}_B)\right] dr_A \, dr_B \;=\; 1 \tag{5.33}$$

and so

$$\begin{aligned} C^2 \int \Big[&\phi_{1s}^*(\vec{r}_A)\phi_{1s}(\vec{r}_A) + \phi_{1s}^*(\vec{r}_B)\phi_{1s}(\vec{r}_B) + \ldots \\ &\pm \phi_{1s}^*(\vec{r}_A)\phi_{1s}(\vec{r}_B) \pm \phi_{1s}^*(\vec{r}_B)\phi_{1s}(\vec{r}_A)\Big] \, dr_A \, dr_B \;=\; 1 \end{aligned} \tag{5.34}$$

However, because the wavefunctions, $\phi_{1s}(\vec{r})$, associated with the atomic orbitals are normalised

$$\int \phi_{1s}^*(\vec{r}_A)\phi_{1s}(\vec{r}_A) \, dr_A \;=\; \int \phi_{1s}^*(\vec{r}_B)\phi_{1s}(\vec{r}_B) \, dr_B \;=\; 1. \tag{5.35}$$

If the *overlap integral*, $I(R)$, is defined as

$$I(R) = \int \phi_{1s}^{*}(\vec{r}_A)\phi_{1s}(\vec{r}_B)\,\mathrm{d}r_A\,\mathrm{d}r_B \tag{5.36}$$

$$= \int \phi_{1s}^{*}(\vec{r}_B)\phi_{1s}(\vec{r}_A)\,\mathrm{d}r_A\,\mathrm{d}r_B \tag{5.37}$$

the normalisation condition becomes

$$C^2\,[1 + 1 \pm 2I(R)] = 1, \tag{5.38}$$

so

$$C = \frac{1}{\sqrt{2\,[1 \pm I(R)]}}. \tag{5.39}$$

Therefore

(i) If

$$R \longrightarrow \infty \quad \Rightarrow \quad I(R) \longrightarrow 0 \tag{5.40}$$

because at large internuclear separations there is no overlap between the wavefunctions associated with the electron being at proton A and that at proton B, and

$$C = \frac{1}{\sqrt{2}} \tag{5.41}$$

(ii) If

$$R \longrightarrow 0 \quad \Rightarrow \quad I(R) \longrightarrow \pm 1 \tag{5.42}$$

because for small internuclear separations the wavefunctions associated with the electron being at proton A and that at proton B completely overlap, and

$$C = \frac{1}{2} \tag{5.43}$$

The resulting electronic wavefunctions for the H_2^+ molecular ion are displayed in Figure 5.4. From the electron probability distribution $|\psi_+|^2$ in this figure, it can be seen that the symmetric (gerade) state has electron

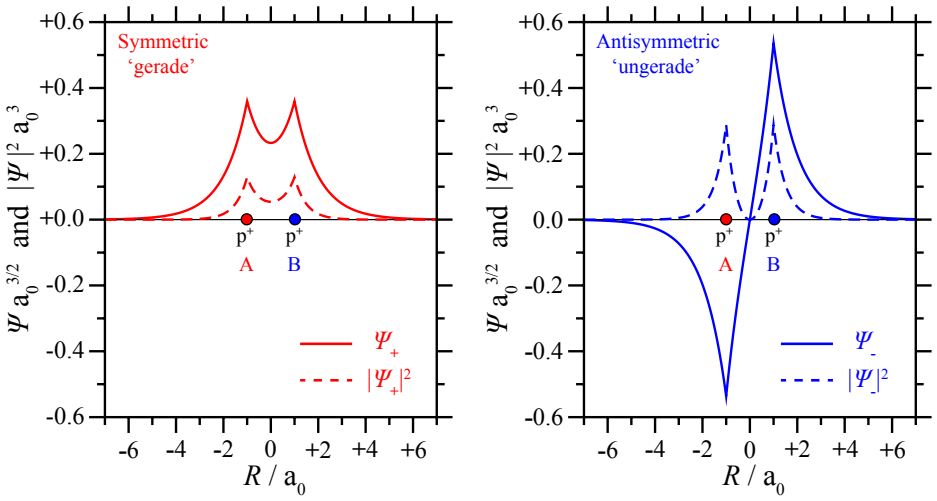

Figure 5.4: Gerade, ψ_+, and ungerade, ψ_-, electronic wavefunctions and electron probability distributions for the ground states of the molecular hydrogen cation H_2^+.

density between the two protons, A and B. This neutralises the proton-proton Coulomb repulsion leading to a stable molecular state in which the electron is shared between the two nuclei in a *covalent bond*. Because this state corresponds to a stable bound state of the molecule the corresponding molecular orbital is often known as a *bonding orbital*.

On the other hand, the antisymmetric ψ_- (ungerade) state exhibits a lower probability of finding the electron located between the two protons. As a result the proton-proton Coulomb repulsion is not compensated and pushes the two nuclei apart . Consequently in this state the molecule is unstable and breaks up, *dissociates*. The corresponding molecular orbital is therefore known as an *antibonding orbital*.

5.3.2 H_2^+ electronic energies

The electronic energies, $E_\pm(R)$, of the lowest-lying gerade and ungerade eigenstates of H_2^+ are given by

$$E_\pm(R) = \frac{\int \psi_\pm^* \hat{H}_{\text{elec}} \psi_\pm \, d\tau}{\int \psi_\pm^* \psi_\pm \, d\tau} \tag{5.44}$$

$$= \frac{A_\pm}{N_\pm} \equiv \frac{\text{expectation value of } \hat{H}_{\text{elec}}}{\text{normalisation constant}}. \tag{5.45}$$

By requiring that the correct normalisation of the wavefunctions as $R \longrightarrow \infty$ gives

$$\psi_\pm = \frac{1}{\sqrt{2}} \left[\phi_{1s}(\vec{r}_A) \pm \phi_{1s}(\vec{r}_B) \right]. \tag{5.46}$$

Therefore,

$$N_\pm = \frac{1}{2} \int \left[\phi_{1s}(\vec{r}_A) \pm \phi_{1s}(\vec{r}_B) \right]^* \left[\phi_{1s}(\vec{r}_A) \pm \phi_{1s}(\vec{r}_B) \right] d\tau \tag{5.47}$$

$$= \frac{1}{2} \left[1 + 1 \pm 2I(R) \right] \tag{5.48}$$

$$= 1 \pm I(R) \tag{5.49}$$

To calculate $A_\pm$,

$$A_\pm = \int \frac{1}{\sqrt{2}} \left[\phi_{1s}(\vec{r}_A) \pm \phi_{1s}(\vec{r}_B) \right]^* \hat{H}_{\text{elec}} \frac{1}{\sqrt{2}} \left[\phi_{1s}(\vec{r}_A) \pm \phi_{1s}(\vec{r}_B) \right] d\tau, \tag{5.50}$$

so therefore

$$\begin{aligned} A_\pm = {} & \frac{1}{2} \int \psi_{1s}^*(\vec{r}_A) \left[-\frac{\nabla_r^2}{2} - \frac{1}{r_A} - \frac{1}{r_B} + \frac{1}{R} \right] \psi_{1s}(\vec{r}_A) \, d\tau + \ldots \\ & \pm \frac{1}{2} \int \psi_{1s}^*(\vec{r}_A) \left[-\frac{\nabla_r^2}{2} - \frac{1}{r_A} - \frac{1}{r_B} + \frac{1}{R} \right] \psi_{1s}(\vec{r}_B) \, d\tau + \ldots \\ & + \frac{1}{2} \int \psi_{1s}^*(\vec{r}_B) \left[-\frac{\nabla_r^2}{2} - \frac{1}{r_A} - \frac{1}{r_B} + \frac{1}{R} \right] \psi_{1s}(\vec{r}_B) \, d\tau + \ldots \\ & \pm \frac{1}{2} \int \psi_{1s}^*(\vec{r}_B) \left[-\frac{\nabla_r^2}{2} - \frac{1}{r_A} - \frac{1}{r_B} + \frac{1}{R} \right] \psi_{1s}(\vec{r}_A) \, d\tau. \end{aligned} \tag{5.51}$$

However, in the H atom

$$\left[-\frac{\nabla_r^2}{2} - \frac{1}{r_A}\right]\psi_{1s}(\vec{r}_A) \;=\; E_{1s}\,\psi_{1s}(\vec{r}_A) \tag{5.52}$$

and

$$\left[-\frac{\nabla_r^2}{2} - \frac{1}{r_B}\right]\psi_{1s}(\vec{r}_B) \;=\; E_{1s}\,\psi_{1s}(\vec{r}_B), \tag{5.53}$$

with similar operators indicated in red and blue in Equation 5.51, therefore

$$\begin{aligned} A_\pm \;=\; & \frac{1}{2}\int \psi_{1s}^*(\vec{r}_A)\left[E_{1s} - \frac{1}{r_B} + \frac{1}{R}\right]\psi_{1s}(\vec{r}_A)\,d\tau + \ldots \\ & \pm\frac{1}{2}\int \psi_{1s}^*(\vec{r}_A)\left[E_{1s} - \frac{1}{r_A} + \frac{1}{R}\right]\psi_{1s}(\vec{r}_B)\,d\tau + \ldots \\ & +\frac{1}{2}\int \psi_{1s}^*(\vec{r}_B)\left[E_{1s} - \frac{1}{r_A} + \frac{1}{R}\right]\psi_{1s}(\vec{r}_B)\,d\tau + \ldots \\ & \pm\frac{1}{2}\int \psi_{1s}^*(\vec{r}_B)\left[E_{1s} - \frac{1}{r_B} + \frac{1}{R}\right]\psi_{1s}(\vec{r}_A)\,d\tau. \end{aligned} \tag{5.54}$$

which can be simplified to

$$\begin{aligned} A_\pm \;=\; \frac{1}{2}\Bigg[& E_{1s}\int \psi_{1s}^*(\vec{r}_A)\,\psi_{1s}(\vec{r}_A)\,d\tau + \int \psi_{1s}^*(\vec{r}_A)\left[-\frac{1}{r_B} + \frac{1}{R}\right]\psi_{1s}(\vec{r}_A)\,d\tau + \ldots \\ & \pm E_{1s}\int \psi_{1s}^*(\vec{r}_A)\,\psi_{1s}(\vec{r}_B)\,d\tau \pm \int \psi_{1s}^*(\vec{r}_A)\left[-\frac{1}{r_A} + \frac{1}{R}\right]\psi_{1s}(\vec{r}_B)\,d\tau + \ldots \\ & + E_{1s}\int \psi_{1s}^*(\vec{r}_B)\,\psi_{1s}(\vec{r}_B)\,d\tau + \int \psi_{1s}^*(\vec{r}_B)\left[-\frac{1}{r_A} + \frac{1}{R}\right]\psi_{1s}(\vec{r}_B)\,d\tau + \ldots \\ & \pm E_{1s}\int \psi_{1s}^*(\vec{r}_B)\,\psi_{1s}(\vec{r}_A)\,d\tau \pm \int \psi_{1s}^*(\vec{r}_B)\left[-\frac{1}{r_B} + \frac{1}{R}\right]\psi_{1s}(\vec{r}_A)\,d\tau\Bigg]. \end{aligned} \tag{5.55}$$

If the integrals of the form

$$J(R) \;=\; \int \psi_{1s}^*(\vec{r}_A)\,\frac{1}{r_B}\,\psi_{1s}(\vec{r}_A)\,d\tau \tag{5.56}$$

which represent the interaction of the electron charge close to proton A with

proton B are then defined as the *Coulomb integrals*, where[3]

$$J(R) \;=\; \frac{1}{R}\Big[1-(1+R)\,\mathrm{e}^{-2R}\Big]. \tag{5.57}$$

And integrals of the form

$$K(R) \;=\; \int \psi^{*}_{1\mathrm{s}}(\vec{r}_{\mathrm{A}})\,\frac{1}{r_{\mathrm{A}}}\,\psi_{1\mathrm{s}}(\vec{r}_{\mathrm{B}})\,\mathrm{d}\tau \tag{5.58}$$

which represent the exchange of the electron between the two nuclei are defined as the *exchange integrals*, where

$$K(R) \;=\; (1+R)\,\mathrm{e}^{-R}. \tag{5.59}$$

Then from Equation 5.55

$$\begin{aligned} A_{\pm} \;=\; \frac{1}{2}\Big[& E_{1\mathrm{s}} \;-\; J(R) \;+\; \frac{1}{R} \;+\ldots \\ & \pm\, E_{1\mathrm{s}}\, I(R) \;\mp\; K(R) \;\pm\; \frac{I(R)}{R} \;+\ldots \\ & +\, E_{1\mathrm{s}} \;-\; J(R) \;+\; \frac{1}{R} \;+\ldots \\ & \pm\, E_{1\mathrm{s}}\, I(R) \;\mp\; K(R) \;\pm\; \frac{I(R)}{R}\Big] \end{aligned} \tag{5.60}$$

$$= \;E_{1\mathrm{s}}\,[1 \;\pm\; I(R)] \;+\; \frac{[1 \;\pm\; I(R)]}{R} \;-\; J(R) \;\mp\; K(R). \tag{5.61}$$

Therefore

$$E_{\pm} \;=\; \frac{A_{\pm}}{N_{\pm}} \tag{5.62}$$

$$= \;E_{1\mathrm{s}} \;+\; \frac{1}{R} \;+\; \frac{-J(R) \;\mp\; K(R)}{1 \;\pm\; I(R)}. \tag{5.63}$$

The general dependence of energies of the two lowest lying electronic states of H_2^+ on the internuclear distance, R, are

[3] See, for example; *Physics of Atoms and Molecules*, B. H. Bransden and C. J. Joachain, Prentice Hall, 2nd Edition (2003)

(i) As $R \longrightarrow \infty$ the overlap, Coulomb and exchange integrals all tend towards zero because of their dependence on e^{-R}.

$$I(R), \quad J(R), \quad \text{and} \quad K(R) \quad \longrightarrow 0 \tag{5.64}$$

$$\Rightarrow \qquad E_- = E_+ = E_{1s} \tag{5.65}$$

(ii) When $R < \infty$ the correction to the energy that depends on the overlap, Coulomb and exchange integrals

$$\frac{-J(R) \mp K(R)}{1 \pm I(R)} \tag{5.66}$$

$\Rightarrow$ Lowers the energy of the gerade state, E_+.

$\Rightarrow$ Raises the energy of the ungerade state, E_-.

(iii) As $R \longrightarrow 0$ the energies of the gerade and ungerade states both tend towards infinity

$$E_\pm \quad \longrightarrow \quad \infty \tag{5.67}$$

because of the Coulomb repulsion between the positively charged nuclei.

(iv) The function, $E_+(R)$, associated with the gerade state, exhibits a minimum. This potential energy minimum corresponds to an internuclear separation for which a stable molecule can exist.

On the other hand, the function, $E_-(R)$, associated with the ungerade state, lies higher than the energy of the separated atoms for all internuclear separations and does not exhibit a minimum. This potential energy curve therefore indicates that a stable molecule cannot form in the antisymmetric state. If excited to this state, the molecule will fall apart, *dissociate*.

These features of the $E_\pm(R)$ functions can be seen in Figure 5.5 in which the results obtained using the orbital approximation described above (continuous curve) are displayed together with the results of an exact calculation of the $E_+(R)$ function (dashed curve). Also indicated in this figure are the equilibrium internuclear distance, R_e, for which the molecule is stable when

in the gerade state, and the dissociation energy, D_e, of this state. This equilibrium dissociation energy is the energy difference between the potential energy minimum at R_e and the energy of the separated atoms.

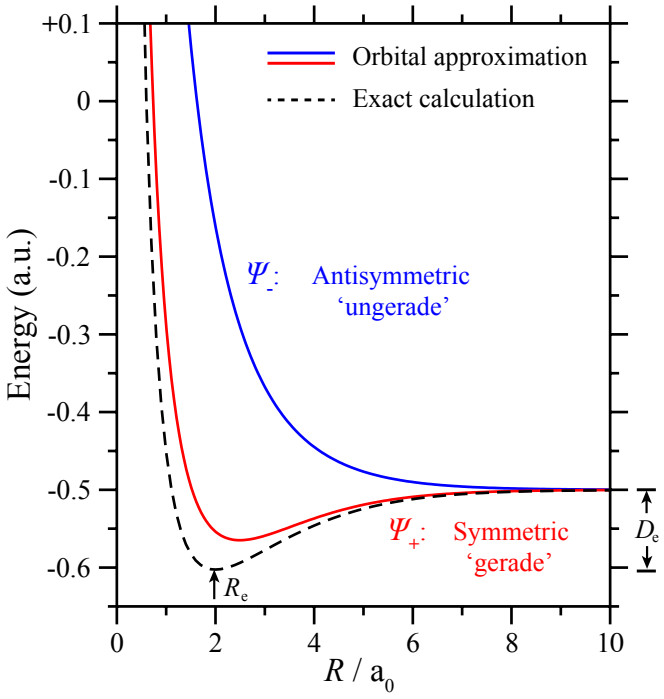

Figure 5.5: Gerade, ψ_+, and ungerade, ψ_-, electronic potential energy functions for the ground states of the molecular hydrogen cation H_2^+. The continuous lines represent the energies obtained using the procedure described here, while the dashed curve is the result of an exact calculation[4]. Also indicated are the equilibrium internuclear distance, R_e, and the dissociation energy, D_e, corresponding to the dashed curve.

[4]W. Kolos, Some Accurate Results for Three Particle Systems, *Act. Phys. Acad. Sci. Hung.*, **27**, 241 (1969).

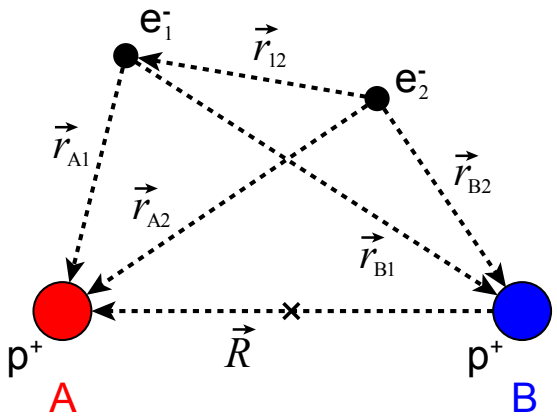

Figure 5.6: Coordinate system describing the neutral hydrogen molecule, H_2. The two protons are labelled by the letters A and B, while the two electrons are labelled by the numbers 1 and 2.

5.4 The neutral hydrogen molecule H_2

The neutral hydrogen molecule, H_2, is the simplest neutral molecule. As in the case of H_2^+;

- The energy level structure of H_2 can be calculated by first determining the electronic wavefunctions and energy eigenvalues within the Born-Oppenheimer approximation
- The H_2 molecule exhibits a covalent bond in which the electrons are shared between the nuclei

However, unlike H_2^+

- Because H_2 contains two electrons, the total wavefunctions must satisfy the Pauli principle and be antisymmetric with respect to exchange of the electrons.

Using the system of coordinates indicated in Figure 5.6, the electronic Hamiltonian for H_2 can be expressed in atomic units as

$$\hat{H}_{\text{elec}} = \underbrace{-\frac{\nabla_1^2}{2} - \frac{\nabla_2^2}{2}}_{\text{e}^- \text{ K. E.}} \underbrace{- \frac{1}{r_{A1}} - \frac{1}{r_{A2}} - \frac{1}{r_{B1}} - \frac{1}{r_{B2}}}_{\text{p}^+ - \text{e}^- \text{ attraction}} + \underbrace{\frac{1}{r_{12}} + \frac{1}{R}}_{\text{repulsion}} \tag{5.68}$$

5.4.1 H_2 electronic wavefunctions

In the case of H_2, the wavefunctions representing the molecule must account for the spin of the electrons. Therefore the total electronic wavefunction, $\psi^{S,T}$, takes the form

$$\psi^{S,T} = \psi(\vec{R};\vec{r}_i)\,\chi^{S,T}, \tag{5.69}$$

where $\psi(\vec{R};\vec{r}_i)$ is the electronic wavefunction without spin, and $\chi^{S,T}$ are the singlet ('S' $\Rightarrow S=0$) and triplet ('T' $\Rightarrow S=1$) two-electron spin wavefunctions (see Section 3.4.1).

To satisfy the Pauli principle the total electronic wavefunctions, $\psi^{S,T}$, must be antisymmetric with respect to exchange of the two electrons. Therefore

- If $\psi(\vec{R};\vec{r}_i)$ is antisymmetric with respect to exchange, the spin part of the wavefunction must be symmetric, i.e., χ^{T}
- If $\psi(\vec{R};\vec{r}_i)$ is symmetric with respect to exchange, the spin part of the wavefunction must be antisymmetric, i.e., χ^{S}

As in the case of H_2^+, the electronic wavefunctions associated with the lowest-lying eigenstates of H_2 can be constructed from atomic orbitals. Considering the 1s orbitals of the H atom, $\phi_{1s}(\vec{r})$, the electronic wavefunctions of the two lowest energy states of H_2 are

$$\psi^{T} = \frac{1}{\sqrt{2}}\left[\phi_{1s}(\vec{r}_{A1})\,\phi_{1s}(\vec{r}_{B2}) - \phi_{1s}(\vec{r}_{A2})\,\phi_{1s}(\vec{r}_{B1})\right]\chi^{T} \tag{5.70}$$

and

$$\psi^{S} = \frac{1}{\sqrt{2}}\left[\phi_{1s}(\vec{r}_{A1})\,\phi_{1s}(\vec{r}_{B2}) + \phi_{1s}(\vec{r}_{A2})\,\phi_{1s}(\vec{r}_{B1})\right]\chi^{S}, \tag{5.71}$$

where $\phi_{1s}(\vec{r}_{A1})$ corresponds to electron 1 at proton A etc. . . and the factor of $1/\sqrt{2}$ in this expression ensures that the wavefunction is normalised at large internuclear separations, i.e., when $R \to \infty$. At smaller internuclear separations the wavefunction must be renormalised. The spatial part of the function ψ^{T} is antisymmetric with respect to exchange of the two electrons, and the spin part of the wavefunction is therefore symmetric. On the

other hand the spatial part of the function ψ^{S} is symmetric with respect to exchange and the spin part is therefore antisymmetric.

The determine the energies, $E_{\pm}(R)$, of these lowest energy eigenstates of H_2, where

$$E_{+}(R) \quad \Rightarrow \quad \psi^{\mathrm{S}} \equiv \psi^{+} \tag{5.72}$$

$$E_{-}(R) \quad \Rightarrow \quad \psi^{\mathrm{T}} \equiv \psi^{-} \tag{5.73}$$

the expectation value of the normalised electronic Hamiltonian must be calculated for a range of internuclear separations, i.e.,

$$E_{\pm}(R) = \frac{\int \psi^{\mathrm{S,T}^*} \hat{H}_{\mathrm{elec}} \, \psi^{\mathrm{S,T}} \, \mathrm{d}\tau}{\int \psi^{\mathrm{S,T}^*} \psi^{\mathrm{S,T}} \, \mathrm{d}\tau} \tag{5.74}$$

$$= \frac{A_{\pm}(R)}{N_{\pm}(R)} \tag{5.75}$$

$$\equiv \frac{\text{expectation value of } \hat{H}_{\mathrm{elec}}}{\text{normalisation factor}}. \tag{5.76}$$

The expectation value, $A_{\pm}$, of the electronic Hamiltonian, $\hat{H}_{\mathrm{elec}}$, can be written explicitly as

$$A_{\pm} = \frac{1}{2} \int \left[\phi_{1\mathrm{s}}(\vec{r}_{\mathrm{A1}}) \, \phi_{1\mathrm{s}}(\vec{r}_{\mathrm{B2}}) \pm \phi_{1\mathrm{s}}(\vec{r}_{\mathrm{A2}}) \, \phi_{1\mathrm{s}}(\vec{r}_{\mathrm{B1}})\right]^* \hat{H}_{\mathrm{el}} \times \left[\phi_{1\mathrm{s}}(\vec{r}_{\mathrm{A1}}) \, \phi_{1\mathrm{s}}(\vec{r}_{\mathrm{B2}}) \pm \phi_{1\mathrm{s}}(\vec{r}_{\mathrm{A2}}) \, \phi_{1\mathrm{s}}(\vec{r}_{\mathrm{B1}})\right] \mathrm{d}\tau \tag{5.77}$$

$$\begin{aligned} = \frac{1}{2} \Bigg[& \int \phi^*_{1\mathrm{s}}(\vec{r}_{\mathrm{A1}}) \, \phi^*_{1\mathrm{s}}(\vec{r}_{\mathrm{B2}}) \, \hat{H}_{\mathrm{elec}} \, \phi_{1\mathrm{s}}(\vec{r}_{\mathrm{A1}}) \, \phi_{1\mathrm{s}}(\vec{r}_{\mathrm{B2}}) \, \mathrm{d}\tau \\ & + \int \phi^*_{1\mathrm{s}}(\vec{r}_{\mathrm{A2}}) \, \phi^*_{1\mathrm{s}}(\vec{r}_{\mathrm{B1}}) \, \hat{H}_{\mathrm{elec}} \, \phi_{1\mathrm{s}}(\vec{r}_{\mathrm{A2}}) \, \phi_{1\mathrm{s}}(\vec{r}_{\mathrm{B1}}) \, \mathrm{d}\tau \\ & \pm \int \phi^*_{1\mathrm{s}}(\vec{r}_{\mathrm{A1}}) \, \phi^*_{1\mathrm{s}}(\vec{r}_{\mathrm{B2}}) \, \hat{H}_{\mathrm{elec}} \, \phi_{1\mathrm{s}}(\vec{r}_{\mathrm{A2}}) \, \phi_{1\mathrm{s}}(\vec{r}_{\mathrm{B1}}) \, \mathrm{d}\tau \\ & \pm \int \phi^*_{1\mathrm{s}}(\vec{r}_{\mathrm{A2}}) \, \phi^*_{1\mathrm{s}}(\vec{r}_{\mathrm{B1}}) \, \hat{H}_{\mathrm{elec}} \, \phi_{1\mathrm{s}}(\vec{r}_{\mathrm{A1}}) \, \phi_{1\mathrm{s}}(\vec{r}_{\mathrm{B2}}) \, \mathrm{d}\tau \Bigg]. \end{aligned} \tag{5.78}$$

The integrals in Equation 5.78 can be solved one line at a time for the electronic Hamiltonian in Equation 5.68 in the following way:

Line 1:

$$\int \phi^*_{1\mathrm{s}}(\vec{r}_{\mathrm{A1}}) \, \phi^*_{1\mathrm{s}}(\vec{r}_{\mathrm{B2}}) \left(-\frac{\nabla_1^2}{2} - \frac{\nabla_2^2}{2} - \frac{1}{r_{\mathrm{A1}}} - \frac{1}{r_{\mathrm{B1}}} - \frac{1}{r_{\mathrm{A2}}} - \frac{1}{r_{\mathrm{B2}}} + \frac{1}{R} + \frac{1}{r_{12}} \right) \phi_{1\mathrm{s}}(\vec{r}_{\mathrm{A1}}) \, \phi_{1\mathrm{s}}(\vec{r}_{\mathrm{B2}}) \, \mathrm{d}\tau$$

(5.79)

The $-\frac{\nabla_1^2}{2}-\frac{1}{r_{A1}}$ and $-\frac{\nabla_2^2}{2}-\frac{1}{r_{B2}}$ terms highlighted in red and blue in Equation 5.79 correspond to the Hamiltonian of the H atom. As a result each of these pairs of terms contribute an energy

$$E_{1s}\int \phi_{1s}^*(\vec{r}_{A1})\,\phi_{1s}^*(\vec{r}_{B2})\,\phi_{1s}(\vec{r}_{A1})\,\phi_{1s}(\vec{r}_{B2})\,d\tau \quad = \quad E_{1s}, \tag{5.80}$$

where E_{1s} is the energy of a H atom in the 1s orbital, to the H_2 molecule. Therefore Equation 5.79 can be simplified to

$$\Rightarrow E_{1s}+E_{1s}+\int\phi_{1s}^*(\vec{r}_{A1})\,\phi_{1s}^*(\vec{r}_{B2})\left(-\frac{1}{r_{B1}}-\frac{1}{r_{A2}}+\frac{1}{R}+\frac{1}{r_{12}}\right)\phi_{1s}(\vec{r}_{A1})\,\phi_{1s}(\vec{r}_{B2})\,d\tau \tag{5.81}$$

$$= \quad E_{1s}+E_{1s}+\frac{1}{R}\int \phi_{1s}^*(\vec{r}_{A1})\,\phi_{1s}(\vec{r}_{A1})\,\phi_{1s}(\vec{r}_{B2})^*\,\phi_{1s}(\vec{r}_{B2})\,d\tau$$
$$+\int \phi_{1s}^*(\vec{r}_{A1})\,\phi_{1s}^*(\vec{r}_{B2})\left(-\frac{1}{r_{B1}}-\frac{1}{r_{A2}}+\frac{1}{r_{12}}\right)\phi_{1s}(\vec{r}_{A1})\,\phi_{1s}(\vec{r}_{B2})\,d\tau \tag{5.82}$$

$$= \quad 2E_{1s}+\frac{1}{R}+J(R) \tag{5.83}$$

where

$$J(R) \quad = \quad \int \phi_{1s}^*(\vec{r}_{A1})\,\phi_{1s}^*(\vec{r}_{B2})\left(-\frac{1}{r_{B1}}-\frac{1}{r_{A2}}+\frac{1}{r_{12}}\right)\phi_{1s}(\vec{r}_{A1})\,\phi_{1s}(\vec{r}_{B2})\,d\tau \tag{5.84}$$

is a *Coulomb integral* representing the interaction of electron 1, in the 1s orbital around proton A, with proton B and with electron 2 in the 1s orbital around it.

Line 2:

$$\int \phi_{1s}^*(\vec{r}_{A2})\,\phi_{1s}^*(\vec{r}_{B1})\left(-\frac{\nabla_1^2}{2}-\frac{\nabla_2^2}{2}-\frac{1}{r_{A1}}-\frac{1}{r_{B1}}-\frac{1}{r_{A2}}-\frac{1}{r_{B2}}+\frac{1}{R}+\frac{1}{r_{12}}\right)\phi_{1s}(\vec{r}_{A2})\,\phi_{1s}(\vec{r}_{B1})\,d\tau \tag{5.85}$$

is equivalent to Equation 5.79 but with the electron labels changed. It therefore results in a equivalent contribution to the electronic energy of the molecule

$$= \quad 2E_{1s}+\frac{1}{R}+J(R). \tag{5.86}$$

Line 3:

$$\int \phi_{1s}^*(\vec{r}_{A1})\,\phi_{1s}^*(\vec{r}_{B2})\left(-\frac{\nabla_1^2}{2}-\frac{\nabla_2^2}{2}-\frac{1}{r_{A1}}-\frac{1}{r_{B1}}-\frac{1}{r_{A2}}-\frac{1}{r_{B2}}+\frac{1}{R}+\frac{1}{r_{12}}\right)\phi_{1s}(\vec{r}_{A2})\,\phi_{1s}(\vec{r}_{B1})\,d\tau \tag{5.87}$$

As in Equation 5.79, the $-\frac{\nabla_1^2}{2}-\frac{1}{r_{B1}}$ and $-\frac{\nabla_2^2}{2}-\frac{1}{r_{A2}}$ terms highlighted in red and blue in Equation 5.87 correspond to the Hamiltonian of the H atom. As a result each of these pairs of terms contribute an energy

$$E_{1s}\int \phi_{1s}^*(\vec{r}_{A1})\,\phi_{1s}^*(\vec{r}_{B2})\,\phi_{1s}(\vec{r}_{A2})\,\phi_{1s}(\vec{r}_{B1})\,d\tau \quad = \quad E_{1s}\,I(R)^2 \tag{5.88}$$

where

$$I(R) \quad = \quad \int \phi_{1s}^*(\vec{r}_{A1})\,\phi_{1s}(\vec{r}_{B1})\,dr_1 \tag{5.89}$$

$$= \quad \int \phi_{1s}^*(\vec{r}_{B2})\,\phi_{1s}(\vec{r}_{A2})\,dr_2 \tag{5.90}$$

is an *overlap integral*, and E_{1s} is the energy of a H atom in the 1s state. Therefore Equation 5.87 can be simplified to

$$\Rightarrow \pm\Big[E_{1s}I(R)^2 + E_{1s}I(R)^2 + \int \phi_{1s}^*(\vec{r}_{A1})\,\phi_{1s}^*(\vec{r}_{B2})\left(-\frac{1}{r_{A1}}-\frac{1}{r_{B2}}+\frac{1}{R}+\frac{1}{r_{12}}\right)\phi_{1s}(\vec{r}_{A2})\,\phi_{1s}(\vec{r}_{B1})\,d\tau\Big] \tag{5.91}$$

$$= \pm\Big[E_{1s}I(R)^2 + E_{1s}I(R)^2 + \frac{1}{R}\int \phi_{1s}^*(\vec{r}_{A1})\,\phi_{1s}(\vec{r}_{B1})\,\phi_{1s}(\vec{r}_{B2})^*\,\phi_{1s}(\vec{r}_{A2})\,d\tau + \int \phi_{1s}^*(\vec{r}_{A1})\,\phi_{1s}^*(\vec{r}_{B2})\left(-\frac{1}{r_{A1}}-\frac{1}{r_{B2}}+\frac{1}{r_{12}}\right)\phi_{1s}(\vec{r}_{A2})\,\phi_{1s}(\vec{r}_{B1})\,d\tau\Big] \tag{5.92}$$

$$= \pm\left(2E_{1s}+\frac{1}{R}\right)I(R)^2 \quad \pm \quad K(R) \tag{5.93}$$

where

$$K(R) \quad = \quad \int \phi_{1s}^*(\vec{r}_{A1})\,\phi_{1s}^*(\vec{r}_{B2})\left(-\frac{1}{r_{A1}}-\frac{1}{r_{B2}}+\frac{1}{r_{12}}\right)\phi_{1s}(\vec{r}_{A2})\,\phi_{1s}(\vec{r}_{B1})\,d\tau \tag{5.94}$$

is an *exchange integral* representing the exchange of the electrons between the two protons.

Line 4:

$$\int \phi^*_{1s}(\vec{r}_{A2})\,\phi^*_{1s}(\vec{r}_{B1})\left(-\frac{\nabla_1^2}{2}-\frac{\nabla_2^2}{2}-\frac{1}{r_{A1}}-\frac{1}{r_{B1}}-\frac{1}{r_{A2}}-\frac{1}{r_{B2}}+\frac{1}{R}+\frac{1}{r_{12}}\right)\phi_{1s}(\vec{r}_{A1})\,\phi_{1s}(\vec{r}_{B2})\,d\tau \tag{5.95}$$

is equivalent to Equation 5.87 but with the electron labels changed. It therefore results in a equivalent contribution to the electronic energy of the molecule

$$= \pm\left(2E_{1s}+\frac{1}{R}\right)I(R)^2 \pm K(R). \tag{5.96}$$

Combining each of these results, Equation 5.78 becomes

$$\begin{aligned} A_\pm = \frac{1}{2}\Big[& 2E_{1s} + \frac{1}{R} + J(R) \\ & +2E_{1s} + \frac{1}{R} + J(R) \\ & \pm(2E_{1s}+\frac{1}{R})\,I(R)^2 \pm K(R) \\ & \pm(2E_{1s}+\frac{1}{R})\,I(R)^2 \pm K(R)\Big] \end{aligned} \tag{5.97}$$

$$= \left(2E_{1s}+\frac{1}{R}\right) \pm \left(2E_{1s}+\frac{1}{R}\right)I(R)^2 + J(R) \pm K(R) \tag{5.98}$$

$$= \left(2E_{1s}+\frac{1}{R}\right)\left(1 \pm I(R)^2\right) + J(R) \pm K(R) \tag{5.99}$$

Returning to Equation 5.75, the normalisation factor, $N_\pm$, can be written

explicitly as

$$N_\pm = \frac{1}{2}\int \left[\phi_{1s}(\vec{r}_{A1})\,\phi_{1s}(\vec{r}_{B2}) \pm \phi_{1s}(\vec{r}_{A2})\,\phi_{1s}(\vec{r}_{B1})\right]^* \times \left[\phi_{1s}(\vec{r}_{A1})\,\phi_{1s}(\vec{r}_{B2}) \pm \phi_{1s}(\vec{r}_{A2})\,\phi_{1s}(\vec{r}_{B1})\right] \mathrm{d}\tau \quad (5.100)$$

$$= \frac{1}{2}\Bigg[\int \phi^*_{1s}(\vec{r}_{A1})\,\phi^*_{1s}(\vec{r}_{B2})\,\phi_{1s}(\vec{r}_{A1})\,\phi_{1s}(\vec{r}_{B2})\,\mathrm{d}r_1\mathrm{d}r_2 + \int \phi^*_{1s}(\vec{r}_{A2})\,\phi^*_{1s}(\vec{r}_{B1})\,\phi_{1s}(\vec{r}_{A2})\,\phi_{1s}(\vec{r}_{B1})\,\mathrm{d}r_1\mathrm{d}r_2 \pm \int \phi^*_{1s}(\vec{r}_{A1})\,\phi^*_{1s}(\vec{r}_{B2})\,\phi_{1s}(\vec{r}_{A2})\,\phi_{1s}(\vec{r}_{B1})\,\mathrm{d}r_1\mathrm{d}r_2 \pm \int \phi^*_{1s}(\vec{r}_{A2})\,\phi^*_{1s}(\vec{r}_{B1})\,\phi_{1s}(\vec{r}_{A1})\,\phi_{1s}(\vec{r}_{B2})\,\mathrm{d}r_1\mathrm{d}r_2\Bigg] \quad (5.101)$$

This can be rearranged to give

$$N_\pm = \frac{1}{2}\Bigg[\int \phi^*_{1s}(\vec{r}_{A1})\,\phi_{1s}(\vec{r}_{A1})\,\mathrm{d}r_1 \int \phi^*_{1s}(\vec{r}_{B2})\,\phi_{1s}(\vec{r}_{B2})\,\mathrm{d}r_2 + \int \phi^*_{1s}(\vec{r}_{A2})\,\phi_{1s}(\vec{r}_{A2})\,\mathrm{d}r_2 \int \phi^*_{1s}(\vec{r}_{B1})\,\phi_{1s}(\vec{r}_{B1})\,\mathrm{d}r_1 \pm \int \phi^*_{1s}(\vec{r}_{A1})\,\phi_{1s}(\vec{r}_{B1})\,\mathrm{d}r_1 \int \phi^*_{1s}(\vec{r}_{B2})\,\phi_{1s}(\vec{r}_{A2})\,\mathrm{d}r_2 \pm \int \phi^*_{1s}(\vec{r}_{A2})\,\phi_{1s}(\vec{r}_{B2})\,\mathrm{d}r_2 \int \phi^*_{1s}(\vec{r}_{B1})\,\phi_{1s}(\vec{r}_{A1})\,\mathrm{d}r_1\Bigg] \quad (5.102)$$

which contains integrals over the square of individual wavefunctions

$$\int \phi^*_{1s}(\vec{r}_{N,i})\,\phi_{1s}(\vec{r}_{N,i})\,\mathrm{d}r_i = 1 \quad (5.103)$$

and overlap integrals

$$\int \phi^*_{1s}(\vec{r}_{N,i})\,\phi_{1s}(\vec{r}_{M,i})\,\mathrm{d}r_i = I(R) \quad (5.104)$$

with the nuclei A and B labelled M and N and the electrons $i = 1, 2$. Inserting these values into Equation (5.102) leads to

$$N_\pm = \frac{1}{2}\left[1 \cdot 1 + 1 \cdot 1 \pm I(R) \cdot I(R) \pm I(R) \cdot I(R)\right] \quad (5.105)$$

$$= 1 \pm I(R)^2 \quad (5.106)$$

Finally, inserting the results in Equation 5.106 and Equation 5.99 into Equation 5.75 leads to

$$E_{\pm} = \frac{\left(2E_{1s} + \frac{1}{R}\right)\left(1 \pm I(R)^2\right) + J(R) \pm K(R)}{1 \pm I(R)^2} \tag{5.107}$$

$$= 2E_{1s} + \frac{1}{R} + \frac{J(R)}{1 \pm I(R)^2} \pm \frac{K(R)}{1 \pm I(R)^2} \tag{5.108}$$

The overlap, $I(R)$, Coulomb, $J(R)$, and exchange, $K(R)$, integrals in this expression have the following dependence on the internuclear distance R:

- Overlap integral, $I(R)$: Because the wavefunctions associated with the $\phi_{1s}(\vec{r})$ atomic orbital are normalised, the overlap integral

$$I(R) = \int \phi^*_{1s}(\vec{r}_{N,i})\,\phi^*_{1s}(\vec{r}_{N,i})\,\mathrm{d}\tau \tag{5.109}$$

$$< 1 \tag{5.110}$$

  for all values of R. Therefore in Equation 5.108

$$1 \pm I(R)^2 > 0. \tag{5.111}$$

- Coulomb integral, $J(R)$: In general

$$J(R) > 0 \tag{5.112}$$

  for all values of R.

- Exchange integral, $K(R)$: In general

$$K(R) < 0 \tag{5.113}$$

  for all values of R.

Therefore based upon these considerations and Equation 5.108,

- The state ψ^{S} with energy E_+ is shifted to lower energy by the corrections associated with the overlap, Coulomb and exchange integrals.

- The state ψ^{T} with energy E_- is shifted to higher energy by the corrections associated with the overlap, Coulomb and exchange integrals.

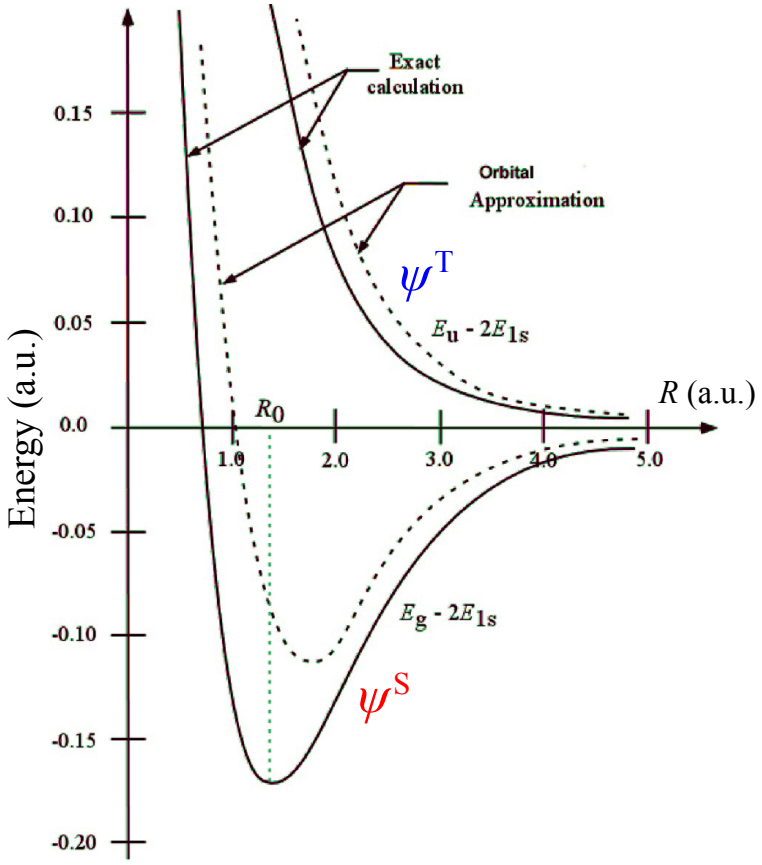

Figure 5.7: Gerade, ψ^T, and ungerade, ψ^T, electronic potential energy functions for the ground states of the neutral hydrogen molecule H_2. The continuous curves represent the results obtained using the procedure described above, while the dashed curves are the results of exact calculations.

The dependence of the energies of these two states on the internuclear distance can be seen in Figure 5.7.

The most important factor for the stability of a molecule is that the bonding electrons neutralise the mutual Coulomb repulsion of the nuclei, i.e., cancel the effective of the repulsive $1/R$ term in the Hamiltonian (Equation 5.68). The molecules formed are more stable if there is a significant probability that the electrons are located in the region between the two nuclei.

In the triplet state, ψ^{T}, the two electrons keep away from each other because the spatial part of the electronic wavefunction is antisymmetric with respect to exchange. Consequently, a stable molecule cannot be formed in this state.

In the singlet state, ψ^{S}, the probability of finding the electrons located between the two nuclei is non-zero because the spatial part of the electronic wavefunction is symmetric with respect to exchange of the two electrons. As can be seen in Figure 5.7 this leads to a minimum in the electronic energy at an internuclear separation of $R \simeq 1.4\, a_0$ about which a stable molecule is formed.

5.4.2 Molecular orbitals

The singlet, ψ^{S}, and triplet, ψ^{T}, wavefunctions (Equation 5.71 and Equation 5.71) associated with the two lowest energy eigenstates of H_2 cannot be expressed directly as a product of one-electron atomic orbitals. However, they can be defined in terms of the one-electron molecular orbitals of H_2^+ (see Section 5.3.1). The wavefunctions associated with these one-electron molecular orbitals are

$$1\sigma_{\mathrm{g}} \;=\; \psi_{+} \;=\; \frac{1}{\sqrt{2}}\left[\phi_{1\mathrm{s}}(\vec{r}_{\mathrm{A}}) + \phi_{1\mathrm{s}}(\vec{r}_{\mathrm{B}})\right] \tag{5.114}$$

$$1\sigma_{\mathrm{u}} \;=\; \psi_{-} \;=\; \frac{1}{\sqrt{2}}\left[\phi_{1\mathrm{s}}(\vec{r}_{\mathrm{A}}) - \phi_{1\mathrm{s}}(\vec{r}_{\mathrm{B}})\right], \tag{5.115}$$

where $1\sigma_{\mathrm{g}}$ and $1\sigma_{\mathrm{u}}$ denote the symmetric 'gerade' and antisymmetric 'ungerade', one-electron orbitals with principal quantum number $n = 1$, and zero electronic angular momentum. This is the molecular analog of the

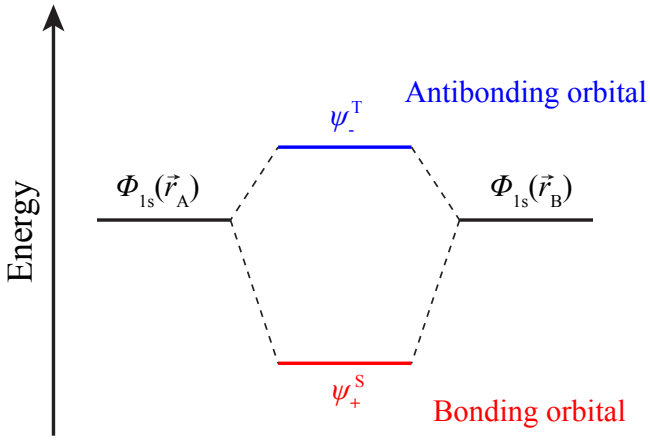

Figure 5.8: Schematic diagram of the singlet (bonding), and triplet (antibonding) orbitals of H_2 at large large internuclear separation (outer energy levels) and at $R = R_e$.

labelling of atomic orbitals as 1s, 2p, ... Using this notation, the ground ψ^S state of H_2 is denoted

$$1\sigma_g^2 \tag{5.116}$$

while the excited ψ^T state is denoted

$$1\sigma_g\, 1\sigma_u. \tag{5.117}$$

A simplified schematic diagram of the formation of these orbitals at large internuclear separation and at $R = R_e$ can be seen in Figure 5.8. Because the singlet state, which is in general shifted to lower energy in the molecular bond and corresponds to the stable molecular orbital ψ^S, it is known as a *bonding orbital*. On the other hand, because it the triplet state is shifted to higher energy for all internuclear distances and corresponds to a purely repulsive molecular potential, ψ^T is known as an *antibonding orbital*.

The above approach to constructing molecular orbitals as linear combinations of atomic orbitals can also be extended to heteronuclear diatomic molecules with two different nuclei A and B. In these cases the molecular orbitals

$$\psi_i \quad = \quad C_A\phi_a(\vec{r}_{Ai}) + C_B\phi_b(\vec{r}_{Bi}) \tag{5.118}$$

differ from those of homonuclear diatomic molecules such as H_2 in that there is no reflection symmetry in the plane perpendicular to the molecular bond and therefore no designation of 'gerade' and 'ungerade'. Consequently

$$|C_A|^2 \neq |C_B|^2. \tag{5.119}$$

In these heteronuclear diatomic molecules the energy levels of the two atoms forming the molecular bond are generally not degenerate at large internuclear separation. Therefore in addition, to mixing of levels with the same values of ℓ, the molecular bond can also be composed of *hybrid orbitals*, e.g., mixtures of s- and p-orbitals.

5.5 Nuclear motion

Within the Born-Oppenheimer approximation the total wavefunction of a molecule with N nuclei and i electrons can be expressed as

$$\Psi(\vec{R}_N;\vec{r}_i) = \nu(\vec{R}_N)\,\psi(\vec{R}_N;\vec{r}_i), \tag{5.120}$$

and the solution to the electronic Schrödinger equation gives the potential in which the nuclear motion takes place.

In general a molecule with N nuclei has $3N$ nuclear degrees of freedom arising form three types of nuclear motion.

1. Translational motion: The free motion of the entire molecule in three-dimensional space, i.e., 3 degrees of freedom.

2. Vibrational motion: The vibrational motion of the nuclei about their equilibrium position. For a molecule with N nuclei there are $3N-6$ vibrational modes (or $3N-5$ if it is a linear molecule, e.g., a diatomic molecule).

3. Rotational motion: The rotational motion of the molecule about its center of mass. In general there are three axes about which this motion can take place leading to 3 rotational degrees of freedom. However, for a linear molecule, e.g., a diatomic molecule, there are only two distinct rotational axes and therefore only two rotational degrees of freedom.

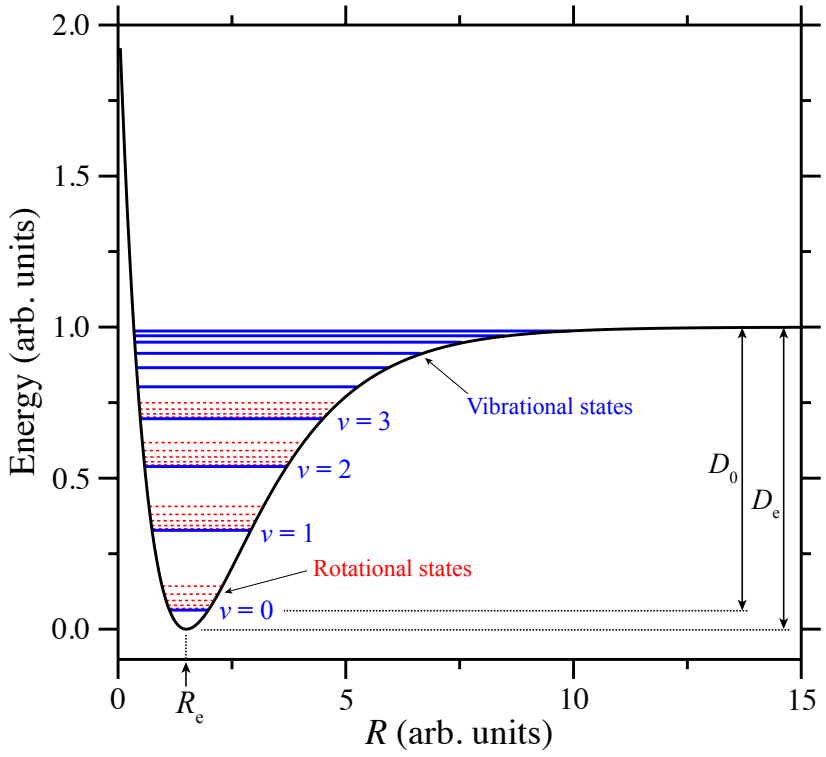

Figure 5.9: Schematic diagram of a typical molecular potential energy curve in which stable nuclear motion can take place. The energies of the vibrational (blue - continuous lines) and rotational (red - dashed lines) states are indicated along with the equilibrium internuclear distance, R_e, the equilibrium dissociation energy, D_e, and the dissociation energy from the lowest vibrational state with $v = 0$, i.e., D_0.

For a diatomic molecule with nuclei A and B, reduced mass μ_{AB}, and an internuclear separation $R = |\vec{R}|$, the nuclear Schrödinger equation has the form

$$\left[-\frac{\hbar^2}{2\mu_{AB}}\nabla_R^2 + V(R)\right] v(R) \quad = \quad E\, v(R). \tag{5.121}$$

Writing ∇_R^2 in spherical polar coordinates leads to

$$-\frac{\hbar^2}{2\mu_{AB}}\nabla_R^2 = -\frac{\hbar^2}{2\mu_{AB}}\frac{1}{R^2}\Bigg[\overbrace{\frac{\partial}{\partial R}\left(R^2\frac{\partial}{\partial R}\right)}^{\text{Radial}}+\ldots + \underbrace{\frac{1}{\sin\theta}\frac{\partial}{\partial\theta}\left(\sin\theta\frac{\partial}{\partial\theta}\right)+\frac{1}{\sin^2\theta}\left(\frac{\partial^2}{\partial\phi^2}\right)}_{\text{Angular}}\Bigg]. \quad (5.122)$$

Since the square of the angular momentum operator, $\hat{\vec{J}}^2$, in spherical polar coordinates is

$$\hat{\vec{J}}^2 = -\hbar^2\left[\frac{1}{\sin\theta}\frac{\partial}{\partial\theta}\left(\sin\theta\frac{\partial}{\partial\theta}\right)+\frac{1}{\sin^2\theta}\left(\frac{\partial^2}{\partial\phi^2}\right)\right]. \quad (5.123)$$

The expression in Equation 5.122 can be simplified to

$$-\frac{\hbar^2}{2\mu_{AB}}\nabla_R^2 = -\frac{\hbar^2}{2\mu_{AB}}\left[\frac{1}{R^2}\frac{\partial}{\partial R}\left(R^2\frac{\partial}{\partial R}\right)\right]+\frac{\hat{\vec{J}}^2}{2\mu_{AB}R^2}. \quad (5.124)$$

Separating the nuclear wavefunction into radial, $F(R)$, and angular, $Y(\theta,\phi)$, parts leads to

$$\nu(R) = \underbrace{\frac{F(R)}{R}}_{\text{Vib.}}\underbrace{Y(\theta,\phi)}_{\text{Rot.}} \quad (5.125)$$

corresponding to a separation into vibrational motion and rotational motion as indicated. Therefore in terms of the vibrational energy, E_{vib}, and the rotational energy, E_{rot}, Equation 5.121 becomes

$$\left(-\frac{\hbar^2}{2\mu_{AB}}\left[\frac{1}{R^2}\frac{\partial}{\partial R}\left(R^2\frac{\partial}{\partial R}\right)\right]+V(R)+\frac{\hat{\vec{J}}^2}{2\mu_{AB}R^2}\right)\frac{F(R)}{R}Y(\theta,\phi) = (E_{vib}+E_{rot})\frac{F(R)}{R}Y(\theta,\phi). \quad (5.126)$$

5.5.1 Rotation

The rotational motion of a diatomic molecule is a free rotation and, as in the case of the orbital angular momentum of the electron in the H atom, the

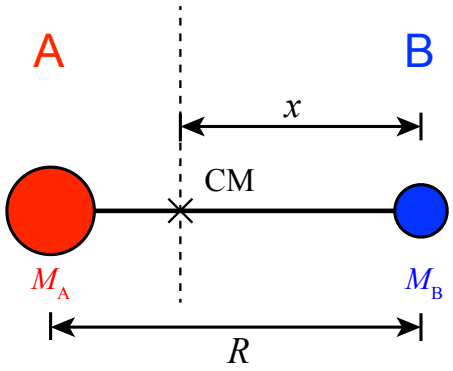

Figure 5.10: Schematic diagram of a rigid rotor with nuclei A and B of mass, M_A and M_B, respectively, separated by a fixed internuclear distance R. The position of nucleus B with respect to the center-of-mass of the two-body system, CM, is denoted x.

eigenfunctions that satisfy the rotational part of the nuclear Schrödinger equation are the spherical harmonic functions, $Y_{JM_J}(\theta,\phi)$. Therefore

$$\frac{\hat{\vec{J}}^2}{2\mu_{AB}R^2}\,Y_{JM_J}(\theta,\phi) \;=\; E_{rot}\,Y_{JM_J}(\theta,\phi), \tag{5.127}$$

and the rotational energy of the molecule is

$$E_{rot} \;=\; \frac{\hbar^2}{2\mu_{AB}R^2}\,J(J+1), \tag{5.128}$$

where J is the rotational quantum number which takes values $J = 0, 1, 2, \ldots$.

If the molecule is assumed to behave as a rigid rotor, i.e., the internuclear distance remains constant and is not affected by the molecule's rotation, its moment of inertial, I, can be expressed as

$$I \;=\; M_A(R-x)^2 + M_B x^2, \tag{5.129}$$

where M_A and M_B are the masses of the two nuclei, R is the internuclear distance, and x is the distance of nucleus B from the center of mass of the system (see Figure 5.10). If $R = R_e$, in the frame of reference associated with the center of mass this becomes

$$I_e \;=\; \mu_{AB}R_e^2. \tag{5.130}$$

and therefore

$$E_{\text{rot}} = \frac{\hbar^2}{2\,I_{\text{e}}}\,J(J+1) \tag{5.131}$$

$$= B\,J(J+1), \tag{5.132}$$

where

$$B = \frac{\hbar^2}{2\mu_{\text{AB}}\,R_{\text{e}}^2} = \frac{\hbar^2}{2\,I_{\text{e}}} \tag{5.133}$$

is known as the *rotational constant*. From this expression it can be seen that

$$E_{\text{rot}} \propto \frac{1}{\mu_{\text{AB}}} \tag{5.134}$$

$$\propto \omega_{\text{rot}}, \tag{5.135}$$

where for a fixed rotational quantum number ω_{rot} is the angular rotational frequency of the molecule. If $J = 0$ the molecule does not rotate and $E_{\text{rot}} = 0$.

5.5.2 Vibration

Using the above solution for the rotational energy of the molecule, the nuclear Schrödinger equation in Equation 5.126 can be rewritten in the form

$$-\frac{\hbar^2}{2\mu_{\text{AB}}}\,\frac{1}{R^2}\,\frac{\partial}{\partial R}\left(R^2\frac{\partial}{\partial R}\right)\frac{F(R)}{R} + \left[\frac{\hbar^2}{2\mu_{\text{AB}}R_{\text{e}}^2}\,J(J+1) + V(R)\right]\frac{F(R)}{R} = E\,\frac{F(R)}{R} \tag{5.136}$$

However,

$$-\frac{\hbar^2}{2\mu_{\text{AB}}}\,\frac{1}{R^2}\,\frac{\partial}{\partial R}\left(R^2\frac{\partial}{\partial R}\right)\frac{F(R)}{R} = -\frac{\hbar^2}{2\mu_{\text{AB}}}\,\frac{1}{R}\,\frac{\partial^2 F(R)}{\partial R^2}, \tag{5.137}$$

so Equation 5.138 can be reduced to

$$-\frac{\hbar^2}{2\mu_{\text{AB}}}\,\frac{1}{R}\,\frac{\partial^2 F(R)}{\partial R^2} + \left[\frac{\hbar^2}{2\mu_{\text{AB}}R_{\text{e}}^2}\,J(J+1) + V(R)\right]\frac{F(R)}{R} = E\,\frac{F(R)}{R} \tag{5.138}$$

which, then multiplying across by R to remove the factors indicated in red in the denominator of each term leads to

$$\left[-\frac{\hbar^2}{2\mu_{AB}}\frac{\partial^2}{\partial R^2}+\frac{\hbar^2}{2\mu_{AB}R_e^2}J(J+1)+V(R)\right]F(R) \;=\; E\,F(R), \tag{5.139}$$

where

$$\left[-\frac{\hbar^2}{2\mu_{AB}}\frac{\partial^2}{\partial R^2}+V(R)\right]F(R) \;=\; E_{vib}\,F(R), \tag{5.140}$$

gives the vibrational energy.

For a stable molecule $V(R)$ has a minimum at $R = R_e$ (see Figure 5.9), and this minimum contains the quantised motional (vibrational and rotational) states. Because the nuclear motion of the stable molecule is confined around this equilibrium internuclear position, a first approximation to the form of $V(R)$ can be obtained considering the molecular potential very close to R_e.

To do this the potential $V(R)$ can be expanded in a Taylor series about $R = R_e$, such that for a general function $f(x)$ expanded about $x = a$,

$$f(x) \;=\; f(a)+f'(a)\frac{(x-a)}{1!}+f''(a)\frac{(x-a)^2}{2!}+\ldots. \tag{5.141}$$

Therefore

$$V(R) = \;=\; V(R_e)+\frac{(R-R_e)}{1}\left.\frac{dV}{dR}\right|_{R=R_e}+\frac{(R-R_e)^2}{2}\left.\frac{d^2V}{dR^2}\right|_{R=R_e}+\ldots \tag{5.142}$$

neglecting higher order terms provided $(R - R_e)$ remains small. However, at the minimum of the potential

$$\left.\frac{dV}{dR}\right|_{R=R_e} \;=\; 0, \tag{5.143}$$

therefore to second order

$$V(R) = \;=\; V(R_e)+\frac{1}{2}k\,(R-R_e)^2, \tag{5.144}$$

where k is a constant. Since the second term of this equation corresponds to the potential associated with a harmonic oscillator, k is the *spring constant*.

The Schrödinger equation for the vibrational motion (Equation 5.145) therefore becomes

$$\Bigg[\underbrace{-\frac{\hbar^2}{2\mu_{\mathrm{AB}}}\frac{\partial^2}{\partial R^2} + \frac{1}{2}k\,(R-R_{\mathrm{e}})^2}_{\text{Quantum harmonic oscillator}} + V(R_{\mathrm{e}}) \Bigg] F(R) \;=\; E_{\mathrm{vib}}\,F(R), \tag{5.145}$$

where $V(R_{\mathrm{e}})$ is the electronic energy at $R = R_{\mathrm{e}}$.

For a quantum harmonic oscillator the eigenvalues, E_v, are given by

$$E_v \;=\; \hbar\omega_0(v+\frac{1}{2}), \tag{5.146}$$

where $v = 0, 1, 2, \ldots$ is the vibrational quantum number. For a harmonic oscillator with a fundamental vibrational frequency, ω_0,

$$\omega_0 \;=\; \sqrt{\frac{k}{\mu_{\mathrm{AB}}}}, \tag{5.147}$$

therefore

$$E_v \;=\; \hbar\sqrt{\frac{k}{\mu_{\mathrm{AB}}}}\,(v+\frac{1}{2}). \tag{5.148}$$

Form this expression it can be seen that for $v = 0$,

$$E_{v=0} \;=\; \frac{1}{2}\hbar\sqrt{\frac{k}{\mu_{\mathrm{AB}}}} \;\neq\; 0. \tag{5.149}$$

This non-zero energy associated with the vibrational ground state is known as the *zero-point energy* of the oscillator.

5.6 Total energy of a diatomic molecule

From the above the total energy, E_{AB}, of a diatomic molecule (rigid rotor) can be expressed in the harmonic approximation as

$$E_{\mathrm{AB}} \;=\; \underbrace{V(R_{\mathrm{e}})}_{\text{Electronic}} \;+\; \underbrace{B\,J(J+1)}_{\text{Rotational}} \;+\; \underbrace{\hbar\sqrt{\frac{k}{\mu_{\mathrm{AB}}}}\,(v+\frac{1}{2})}_{\text{Vibrational}}. \tag{5.150}$$

This expression is valid when:

1. v is small; i.e., near the bottom of the potential where the harmonic approximation is reasonable

2. J is small; i.e., when centrifugal distortion, which can occur when the molecule is rapidly rotating and can cause an increase in the bond length, does not play a significant role.

However, corrections can be made to the expression in Equation 5.150 to account for effects of high rotational and vibrational excitation. To improve the precision with which the rotational energy can be determined:

i. To account for changes in the mean internuclear separation with high vibrational excitation (high v), the rotational constant, B_v, can be adjusted to be dependent on the vibrational quantum number such that

$$B_v = \int_0^\infty F^*(v) \frac{\hbar^2}{2\mu_{AB}R^2} F(R)\, dR. \tag{5.151}$$

ii. For high J the effects of centrifugal distortion of the molecular bond can be accounted for be introducing a second order correction, $E_J^{(2)}$, to the rotational energy which is dependent upon D_v the *centrifugal distortion constant*,

$$E_J^{(2)} = -D_v J^2(J+1)^2. \tag{5.152}$$

Note: D_v is several orders of magnitude smaller than B_v, e.g., in the ground state of the CO molecule $B_v \sim 2\,\text{cm}^{-1}$ while $D_v \sim 0.000\,006\,\text{cm}^{-1}$.

Combining these two corrections leads to

$$E_J = B_v J(J+1) - D_v J^2(J+1)^2. \tag{5.153}$$

To describe the vibrational energies more precisely it is necessary to consider how the real molecular potential energy curve deviates form that of a harmonic oscillator. The main deviations occur for the more highly excited vibrational states (see Figure 5.11), where the anharmonicity of the true molecular potential become significant. As shown in Figure 5.11 a more appropriate analytic potential energy function which can be used to

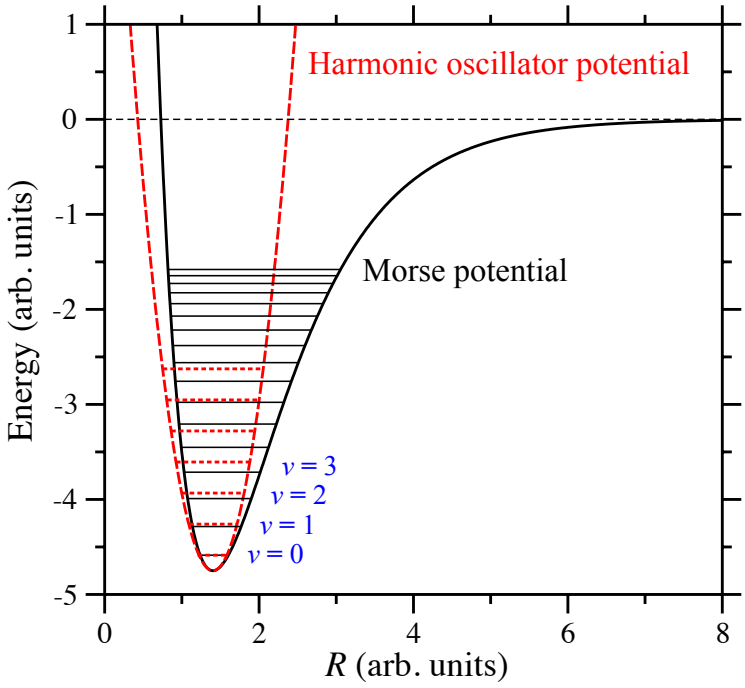

Figure 5.11: Schematic diagram of the Morse (continuous lines/curve) and harmonic oscillator (dashed lines/curve) potentials with their associated energy level structure.

model that of a diatomic molecule is the *Morse potential*, $V_{\text{Morse}}(R)$, where

$$V_{\text{Morse}}(R) = -D_e + D_e\left[1 - e^{-\alpha(R-R_e)}\right]^2 \tag{5.154}$$

$$= D_e\left[e^{-2\alpha(R-R_e)} - 2e^{-\alpha(R-R_e)}\right], \tag{5.155}$$

where the constant α is related to the force constant of the harmonic oscillator and can be determined by expanding $V_{\text{Morse}}(R)$ in powers of $(R - R_e)$, i.e.,

$$V_{\text{Morse}}(R) \simeq D_e\left[-1 + \alpha^2(R - R_e) + \ldots\right]. \tag{5.156}$$

Hence,

$$\alpha = \sqrt{\frac{k}{2\,D_e}}. \tag{5.157}$$

The Morse potential supports a finite number of vibrational states and as can be seen in Figure 5.11 these become more closely spaced in energy as they approach the dissociation limit. In the Morse potential the vibrational energy of each state can be expressed as

$$E_v = \hbar\,\omega_0\,(v + \frac{1}{2}) - \frac{\left[\hbar\,\omega_0\,(v + \frac{1}{2})\right]}{4\,D_e}, \tag{5.158}$$

where

$$\omega_0 = \alpha\sqrt{\frac{2\,D_e}{\mu_{AB}}}. \tag{5.159}$$

5.7 Spectra of diatomic molecules

Molecular spectra are composed of three main kinds of transitions.

1. *Pure rotational transitions*

   - These are transitions which do not involve any change in electronic state or vibrational state of the molecule.
   - They are only strong for molecules with non-zero *electric dipole moments* with which an oscillating electromagnetic field can interact. Examples of such molecules are LiF and HCl.

- Homonuclear diatomic molecules, e.g, H_2, D_2 or H_2^+ do not undergo pure rotational transitions within the electric dipole approximation.
- Pure rotational transitions occur at frequencies on the order of the rotational energy level spacings within a molecule, i.e, on the same order of magnitude as the rotational constant B. They therefore lie in the microwave region of the electromagnetic spectrum ($\nu = 1 - 100$ GHz).
- The selection rule for pure rotational transitions within the electric dipole approximation is that

$$\Delta J = \pm 1 \tag{5.160}$$

  for linear molecules, including diatomics. (Note: non-linear polyatomic molecules can undergo pure rotational transition for which $\Delta J = 0$).

Since the rotational energy, E_J, of a state in a diatomic molecule is

$$E_J = B\,J(J+1), \tag{5.161}$$

the energy difference between the states, J and $J' = J + 1$, involved in a pure rotational transition is

$$\begin{aligned} \Delta E_J &= E_{J+1} - E_J && (5.162)\\ &= B\,(J+1)(J+2) - B\,J(J+1) && (5.163)\\ &= 2B\,(J+1). && (5.164) \end{aligned}$$

Therefore as J increases the differences in energy between rotational states J and J', which correspond to the frequencies of the pure rotational transitions, increase by $2B$. Pure rotational spectra are therefore composed of series of sharp spectral lines separated in energy by an interval of $2B$ (see Figure 5.12). From such a spectrum the rotational constant can be accurately determined and hence if the reduced mass of the systems is known the internuclear distance can be deduced.

2. *Vibration-rotation transitions*

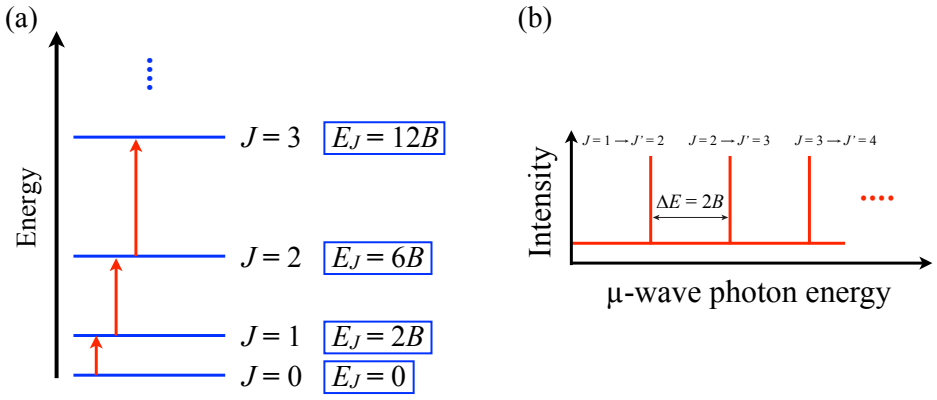

Figure 5.12: Schematic diagram of (a) the rotational energy level structure, and (b) a pure rotational spectrum of a heteronuclear diatomic molecule.

- These are transitions which do not involve a change in the electronic state of the molecule, but do involve changes in the rotational and vibrational states.
- Vibration-rotation transitions occur at frequencies on the order of the vibrational energy level spacings within a molecule, i.e., on the same order of magnitude as the spring constant k associated with the molecular bond. They therefore lie in the infrared region of the electromagnetic spectrum.
- The selection rules for vibration-rotation transitions, within the electric dipole approximation, are that

$$\Delta v = \pm 1 \tag{5.165}$$

and

$$\Delta J = \pm 1. \tag{5.166}$$

This vibrational selection rule is that associated with a quantum harmonic oscillator. Along with these transitions in which the vibrational quantum number changes by ± 1, overtone transitions for which $\Delta v = \pm 2, \pm 3, \ldots$ can also occur but are much weaker.

Rotation-vibration spectra of diatomic molecules typically exhibit two groupings of lines relating to each allowed change in the rotational

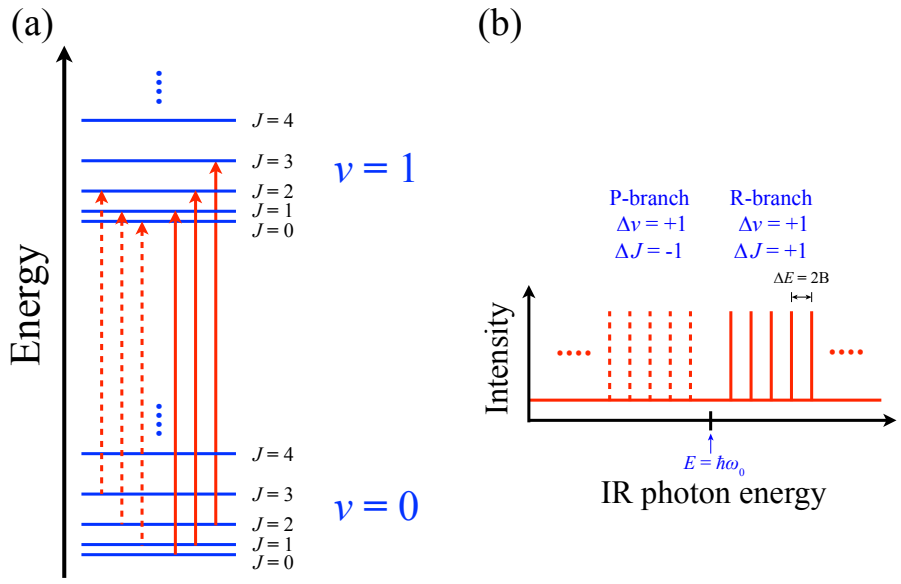

Figure 5.13: Schematic diagram of (a) the rotational and vibrational energy level structure, and (b) a typical rotation-vibration spectrum of a heteronuclear diatomic molecule.

quantum number. One group associated with $\Delta J = -1$ transitions, and the other associated with $\Delta J = +1$ transitions. These are known as the *P-branch* and the *R-branch*, respectively.

The P-branch transitions, for which $\Delta J = -1$, involve states separated in energy by, $\Delta E_{\text{ro-vib}}$, where

$$\Delta E_{\text{ro-vib}} = E(v+1, J-1) - E(v, J) \tag{5.167}$$

$$= -2B\,J + \hbar\omega_0. \tag{5.168}$$

where the first term in Equation 5.170 corresponds to the change in the rotational energy and the second term corresponds to the change in the vibrational energy.

On the other hand, the R-branch transitions, for which $\Delta J = +1$, involve states separated in energy by

$$\Delta E_{\text{ro-vib}} = E(v+1, J+1) - E(v, J) \tag{5.169}$$

$$= 2B\,(J+1) + \hbar\omega_0, \tag{5.170}$$

The P- and R-branch transitions in rotation-vibration spectra are therefore are composed of sets spectral lines equally spaced by $2B$ and located on either side of the energy difference corresponding to the pure vibrational interval, $\hbar\omega_0$, as indicated in Figure 5.13. In such spectra the rotational constant of the molecule, B, can be determined from the spacing between the spectral lines in each of the branches. This then allows the moment of inertia of the molecule and the equilibrium internuclear separation to be calculated. The position, $\hbar\omega_0$, of the missing line that would correspond to the forbidden $\Delta J = 0$ transition gives the spring constant.

3. *Electronic transitions*

Diatomic molecules have axial symmetry and are not spherically symmetric as atoms are. As a result, the molecular axis defines a fixed direction in space onto which the angular parts of the electronic wavefunctions have a constant projection, L_z (where the molecular axis is defined as the z axis). Consequently, the electronic eigenfunctions of the molecule are simultaneous eigenstates of $\hat{H}_{\text{elec}}$ and $\hat{L}_z$. In general, when acting on an angular wavefunction $Y(\theta, \phi)$, the operator $\hat{L}_z$ has eigenvalues $\hbar M_L$, i.e.,

$$\hat{L}_z\, Y(\theta, \phi) \quad = \quad M_L\, \hbar\, Y(\theta, \phi), \tag{5.171}$$

where $M_L = 0, \pm 1, \pm 2, \ldots, \pm L$. In this case, where the z axis is chosen the be the axis of the molecule, the quantum number M_L is denoted Λ such that

$$\hat{L}_z\, Y(\theta, \phi) \quad = \quad \Lambda\, \hbar\, Y(\theta, \phi), \tag{5.172}$$

with Λ defined as the projection of the total electronic orbital angular momentum onto the internuclear axis.

This value of Λ can them be used in the construction the term symbol describing the electronic state of a diatomic molecule which has the form

$$^{2S+1}\Lambda^{+,-}_{\text{g,u}} \tag{5.173}$$

where S is the total electron spin quantum number, g (gerade) and u (ungerade) represent the symmetry of the electronic wavefunctions in the case of homonuclear diatomic molecules, and + and − indicate the reflection symmetry of the electronic wavefunction in a plane containing the internuclear axis. In such a term symbol $\Lambda \equiv |\Lambda|$.

In the same way that the letters S, P, D, F,... are used to denote the orbital angular momentum in the term symbols of atoms, the value of Λ, is indicated in the molecular term symbol in Equation 5.173 by the greek letters $\Sigma, \Pi, \Delta, \Phi, \ldots$.

$\lvert\Lambda\rvert =$	0	1	2	3	...
	Σ	Π	Δ	Φ	...

For one-electron molecular orbitals, these labels are written as lower case characters (as for one-electron atomic orbitals), i.e.,

$\lambda =$	0	1	2	3	...
	σ	π	δ	ϕ	...

The selection rules for allowed electric dipole transitions between different electronic states are then

$$\Delta\Lambda = 0, \pm 1 \tag{5.174}$$

$$\Delta S = 0 \tag{5.175}$$

$$\mathrm{g} \rightarrow \mathrm{u} \quad \text{or} \quad \mathrm{u} \rightarrow \mathrm{g} \quad (\text{i.e., } \mathrm{g} \nrightarrow \mathrm{g} \quad \text{and} \quad \mathrm{u} \nrightarrow \mathrm{u}) \tag{5.176}$$

$$+ \rightarrow + \quad \text{or} \quad - \rightarrow - \quad (\text{i.e., } + \nrightarrow - \quad \text{and} \quad - \nrightarrow +) \tag{5.177}$$

$$\Delta v = \text{any value} \tag{5.178}$$

$$\Delta J = 0, \pm 1 \tag{5.179}$$

The energy differences between the electronic states of a molecule are much larger than those between rotational or vibrational states. Electronic transitions therefore typically occur in the ultraviolet or vacuum ultraviolet regions of the electromagnetic spectrum. Because the equilibrium internuclear distance and rotational constants of different electronic states can be very different, the different rotational

transitions do not necessarily give rise to series of equally spaced lines as seen in pure rotational spectra or vibration-rotation spectra. Instead, each electronic transition is split into bands of closely spaced rotational lines associated with each initial and final vibrational state.

5.7.1 Franck-Condon principle

If it is assumed that the time required for the electronic wavefunction of a molecule to change when a transition occurs, is so fast that the nuclei do not move in this time, the spectral intensities of the transitions between each pair of vibrational states of the initial and final electronic states can be determined from the overlap of their vibrational wavefunctions.

From Fermi's golden rule (see Section 4.1, Equation 4.4) the probability of a transition occurring between an initial state, i, and a final state, f, is

$$T_{\mathrm{if}} = \left| \int \Psi_{\mathrm{f}}^{*} \, V_{\mathrm{dip}} \Psi_{\mathrm{i}} \, \mathrm{d}\tau \right|^2 \tag{5.180}$$

$$\propto \left| \int \Psi_{\mathrm{f}}^{*} \, \hat{\vec{\mu}}_{\mathrm{elec}} \Psi_{\mathrm{i}} \, \mathrm{d}\tau \right|^2 \tag{5.181}$$

$$\propto \left| \int \Psi_{\mathrm{f}}^{*} \, \hat{\vec{r}} \, \Psi_{\mathrm{i}} \, \mathrm{d}\tau \right|^2 . \tag{5.182}$$

For a diatomic molecule with a total wavefunction

$$\Psi(\vec{R};\vec{r}) = \nu(\vec{R}) \, \psi(\vec{R};\vec{r}), \tag{5.183}$$

considering only the vibrational part, $F(\vec{R})$, of the nuclear wavefunction, $\nu(\vec{R})$, (see Section 5.5) the transition probability can therefore be written as

$$T_{\mathrm{if}} \propto \left| \int F_{\mathrm{f}}^{*}(\vec{R}) \, \psi_{\mathrm{f}}^{*}(\vec{R};\vec{r}) \, \hat{\vec{r}} \, F_{\mathrm{i}}(\vec{R}) \, \psi_{\mathrm{i}}(\vec{R};\vec{r}) \, \mathrm{d}\tau \right|^2 \tag{5.184}$$

$$= \underbrace{\left| \int \psi_{\mathrm{f}}^{*}(\vec{R};\vec{r}) \, \hat{\vec{r}} \, \psi_{\mathrm{i}}(\vec{R};\vec{r}) \, \mathrm{d}r \right|^2}_{\text{Electronic transition moment}} \times \underbrace{\left| \int F_{\mathrm{f}}^{*}(\vec{R}) \, F_{\mathrm{i}}(\vec{R}) \, \mathrm{d}R \right|^2}_{\text{Franck-Condon factor}} \tag{5.185}$$

where,

$$\int F_{\mathrm{f}}^{*}(\vec{R}) \, F_{\mathrm{i}}(\vec{R}) \, \mathrm{d}R \tag{5.186}$$

is known as the *Franck-Condon overlap integral* (see Figure 5.14), and, as indicated,

$$\left| \int F_{\mathrm{f}}^{*}(\vec{R})\, F_{\mathrm{i}}(\vec{R})\, \mathrm{d}R \right|^{2} \tag{5.187}$$

is the *Franck-Condon factor*.

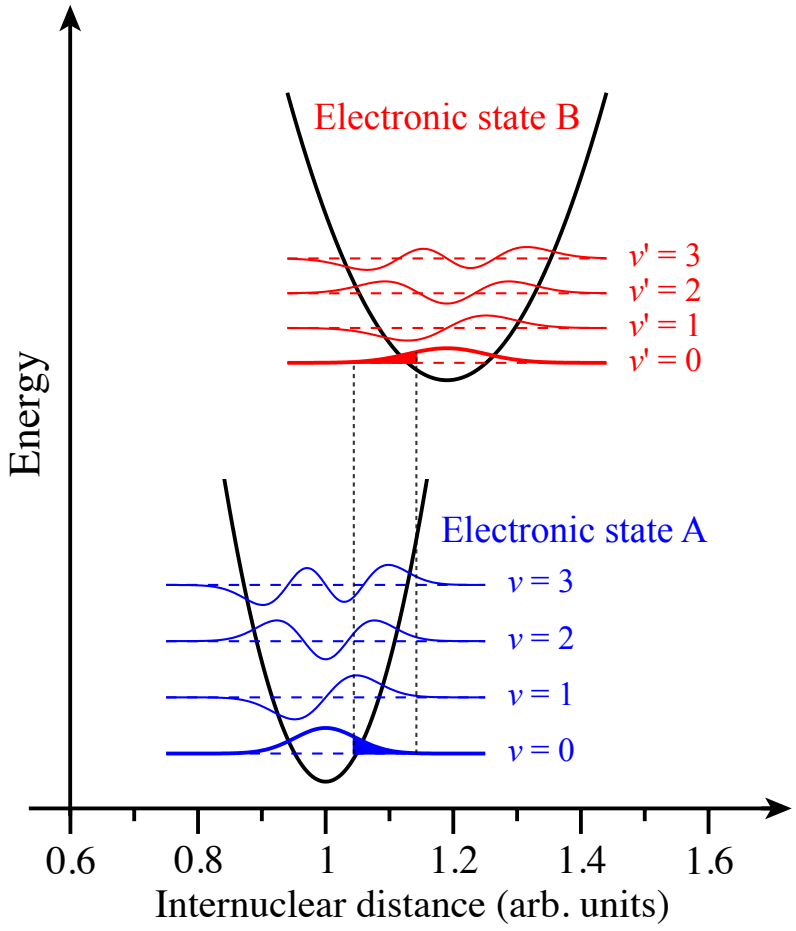

Figure 5.14: The overlap (shaded regions) of the $v = 0$ and $v' = 0$ vibrational wavefunctions, $F(\vec{R})$, of two electronic states, labelled A and B, respectively.

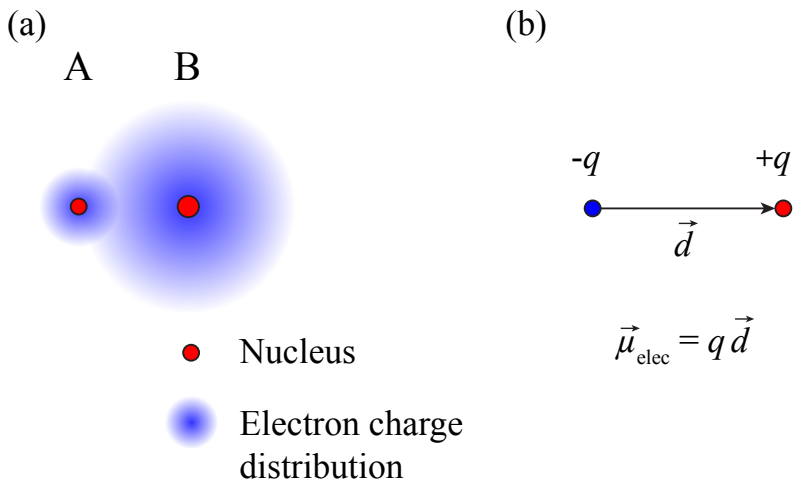

Figure 5.15: (a) Schematic diagram of an ionically bound molecule AB in which the electron charge (shaded blue regions) is localised more closely toward one end of the molecular bond (close to nucleus B) than the other. (b) The electric dipole moment, $\vec{\mu}_{\text{elec}}$, associated with two charges, $-q$ and $+q$, separated by a distance $\vec{d}$.

5.8 Ionically bound molecules

The homonuclear diatomic molecules discussed above are covalently bound, with electrons shared equally between the two nuclei. They therefore do not exhibit any electric dipole moment, i.e, the electron charge is distributed equally between the two nuclei, or pure rotational spectra. On the other hand, molecules that exhibit strong pure rotational spectra must have a significant electric dipole moment, $\vec{\mu}_{\text{elec}}$, i.e., an uneven distribution of electron charge between the two nuclei with one end of the molecular bond more negatively charged than the other [see for example Figure 5.15(a)]. The interaction of this electric dipole moment with an electromagnetic field gives rise to a torque on the molecule and a change in its rotational state.

The heteronuclear isotopomers of the molecular hydrogen cation and neutral hydrogen molecule, e.g., HD^+, HT^+, HD, and HT have small electric dipole moments, because of the slightly different masses of the two nuclei, and very weak pure rotational spectra. However, ionically bound

molecules, e.g, HCl, HF, or LiF have significant electric dipole moments (on the order of 3.33×10^{-30} Cm $\equiv$ 1 debye, or 1 D) and therefore strong pure rotational spectra.

Ionic bonds are most readily formed between atoms one of which has one electron outside an otherwise closed shell, e.g., the alkali metal atoms Li, Ns, Rb, Cs, and the other of which is one electron short of a closed shell, e.g, the halogen atoms F, Cl, Br, I.

5.8.1 Dissociation energy of alkali metal halides

The form and strength of an ionic bond can be seen by considering the *electron affinity*, A, of the atoms involved. This is the binding energy of a single electron attached to the neutral atom to form a negative ion (*anion*). In the case of Na and Cl, e.g,

$$\mathrm{Na} + \mathrm{e}^- \rightarrow \mathrm{Na}^- \tag{5.188}$$

$$\mathrm{Cl} + \mathrm{e}^- \rightarrow \mathrm{Cl}^- \tag{5.189}$$

the electron affinities are

$$\frac{A_{\mathrm{Na}}}{e} = 0.54 \text{ eV} \tag{5.190}$$

$$\frac{A_{\mathrm{Cl}}}{e} = 3.62 \text{ eV}, \tag{5.191}$$

indicating that an additional electron would be bound more tightly to the Cl atom than to the Na atom. On the other hand, the ionisation energies, I, of the two atoms are

$$\frac{I_{\mathrm{Na}}}{e} = 5.14 \text{ eV} \tag{5.192}$$

$$\frac{I_{\mathrm{Cl}}}{e} = 12.97 \text{ eV}. \tag{5.193}$$

From these values of the electron affinities and ionisation energies it can be seen that energy is required to remove an electron from the Na atom and attach it to the Cl atom, but this energy is less than that required to remove an electron from the Cl atom and attach it to the Na atom. This energy, E, is

$$E = I_{\mathrm{Na}} - A_{\mathrm{Cl}} \tag{5.194}$$

$$\equiv 1.52 \text{ eV}. \tag{5.195}$$

However, if this electron transfer is achieved the resulting Na^+ and Cl^- ions will interact via an attractive Coulomb interaction. The interatomic (or internuclear) distance, R, for which the this Coulomb energy matches the energy loss associated with the transfer of the electron between the two atoms can therefore be determined to be

$$E_C = \frac{e^2}{4\pi\epsilon_0 R} \quad (5.196)$$
$$\equiv 1.52 \text{ eV}. \quad (5.197)$$

Therefore,

$$R = 9.47 \times 10^{-10} \text{ m} \quad (5.198)$$
$$= 17.9\, a_0, \quad (5.199)$$

and this is approximately the equilibrium internuclear distance at which a stable, ionically bound, NaCl molecule will form.

The true equilibrium internuclear distance in the ground electronic state of NaCl, determined from measurements of the rotational constant, is $R_e = 4.5\, a_0$, and at this separation the energy, E_C, associated with the Coulomb attraction between the Na^+ and Cl^- ions is

$$\frac{E_C(R_e)}{e} = 6 \text{ eV}. \quad (5.200)$$

This is therefore the energy required to separate the two nuclei and produce two atomic ions. However, considering the energy saved by transferring the electron from the Cl^- back to the Na^+ in the dissociation process, the dissociation energy, D_e, of NaCl to from two neutral ground state atoms is

$$D_e = E_C(R_e) - (I_{Na} - A_{Cl}) \quad (5.201)$$
$$\equiv 4.48 \text{ eV}. \quad (5.202)$$

This simple argument leads to a dissociation energy for NaCl that is very close to the true value of $D_e \equiv 4.26$ eV. The causes of the discrepancy between these values are associated with

1. The assumption that the Na^+ and Cl^- ions are point charges, while in a more complete description of the molecule it is necessary to take into account their finite sizes.

2. Not accounting for the effects of the overlap of the electronic wavefunctions of the two ions on the energy of the system. At small internuclear distances this will raise the energy of the molecule.

5.8.2 Ionic character of a bond

The ionic bonds in molecules are not purely ionic, in that the bonding electron is not completely localised at of the nuclei. If the bond was purely ionic the electric dipole moment of the molecule would be

$$\mu_{\text{elec}} = e R_{\text{e}}. \tag{5.203}$$

In NaCl, with an equilibrium internuclear distance of $R_{\text{e}} = 4.54\, a_0 = 2.40 \times 10^{-10}$ m, a purely ionic bond would lead to a dipole moment of

$$\mu_{\text{elec}} = 3.8 \times 10^{-29} \text{ Cm} \tag{5.204}$$

$$= 11.5 \text{ debye}. \tag{5.205}$$

However, the measured electric dipole moment is

$$\mu_{\text{expt}} = 9.0 \text{ debye}. \tag{5.206}$$

Therefore there must be a non-zero probability of finding the electron located close to the Na^+ atom. In such a situation the fractional ionic character, f_{ionic}, of the bond can be defined as

$$f_{\text{ionic}} = \frac{\mu_{\text{expt}}}{e R_{\text{e}}} \tag{5.207}$$

$$= 0.78 \quad \text{for NaCl}. \tag{5.208}$$

In this way:

$$\text{If } f_{\text{ionic}} = 1 \Rightarrow \text{Completely ionic bond} \tag{5.209}$$

$$\text{If } f_{\text{ionic}} = 0 \Rightarrow \text{Completely covalent bond} \tag{5.210}$$

The ionic character of the bonds in the ground electronic states of a selection of alkali metal halide molecules are listed in Table 5.1

	R_e (10^{-10} m)	$\mu_{elec} = e\,R_e$ (debye)	μ_{expt} (debye)	f_{ionic}
LiF	1.56	7.49	6.32	0.84
NaCl	2.40	11.52	9.00	0.78
KBr	2.82	13.54	10.62	0.78

Table 5.1: Ionic character of the bonds in the ground electronic states of the alkali metal halide molecules LiF, NaCl and KBr.

Part III

Atoms in electric and magnetic fields

Chapter 6

Introduction

Atoms can be very sensitive to electric and magnetic fields. These fields cause energy shifts and energy splittings of the field-free electronic structure. As a result, samples of atoms can be used as very sensitive probes of electric and magnetic fields. However, in atomic clocks, and when atoms are used in tests of fundamental physics, this sensitivity means that it is essential to control and minimise these fields. In addition, electric and magnetic fields can be used to accelerate, decelerate and trap neutral atoms and antiatoms.

6.1 Hamiltonian operator

The Hamiltonian operator, $\hat{H}$, for an isolated atom with many electrons in the absence of external electric or magnetic fields can be expressed as

$$\hat{H} = \hat{H}_0(\vec{r}_1, \vec{r}_2, \ldots, \vec{r}_i) + \hat{H}_{\mathrm{SO}}, \tag{6.1}$$

where $\hat{H}_{\mathrm{SO}}$ accounts for the spin-orbit interaction in the atom.

In the presence of an external magnetic field $\vec{B}$, and electric field $\vec{F}$, the Hamiltonian operator becomes

$$\hat{H} = \hat{H}_0 + \hat{H}_{\mathrm{SO}} + V_B + V_F, \tag{6.2}$$

where V_B and V_F represent the interactions with the magnetic and electric fields, respectively. The interaction of the atom with the magnetic field

is known as the *Zeeman interaction* as it was first observed by the Dutch physicist Pieter Zeeman in 1896. The interaction with the electric fields is known as the *Stark interaction* after the early experimental work by Johannes Stark on its observation.

6.1.1 First order perturbation theory

When contributions from the applied electric and magnetic fields are small compared to the field-free Hamiltonian, i.e., when

$$\hat{H}_0 \gg \hat{H}_{\mathrm{SO}},\, V_B \text{ and } V_F, \tag{6.3}$$

the fields can be considered to only perturb the field-free electronic structure. In this situation the energy shifts arising from the interactions with the external fields are small compared to the energy spacings between states with difference values of n in the atom, and the energy shift, ΔE, of a state ψ_0 is given by the expectation value of the perturbing potential, V, i.e,

$$\Delta E \simeq \int \psi_0^* V \psi_0 \, \mathrm{d}\tau. \tag{6.4}$$

The total energy, E_{tot}, of the state in the presence of the field is then

$$E_{\mathrm{tot}} = E_0 + \Delta E, \tag{6.5}$$

where

$$\hat{H}_0 \psi_0 = E_0 \psi_0, \tag{6.6}$$

and

$$E_0 \gg \Delta E. \tag{6.7}$$

Chapter 7

Atoms in magnetic fields

7.1 Introduction

The Zeeman effects arises from the interaction of the magnetic dipole moment of an atom, $\vec{\mu}_{\rm mag}$, with an external magnetic field, $\vec{B}$. The interaction potential, V_B, is therefore

$$V_B = -\vec{\mu}_{\rm mag} \cdot \vec{B}. \tag{7.1}$$

Within the atom there are two sources of magnetic dipole moments. The magnetic dipole associated with the total electron spin, $\vec{\mu}_S$, and the magnetic dipole moment associated with the total electron orbital angular momentum, $\vec{\mu}_L$. As in the treatment of the spin-orbit interaction in Section 3.7,

$$\vec{\mu}_S = -g_{\rm e}\mu_{\rm B}\frac{\vec{S}}{\hbar}, \tag{7.2}$$

where $g_{\rm e} \simeq 2$ is the electron spin g-factor, and $\mu_{\rm B}$ is the Bohr magneton, and

$$\vec{\mu}_L = -g_{\rm L}\mu_{\rm B}\frac{\vec{L}}{\hbar}, \tag{7.3}$$

where $g_{\rm L} = 1$ is the orbital g-factor. In the following the Zeeman effect will be considered in three different situations:

1. For states in which the total electron spin is zero, i.e., $S = 0$.
2. For states in which $S \neq 0$ and the Zeeman interaction (energy shift) is small compared to the spin-orbit energy splitting.

3. For states in which $S \neq 0$ and the Zeeman interaction (energy shift) is large compared to the spin-orbit energy splitting.

7.2 Zeeman effect when $S = 0$

In terms for which $S = 0$, an atom exhibits no magnetic dipole moment associated with its total electron spin, i.e, $\vec{\mu}_S = 0$, therefore

$$V_B = -\vec{\mu}_L \cdot \vec{B}. \tag{7.4}$$

For a magnetic field $\vec{B} = (0, 0, B_z)$ acting in the z-direction

$$V_B = \frac{\mu_B}{\hbar} \vec{L} \cdot \vec{B} \tag{7.5}$$

$$= \frac{\mu_B}{\hbar} L_z B_z. \tag{7.6}$$

Therefore the resulting Zeeman energy shift, ΔE_B, is

$$\Delta E_B = \int \psi_0^* V_B \psi_0 \, d\tau \tag{7.7}$$

$$= \int \psi_0^* \frac{\mu_B}{\hbar} \hat{L}_z B_z \psi_0 \, d\tau \tag{7.8}$$

$$= \frac{\mu_B}{\hbar} B_z \int \psi_0^* \hat{L}_z \psi_0 \, d\tau. \tag{7.9}$$

However, from the properties of the angular momentum operators

$$\hat{L}_z \psi_0 = \hbar M_L \psi_0, \tag{7.10}$$

so

$$\Delta E_B = \mu_B M_L B_z \int \psi_0^* \psi_0 \, d\tau \tag{7.11}$$

$$= \mu_B M_L B_z, \tag{7.12}$$

provided that the field-free wavefunctions, ψ_0, are normalised.

In this situation, when $S = 0$, each term with total orbital angular momentum quantum number L is therefore split into $2L + 1$ equally spaced

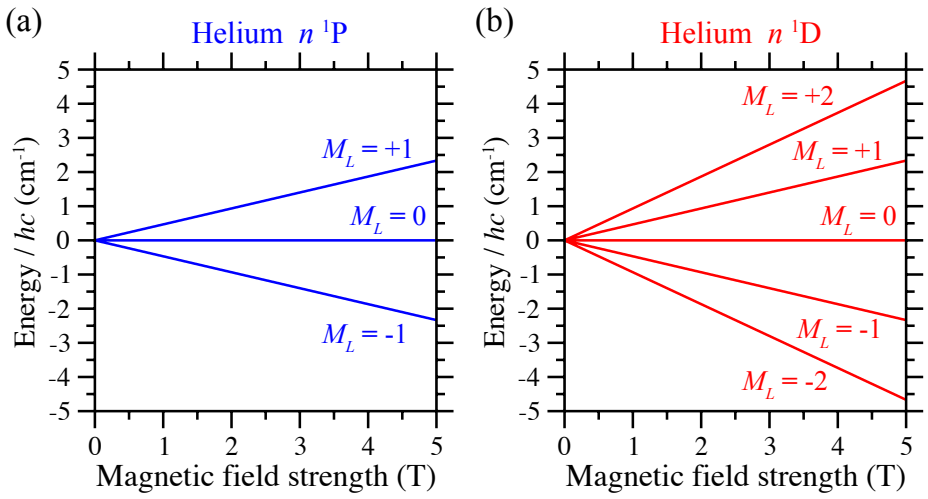

Figure 7.1: The Zeeman effect in the absence of spin, i.e., when $S = 0$, in (a) the $n\,^1$P term, and (b) the $n\,^1$D term in He.

sublevels by the magnetic field. This can be seen in Figure 7.1 in the case of the singlet-P and singlet-D ($S = 0$) terms in He.

In the absence of electron spin the electric dipole selection rules for transitions between Zeeman sublevels require that

$$\Delta M_L = 0, \pm 1. \tag{7.13}$$

Therefore each spectral line is split into three components, one associated with the $\Delta M_L = -1$ transitions, one associated with the $\Delta M_L = 0$ transitions, and one associated with the $\Delta M_L = +1$ transitions, as indicated in Figure 7.2. This splitting of a single spectral line into three components when $S = 0$ is often known as the *normal Zeeman effect*.

7.3 Zeeman effect when $S \neq 0$ (weak-field regime)

For states in which $S \neq 0$, the magnetic dipole moments associated with the electron spin and orbital angular momentum must both be accounted for when treating the interaction of the atom with a magnetic field. In the weak-field limit, i.e., when the applied magnetic field is weaker than the internal magnetic fields in the atom and the Zeeman energy shift is therefore smaller

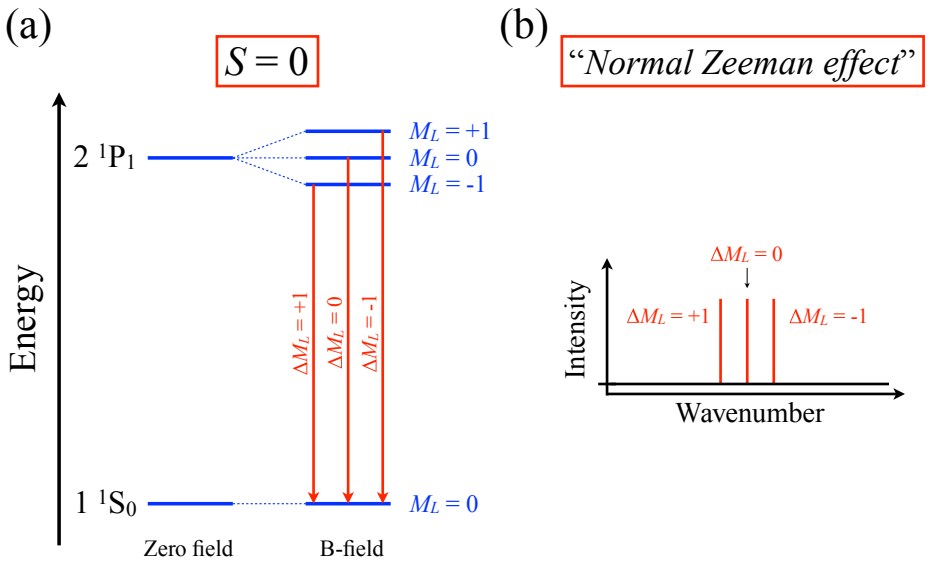

Figure 7.2: Schematic diagrams (a) indicating the electric dipole allowed transitions between Zeeman sublevels when $S = 0$, and (b) the corresponding spectral intensity distributions.

than the spin-orbit energy splitting, the spin-orbit interaction couples $\vec{L}$ and $\vec{S}$ so that

$$\vec{J} = \vec{L} + \vec{S}. \tag{7.14}$$

If the external magnetic field is too weak to uncouple the $\vec{L}$ and $\vec{S}$ vectors, M_L and M_S are not good quantum numbers with which to describe the system. This must be taken into account when calculating the effect of the magnetic field on the atomic energy level structure.

In this case

$$V_B = -\vec{\mu}_S \cdot \vec{B} - \vec{\mu}_L \cdot \vec{B} \tag{7.15}$$

$$= (g_e \vec{S} + g_L \vec{L}) \frac{\mu_B}{\hbar} \cdot \vec{B} \tag{7.16}$$

$$= \frac{\mu_B}{\hbar} \vec{B} \cdot (\vec{L} + 2\vec{S}) \tag{7.17}$$

$$= \frac{\mu_B}{\hbar} \vec{B} \cdot (\vec{J} + \vec{S}). \tag{7.18}$$

If $\vec{B} = (0, 0, B_z)$, the energy shift resulting from the Zeeman interaction is given by the expectation value of V_B, so

$$\Delta E_B = \int \psi_0^* \frac{\mu_B}{\hbar} B_z \hat{J}_z \psi_0 \, d\tau + \int \psi_0^* \frac{\mu_B}{\hbar} \vec{B} \cdot \vec{S} \psi_0 \, d\tau \tag{7.19}$$

$$= \mu_B M_J B_z + \int \psi_0^* \frac{\mu_B}{\hbar} \vec{B} \cdot \vec{S} \psi_0 \, d\tau. \tag{7.20}$$

In the *LS*-coupling regime the total spin vector $\vec{S}$ precesses about the total orbital angular momentum vector $\vec{J}$ with a constant projection S_J along the vector $\vec{J}$. However, it does not have a constant projection along $\vec{B}$. This can be seen schematically in Figure 7.3. In this situation the projection S_J is give by[1]

$$S_J = \frac{\vec{S} \cdot \vec{J}}{|\vec{J}|}. \tag{7.21}$$

This can be written in vector form by multiplying by the unit vector in the direction defined by $\vec{J}$ so that

$$\vec{S}_J = \frac{\vec{S} \cdot \vec{J}}{|\vec{J}|} \frac{\vec{J}}{|\vec{J}|}, \tag{7.22}$$

and when written in operator form

$$\hat{\vec{S}}_J = \frac{\hat{\vec{S}} \cdot \hat{\vec{J}}}{\hat{\vec{J}}^2} \hat{\vec{J}}. \tag{7.23}$$

[1]Note: For two vectors $\vec{a}$ and $\vec{b}$ with an angle θ between them, $\vec{a} \cdot \vec{b} = |\vec{a}||\vec{b}| \cos\theta$, so the projection of $\vec{a}$ onto $\vec{b}$ is $|\vec{a}| \cos\theta = \vec{a} \cdot \vec{b} \, / \, |\vec{b}|$.

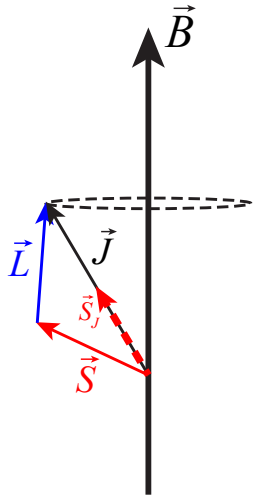

Figure 7.3: Schematic diagram illustrating the precession of the total angular momentum vector $\vec{J}$, in a weak magnetic field $\vec{B}$. In this situation, the total spin vector $\vec{S}$ precesses about $\vec{J}$ with a constant projection S_J indicated by the dashed red line.

Then using the fact that $\hat{\vec{J}} = \hat{\vec{L}} + \hat{\vec{S}}$ can be rearranged such that

$$\hat{\vec{L}} = \hat{\vec{J}} - \hat{\vec{S}} \tag{7.24}$$

and therefore

$$\hat{\vec{L}}^2 = \hat{\vec{J}}^2 + \hat{\vec{S}}^2 - 2\,\hat{\vec{J}} \cdot \hat{\vec{S}}, \tag{7.25}$$

and

$$\hat{\vec{J}} \cdot \hat{\vec{S}} = \frac{1}{2}\left[\hat{\vec{J}}^2 + \hat{\vec{S}}^2 - \hat{\vec{L}}^2\right]. \tag{7.26}$$

Since the vector $\vec{S}_J$ has a constant projection on the external magnetic field $\vec{B}$, the total energy shift resulting from the Zeeman interaction (Equation 7.20)

can be expressed as

$$\Delta E_B = \mu_B M_J B_z + \frac{\mu_B}{\hbar} \int \psi_0^* \vec{B} \cdot \vec{S}_J \psi_0 \, d\tau \tag{7.27}$$

$$= \mu_B M_J B_z + \frac{\mu_B}{\hbar} \int \psi_0^* \vec{B} \cdot \frac{\vec{S} \cdot \vec{J}}{|\vec{J}|^2} \vec{J} \psi_0 \, d\tau \tag{7.28}$$

$$= \mu_B M_J B_z + \frac{\mu_B}{\hbar} \int \psi_0^* B_z \left[\frac{\hat{\vec{J}}^2 + \hat{\vec{S}}^2 - \hat{\vec{L}}^2}{2\hat{\vec{J}}^2} \right] J_z \psi_0 \, d\tau \tag{7.29}$$

$$= \mu_B M_J B_z + \mu_B M_J B_z \left[\frac{J(J+1) + S(S+1) - L(L+1)}{2J(J+1)} \right] \tag{7.30}$$

$$= \mu_B M_J g_J B_z, \tag{7.31}$$

where

$$g_J = 1 + \left[\frac{J(J+1) + S(S+1) - L(L+1)}{2J(J+1)} \right] \tag{7.32}$$

is known as the *Landé g-factor*.

An example of the weak-field Zeeman effect when $S \neq 0$ can be seen in Figure 7.4 for the case of the $2\,^2\mathrm{P}$ term in the H atom. For the range of magnetic fields considered in this figure, the Zeeman energy shifts of all of the M_J sublevels are smaller than the spin-orbit energy splitting, ΔE_{SO}.

For atomic levels with non-zero total electron spin the electric dipole selection rules for transitions between Zeeman sublevels require that

$$\Delta M_J = 0, \pm 1. \tag{7.33}$$

This leads to sets of allowed electric dipole transitions such as those indicated in Figure 7.5(a) in the case of the $3\,^2\mathrm{P}_{1/2}$ and $3\,^2\mathrm{P}_{3/2}$ levels in the Na atom. The transitions indicated in this figure between levels for which $\Delta J = 0$ give rise to spectra of the kind depicted in Figure 7.5(b). The form of such spectra, with two pairs of equally spaced lines separated by a larger interval, has led to this weak-field Zeeman effect when $S \neq 0$ being known as the *anomalous Zeeman effect*.

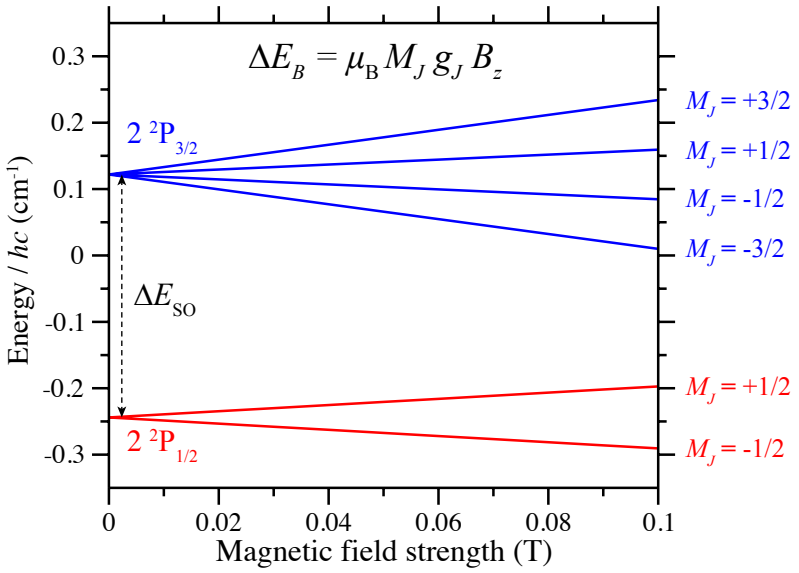

Figure 7.4: The weak-field Zeeman effect in the $2\,^2P_{1/2}$ and $2\,^2P_{3/2}$ levels of the H atom. In zero magnetic field the two levels are separated in energy by the spin-orbit splitting, ΔE_{SO}.

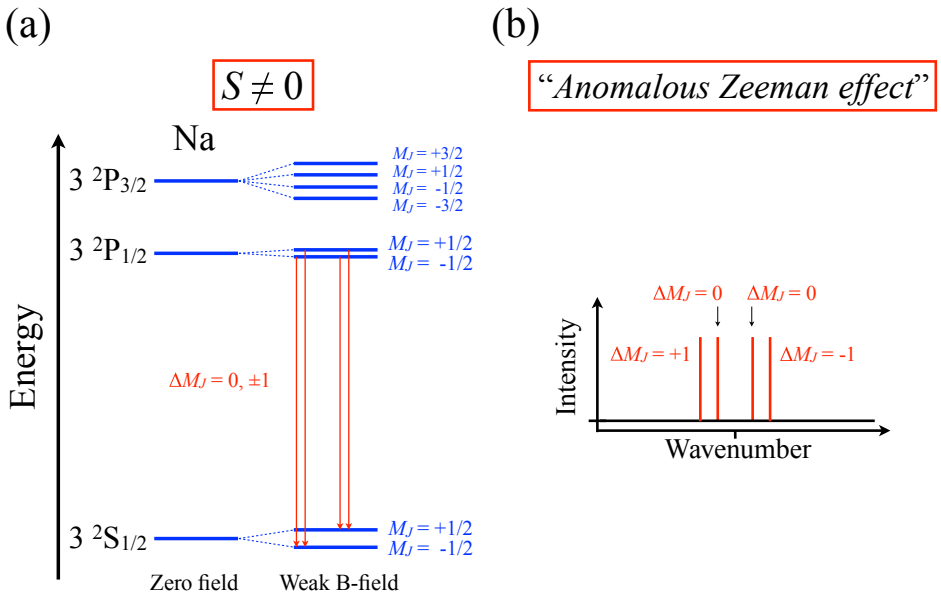

Figure 7.5: Schematic diagrams (a) indicating the electric dipole allowed transitions between Zeeman sublevels when $S \neq 0$ in the Na atom, and (b) the corresponding spectral intensity distributions.

7.4 Zeeman effect when $S \neq 0$ (strong-field regime)

In strong magnetic fields, when

$$V_B \gg \hat{H}_{\mathrm{SO}} \tag{7.34}$$

and therefore

$$\Delta E_B \gg \Delta E_{\mathrm{SO}}, \tag{7.35}$$

the external magnetic field can be considered larger than the internal magnetic fields of the atom and the total orbital angular momentum vector $\vec{L}$ and the total electron spin vector $\vec{S}$ decouple from each other and precess independently about the magnetic field vector. Therefore in this case

$$V_B = -\vec{\mu}_S \cdot \vec{B} - \vec{\mu}_L \cdot \vec{B} \tag{7.36}$$

$$= \frac{\mu_{\mathrm{B}}}{\hbar} g_{\mathrm{e}} \vec{S} \cdot \vec{B} + \frac{\mu_{\mathrm{B}}}{\hbar} g_L \vec{L} \cdot \vec{B} \tag{7.37}$$

$$= \frac{\mu_{\mathrm{B}}}{\hbar} \vec{B} \cdot (\vec{L} + 2\vec{S}). \tag{7.38}$$

As above, if $\vec{B} = (0, 0, B_z)$,

$$V_B = \frac{\mu_{\mathrm{B}}}{\hbar} B_z \, (L_z + 2\, S_z), \tag{7.39}$$

and therefore

$$\Delta E_B = \int \psi_0^* \, \frac{\mu_{\mathrm{B}}}{\hbar} B_z \, (\hat{L}_z + 2\, \hat{S}_z) \, \psi_0 \, \mathrm{d}\tau \tag{7.40}$$

$$= \mu_{\mathrm{B}} B_z \, (M_L + 2 M_S). \tag{7.41}$$

This strong-field regime, in which the magnetic field decouples $\vec{L}$ and $\vec{S}$, is known as the *Paschen-Back regime*.

A schematic diagram of the energy level structure of lowest lying energy levels in the Na atom in the Paschen-Back regime can be seen in Figure 7.6 (right hand side). In this regime the electric dipole selection rules for transitions between Zeeman sublevels require that

$$\Delta M_L = 0, \pm 1 \tag{7.42}$$

$$\Delta S = 0, \tag{7.43}$$

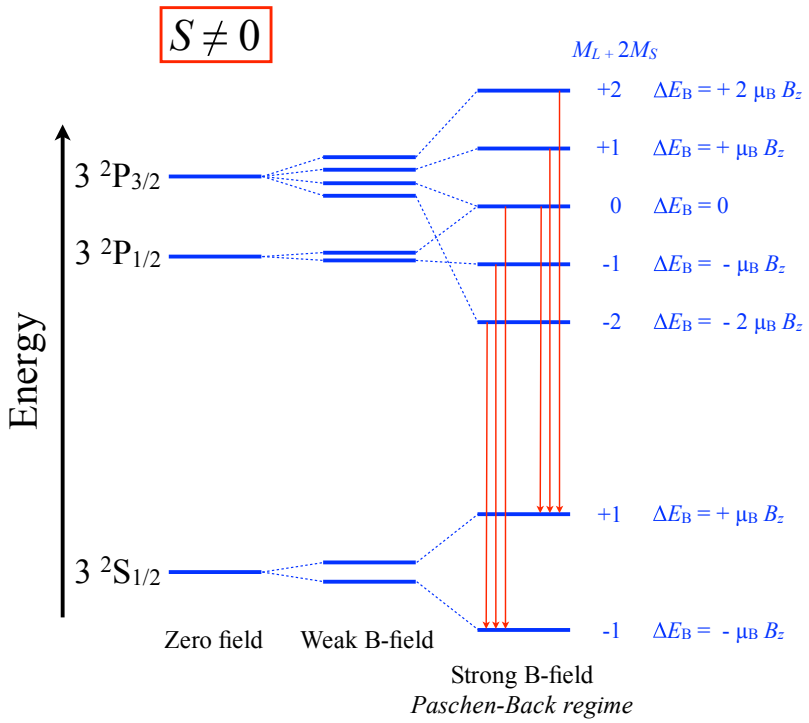

Figure 7.6: Schematic diagrams of the changes in atomic energy level structure when $S \neq 0$ in weak and strong magnetic fields. The red arrows indicate the electric dipole allowed transitions in the Paschen-Back regime.

and in the case of the ground and first excited states of Na are indicated by the red arrows in Figure 7.6.

7.5 The Stern-Gerlach experiment

The seminal experiments of Gerlach and Stern in the early 1920s in which space-quantisation was demonstrated exploited beams of ground-state silver (Ag) atoms. The ground level of Ag is a $^2S_{1/2}$ level, with $S = 1/2$, $L = 0$ and $J = 1/2$. This term exhibits no spin-orbit splitting and so there is now distinction between the Zeeman effect in strong and weak fields with the

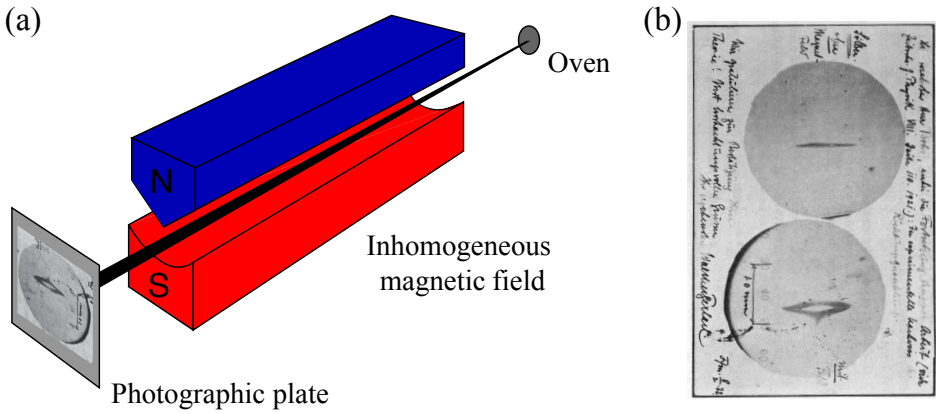

Figure 7.7: (a) Schematic diagram of the apparatus used by Stern and Gerlach to deflect/split beams of silver atoms into their different Zeeman components using inhomogeneous magnetic fields. (b) Images recorded by Gerlach and Stern of the undeflected beam (bottom panel) and the deflected/split beam (bottom panel)[2].

result that

$$\Delta E_B = \mu_B g_J M_J B_z \tag{7.44}$$

$$= \mu_B g_e M_S B_z \tag{7.45}$$

$$= 2\mu_B M_S B_z. \tag{7.46}$$

In Gerlach and Stern's experiments, forces were exerted on the atoms in the $M_J = M_S = \pm 1/2$ Zeeman sublevels by generating inhomogeneous magnetic fields with strong gradients transverse to the direction of propagation of the atomic beam (see Figure 7.7).

When an atom is subjected to a magnetic field $\vec{B}$, its potential energy, V, in the field is given by the Zeeman energy shift, ΔE_B, of the sublevel in which it is prepared. If the magnetic field is inhomogeneous, the potential energy of the atom is therefore position dependent and at any position in the field the atom experiences a force, $\vec{f}$, equal to the negative gradient of

[2]W. Gerlach and O. Stern, Der experimentelle Nachweis des magnetischen Moments des Silberatoms, *Z. Phys.* **8**, 110 (1921); W. Gerlach and O. Stern, Der experimentelle Nachweis der Richtungsquantelung im Magnetfeld, *Z. Phys.* **9**, 349 (1922); W. Gerlach and O. Stern, Das magnetische Moment des Silberatoms, *Z. Phys.* **9**, 353 (1922)

the potential, i.e.,

$$\vec{f} = -\nabla V. \tag{7.47}$$

Considering only the z-component of the field gradient, the force exerted on the atom in the z-dimension, f_z, is therefore

$$f_z = -\frac{\partial V}{\partial z} \tag{7.48}$$

$$= -2\mu_B M_S \frac{\partial B_z}{\partial z}. \tag{7.49}$$

Hence, an equal but opposite force will be exerted on the $M_S = +1/2$ and $M_S = -1/2$ Zeeman sublevels causing the beam to be split as seen in the experiments of Gerlach and Stern (Figure 7.7). In the case depicted in Figure 7.7(a) where the magnetic field is very strong close to the upper magnet pole piece, and weak close to the lower magnet pole piece the magnetic field gradient is greatest in the vertical direction. As a result atoms in the $M_S = +1/2$ sublevel will be forced downwards, and atoms in the $M_S = -1/2$ sublevel will be forced upwards splitting the beam into its two Zeeman components as seen in the lower panel in Figure 7.7(b).

7.6 Multistage Zeeman deceleration of atomic beams

Forces of the same origin as those in the experiments of Gerlach and Stern can also be exploited to decelerate beams of neutral atoms if the magnetic field gradients are generated along the axis of propagation of the beams. This can be achieved if a beam of atoms in a sublevel with $M_J > 0$ enters an electromagnet travelling along the axis of the coil (see Figure 7.8). As an atom in such a state travels into the coil, it experiences a positive magnetic field gradient on the axis of the coil and therefore, if the axis of the coil is chosen to lie along the z-axis, a decelerating force as given by Equation 7.49. Because the energy of the Zeeman sublevel of the atom increases as the atom enters the field, the atoms must lose kinetic energy. If the coil is left on the atoms would then accelerate out the other side when they experience the negative magnetic field gradient. However, if the current flowing in

the coil is switched off rapidly when the atoms have reached the magnetic field maximum, they will only experience the decelerating force and will therefore be slowed down.

Typically in experiments of the kind depicted in Figure 7.8 beams of H atom can be generated with initial speeds of 500 m/s and magnetic fields of up to 2 T can be generated in the coils of the decelerator with gradients on the order of 2 T/cm. At this speed the atoms have an initial kinetic energy of

$$E_{\text{kin}} = \frac{1}{2} M_{\text{H}} v^2 \tag{7.50}$$
$$\simeq 2.0 \times 10^{-22} \text{ J}. \tag{7.51}$$

However, the maximum Zeeman shift of the $M_J = M_S = +1/2$ sublevel in the magnetic field of one decelerator coil is

$$\Delta E_B = 2\mu_{\text{B}} M_S B_z \tag{7.52}$$
$$\simeq 2.0 \times 10^{-23} \text{ J}. \tag{7.53}$$

Therefore all of the kinetic energy of an individual atom cannot be removed in one coil (stage) of the decelerator. Therefore

$$\frac{E_{\text{kin}}}{\Delta E_B} = 10 \tag{7.54}$$

coils (stages) are required to completely decelerate the atoms from 500 m/s to zero velocity in the laboratory-fixed frame of reference. A device of the kind depicted in Figure 7.8 can be employed to achieve this. The decelerated atoms can then be trapped in a magnetic quadrupole trap at the end of the decelerator (see Section 4.4).

[3] N. Vanhaecke, U. Meier, M. Andrist, B. H. Meier, and F. Merkt, Multistage Zeeman deceleration of hydrogen atoms, *Phys. Rev. A* **75**, 031402(R) (2007); S. D. Hogan, A. W. Wiederkehr, H. Schmutz, and F. Merkt, Magnetic Trapping of Hydrogen after Multistage Zeeman Deceleration, *Phys. Rev. Lett.* **101**, 143001 (2008).

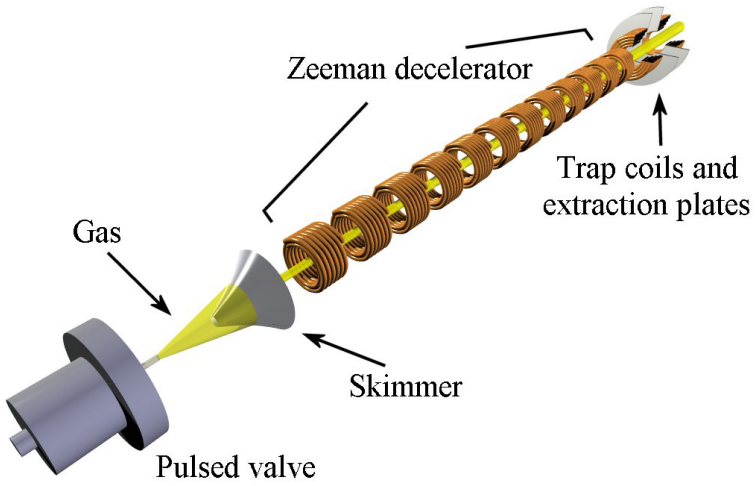

Figure 7.8: Schematic diagram of a multistage Zeeman decelerator used for decelerating beams of H and D atoms[3].

Chapter 8

Hyperfine structure

Atomic nuclei are composed of protons and neutrons. These are Fermions with spin angular momenta of 1/2. When they bind to form the nucleus of an atom the spin angular momenta of these individual particles can be combined, giving rise to a total nuclear spin vector $\vec{I}$.

In the same way that there is a magnetic dipole moment associated with the spin of the electron, a magnet dipole moment, $\vec{\mu}_I$, can be associated with a nuclear spin such that

$$\vec{\mu}_I = g_{\mathrm{N}}\,\mu_{\mathrm{N}}\,\frac{\vec{I}}{\hbar}, \tag{8.1}$$

where

$$\mu_{\mathrm{N}} = \frac{m_{\mathrm{e}}}{m_{\mathrm{p}}}\,\mu_{\mathrm{B}} \tag{8.2}$$

is known as the *nuclear magneton*, and g_{N} is the *nuclear spin g-factor* which depends on the structure of the nucleus. For example, the proton spin g-factor is $g_{\mathrm{p}} = 5.6$, while the neutron spin g-factor is $g_{\mathrm{n}} = -3.8$. The total nuclear spin quantum number depends strongly on the nuclear structure, with some examples given in Table 8.1.

The nuclear magnetic moment in an atom can give rise to energy level shifts that are analogous to those associated with the spin-orbit interaction. However, in this case the energy shifts, ΔE_{HFS}, depend on the interaction of the nuclear magnetic moment with the total electron angular momentum

Isotope	Nuclear spin
H	$I = 1/2$
^{12}C	$I = 0$
^{16}O	$I = 0$
^{13}C	$I = 1/2$
^{14}O	$I = 5/2$

Table 8.1: Nuclear spins of selected atomic isotopes.

and total electron spin, i.e.,

$$\Delta E_{\text{HFS}} \propto \vec{I} \cdot \vec{J} \tag{8.3}$$

and

$$\Delta E_{\text{HFS}} \propto \vec{I} \cdot \vec{S}. \tag{8.4}$$

The energy shifts arising from these interactions are known as the atomic *hyperfine structure* (HFS) of the atom. Hyperfine interactions lift the energy degeneracy of levels with different values of the total angular momentum quantum number including nuclear spin, F. The vector associated with this this total angular momentum quantum number is $\vec{F}$, where

$$\vec{F} = \vec{J} + \vec{I}, \tag{8.5}$$

and the quantum numbers then take the values

$$F = |J - I|, \ldots, |J + I| \text{ in steps of 1.} \tag{8.6}$$

As an example of the hyperfine structure of an atomic energy level, consider the $1\,^2S_{1/2}$ ground state of the H atom. This has

$$S = 1/2 \tag{8.7}$$

$$J = 1/2, \tag{8.8}$$

and because the proton has a spin of 1/2,

$$I = 1/2. \tag{8.9}$$

Therefore the possible values of F are

$$F = 0, 1. \tag{8.10}$$

As a result of the hyperfine interaction, the levels with these two different total orbital angular momenta including nuclear spin are separated in energy by the hyperfine splitting, ΔE_{HFS}. For this particular case

$$\frac{\Delta E_{\mathrm{HFS}}}{hc} = 0.047\ \mathrm{cm}^{-1}. \tag{8.11}$$

The transition between these two hyperfine sublevels occurs at a wavelength of

$$\lambda \simeq 21\ \mathrm{cm}, \tag{8.12}$$

in the radio frequency region of the electromagnetic spectrum. The emission of radiation in the decay of H atoms via this transition is of importance in astronomical spectroscopy of interstellar gas clouds. Because it has a very small Einstein A-coefficient of

$$A_{\mathrm{HFS}} \simeq 2.9 \times 10^{-15}\ \mathrm{s}^{-1}, \tag{8.13}$$

the decay of a sample of ground state H atoms via this transition occurs very slowly with a timescale on the order of

$$\tau_{\mathrm{fl}} = \frac{1}{A_{\mathrm{HFS}}} = 11 \times 10^{6}\ \text{years}. \tag{8.14}$$

Chapter 9

Atoms in electric fields

9.1 Introduction

The Stark effect, i.e., the effect of an externally applied electric field, $\vec{F}$, on the energy level structure of an atom, arises from the interaction of the electric dipole moment of the atom $\vec{\mu}_{\rm elec}$ with the field.

For two equal but opposite charges, $q_1 = +e$ and $q_2 = -e$, separated by a distance $\vec{r}$ (see Figure 9.1), the corresponding electric dipole moment is

$$\vec{\mu}_{\rm elec} = -e\,\vec{r}. \tag{9.1}$$

In the presence of the field the potential energy, V_F, of this dipole is

$$V_F = -\vec{\mu}_{\rm elec} \cdot \vec{F}. \tag{9.2}$$

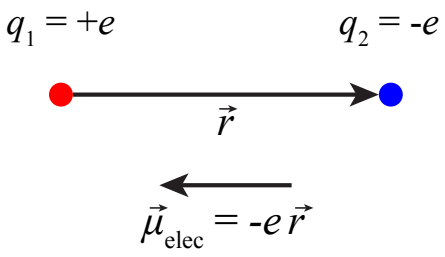

Figure 9.1: The electric dipole moment, $\vec{\mu}_{\rm elec}$, associated with two charges separated by a distance $\vec{r}$.

If the electric field is acts in the z-direction, i.e., if $\vec{F} = (0, 0, F_z)$, considering the expression in Equation 9.1, this then becomes

$$V_F = e F_z z. \tag{9.3}$$

In the following we will consider two regimes. one in which the effect of the electric field on the atom is weak and the Stark shifts are small compared to the energy differences between the unperturbed states with different values of n, i.e.,

$$V_F \ll \frac{e^2}{4\pi\epsilon_0 r}. \tag{9.4}$$

In this case, results from perturbation theory can be applied to determine the effects of the field on the energy level structure. The second regime will be that in which the electric field strongly modifies the potential experienced by the electron in the atom leading to ionisation, i.e.,

$$V_F \gg \frac{e^2}{4\pi\epsilon_0 r}. \tag{9.5}$$

This regime is reached for low values of n in very strong electric fields, or for high values of n in weaker fields.

9.2 Stark effect in weak fields

In general weak electric fields give rise to shifts and splittings of atomic energy levels. Energy levels with different orbital angular momentum quantum numbers that are degenerate in energy exhibit linear Stark shifts, i.e., $\Delta E_F \propto F$, while non-degenerate levels exhibit quadratic Stark shifts, i.e., $\Delta E_F \propto F^2$.

9.2.1 Quadratic Stark effect

In situations where an atom has no intrinsic electric dipole moment, i.e., in non-degenerate states, linear Stark energy shifts do not occur. In such cases states only exhibit quadratic Stark shifts. This can be understood by calculating the expectation value for the Stark Hamiltonian operator, V_F (see Equation 9.3), for a non-degenerate state. Considering for example the

non-degenerate $1\,^2S_{1/2}$ ground state of the H atom with the wavefunction $\psi_{n\ell m} = \psi_{100}$,

$$\Delta E_F = \int \psi^*_{100}\, e\, F_z \hat{z}\, \psi_{100}\, \mathrm{d}\tau \tag{9.6}$$

$$= e F_z \int \underbrace{\psi^*_{100}}_{\text{even}} \underbrace{\hat{z}}_{\text{odd}} \underbrace{\psi_{100}}_{\text{even}}\, \mathrm{d}\tau \tag{9.7}$$

$$= 0. \tag{9.8}$$

This indicates that the part of the operator associated with the electric dipole moment, $\hat{\mu}_{\text{elec}} = e\hat{z}$, is zero and in this state the atom has no intrinsic electric dipole moment.

However, the electric field can polarise the atom by redistributing the charge of the electron. This leads to an induced electric dipole moment the magnitude and direction of which depends on the magnitude and direction of the electric field vector,

$$\vec{\mu}_{\text{elec}} \propto \vec{F}. \tag{9.9}$$

In this case, the energy shift of a non-degenerate state in an electric field can be determined by applying second order perturbation theory. For a perturbing potential V, the the energy shift of a state, $\psi_{n\ell m}$, is given to second order by perturbation theory as

$$\Delta E_V = \int \psi^*_{n\ell m} V\, \psi_{n\ell m}\, \mathrm{d}\tau + \sum_{n'\ell'm' \neq n\ell m} \frac{\left| \int \psi^*_{n'\ell'm'} V\, \psi_{n\ell m}\, \mathrm{d}\tau \right|^2}{E_{n\ell m} - E_{n'\ell'm'}}. \tag{9.10}$$

Therefore in this case

$$\Delta E_V = e^2 F_z^2 \sum_{n'} \sum_{\ell=\ell\pm1} \frac{\left| \int \psi^*_{n'\ell'm'} \hat{z}\, \psi_{n\ell m}\, \mathrm{d}\tau \right|^2}{E_{n\ell m} - E_{n'\ell'm'}}. \tag{9.11}$$

The restrictions on the range of values of ℓ and ℓ' in the sum arises from the form of the $\hat{z}$ operator. Since

$$z = r\cos\theta \tag{9.12}$$

$$= r\sqrt{\frac{4\pi}{3}} Y_{10}, \tag{9.13}$$

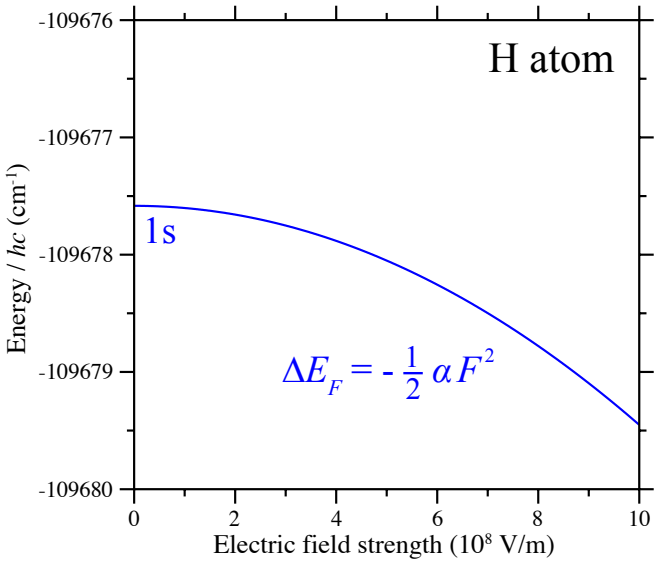

Figure 9.2: The quadratic Stark effect in the $1\,^2S_{1/2}$ ground state of the H atom.

the integral in the sum only has non-zero values when the values of ℓ and ℓ' differ by 1 and the values of m and m' are equal.

In the ground state of the H atom

$$\Delta E_F = e^2 F_z^2 \sum_{n'} \frac{\left|\int \psi^*_{n10}\, \hat{z}\, \psi_{100}\, \mathrm{d}\tau\right|^2}{E_{100} - E_{n'10}} \tag{9.14}$$

$$= -\frac{1}{2}\alpha F_z^2, \tag{9.15}$$

where

$$\alpha = -2e^2 \sum_{n'} \frac{\left|\int \psi^*_{n10}\, \hat{z}\, \psi_{100}\, \mathrm{d}\tau\right|^2}{E_{100} - E_{n'10}} \tag{9.16}$$

is the *electric dipole polarizability*. Since

$$\Delta E_F = -\frac{1}{2}\alpha F_z^2 \tag{9.17}$$

$$= -\left[\frac{1}{2}\alpha F_z\right] F_z, \tag{9.18}$$

comparison with Equation 9.2 indicates that $\alpha F_z/2$ is the induced electric dipole moment of the state in the presence of the field. For the ground state

of the H atom

$$\alpha = 7.42 \times 10^{-41}\,\mathrm{C\,m^2\,V^{-1}}, \tag{9.19}$$

and the corresponding dependence of the ground state energy on the strength of the applied electric field can be seen in Figure 9.2.

The quadratic Stark shift generally lowers the energy of an isolated non-degenerate energy level. This is because the electric dipole moment induced by the field lies parallel to the field vector.

9.2.2 Linear Stark effect

If an atom possesses an intrinsic electric dipole moment, which is the case when the electron is in an orbital with a value of the orbital angular momentum quantum number ℓ that is degenerate in energy with other orbitals with different values of ℓ, the states exhibit linear Stark shifts. For example, in excited states of the H atom for every value of $n > 1$, levels with all allowed values of ℓ are degenerate, as a result excited states of the H atom always exhibit linear Stark shifts. As in the case of the quadratic Stark shift, the Stark Hamiltonian operator (see Equation 9.3) mixes states according to the electric dipole selection rules that require that $\Delta\ell = \pm 1$ and $\Delta m = 0$.

Consider the states with $n = 2$ in the H atom (see Figure 9.3). Because of the selection rules associated with the Stark Hamiltonian operator, the field can only mix the 2s state for which $m_\ell = 0$ (i.e., the state ψ_{200}) with the 2p state for which $m_\ell = 0$ (i.e., the state ψ_{210}). But it will not mix (affect) the 2p states for which $m_\ell = \pm 1$. Therefore the new eigenstates of the complete Hamiltonian

$$\hat{H} = \hat{H}_0 + V_F, \tag{9.20}$$

expressed in terms of the field-free wavefunctions, must take the form

$$\psi_1 = \psi_+ = \frac{1}{\sqrt{2}}\left(\psi_{200} + \psi_{210}\right) \tag{9.21}$$

$$\psi_2 = \psi_- = \frac{1}{\sqrt{2}}\left(\psi_{200} - \psi_{210}\right) \tag{9.22}$$

$$\psi_3 = \psi_{21-1} \tag{9.23}$$

$$\psi_4 = \psi_{21+1}. \tag{9.24}$$

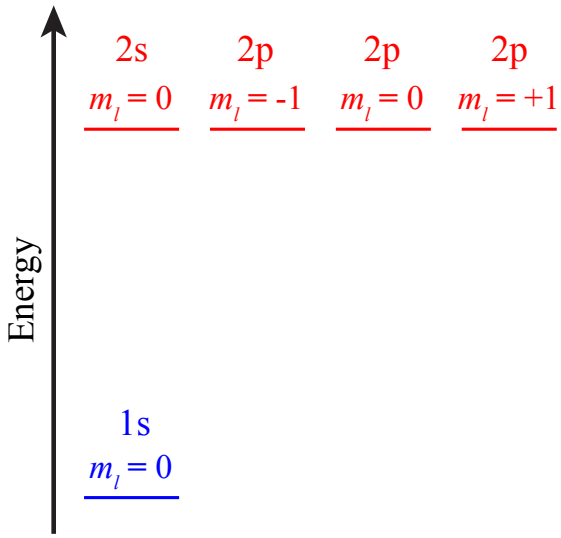

Figure 9.3: Energy levels in the H atom for which $n = 1$ and $n = 2$.

Energy shifts

To determine the energy shifts of the states $\psi_\pm$ in the field first order perturbation theory can be applied and the expectation value of V_F determined, i.e.,

$$\Delta E_F = \int \psi_\pm^* V_F \, \psi_\pm \, \mathrm{d}\tau \tag{9.25}$$

$$= \frac{1}{2} \int (\psi_{200} \pm \psi_{210})^* \, eF_z\hat{z} \, (\psi_{200} \pm \psi_{210}) \, \mathrm{d}\tau \tag{9.26}$$

$$= \frac{1}{2} eF_z \left[\int \psi_{200}^* \, \psi_{200} \, \mathrm{d}\tau + \int \psi_{210}^* \, \psi_{210} \, \mathrm{d}\tau + \ldots \right.$$
$$\left. \pm \int \psi_{200}^* \, \psi_{210} \, \mathrm{d}\tau \pm \int \psi_{210}^* \, \psi_{200} \, \mathrm{d}\tau \right]. \tag{9.27}$$

Expressing each of the wavefunctions as a product of a radial wavefunction and a spherical harmonic function, such that

$$\psi_{200} = R_{20}(r) \, Y_{00}(\theta, \phi), \tag{9.28}$$

$$\psi_{210} = R_{21}(r) \, Y_{10}(\theta, \phi), \tag{9.29}$$

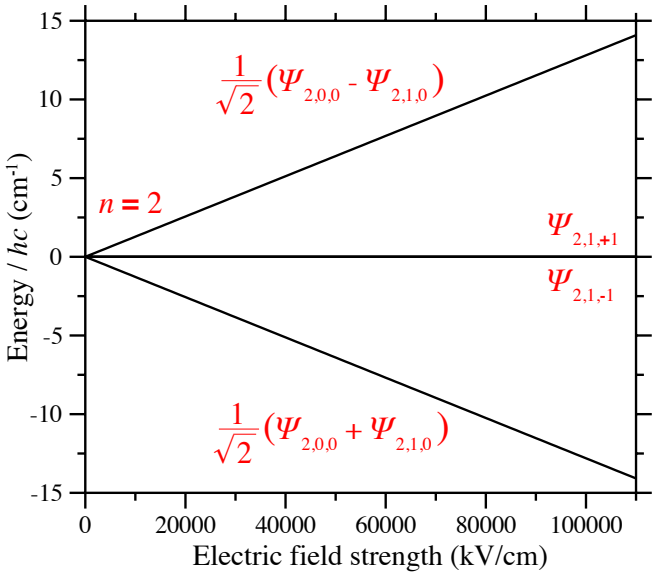

Figure 9.4: The linear Stark effect in the $n = 2$ states in the H atom.

using the analytic forms of these functions in Table 2.2 and in Table 2.1, and expressing the $\hat{z}$ operator in terms of a spherical harmonic function as

$$z = r\cos\theta \tag{9.30}$$

$$= r\sqrt{\frac{4\pi}{3}}\,Y_{10}(\theta,\phi), \tag{9.31}$$

leads to the result that

$$\Delta E_F^{\pm} = \mp 3\,ea_0\,F_z, \tag{9.32}$$

where a_0 is the Bohr radius. Comparing this expression to Equation 9.2 indicates that for these states

$$-\mu_{\text{elec}}^{\pm} = \mp 3\,ea_0, \tag{9.33}$$

and therefore

$$\mu_{\text{elec}}^{\pm} = \pm 3\,ea_0. \tag{9.34}$$

The energy shifts of all four states with $n = 2$ in the H atom in the presence of an electric field are displayed in Figure 9.4. The states $\psi_3 = \psi_{21-1}$

and $\psi_4 = \psi_{21+1}$ are not affected by the field. They therefore do not possess any intrinsic electric dipole moments and do not change their energy as the field strength increases.

Because the wavefunctions $\psi_\pm$ are also eigenstates of the field-free Hamiltonian, no energy is required to mix them as a result an intrinsic electric dipole moment exists within the atom and it is not necessary for the field to induce the dipole moment. Consequently, in this case

$$\Delta E_F \quad \propto \quad F_z. \tag{9.35}$$

Electron charge distributions

The wavefunctions $\psi_\pm$ can be expressed in the form

$$\psi_\pm \quad = \quad \frac{1}{\sqrt{2}} \left(R_{20}\, Y_{00} \pm R_{21}\, Y_{10} \right) \tag{9.36}$$

$$= \quad \frac{1}{\sqrt{8\pi}} \left(R_{20} \pm R_{21}\ \sqrt{3} \cos\theta \right). \tag{9.37}$$

Using these expressions the electron probability distributions $|\psi_\pm|^2\, r^2$ can be calculated and are displayed in Figure 9.5. This shows that in the ψ_- state [Figure 9.5(a)] the electron charge is localised along the electric field axis away from the positively charged proton. As a result the electric dipole moment of the atoms is antiparallel to the electric field vector leading to a positive Stark energy shift. On the other hand in the ψ_+ state [Figure 9.5(b)] the electron charge is localised behind the proton with the result that the electric dipole moment is oriented parallel to the electric field vector. This leads to a negative Stark energy shift.

9.3 Ionisation in strong electric fields

In strong electric fields the Stark Hamiltonian, V_F, significantly modifies the Coulomb potential, V_C, experienced by an electron within an atom and can lead to electric field ionisation. The origin of this effect can be seen by considering the potential energy part, $V(z)$, of the total Hamiltonian

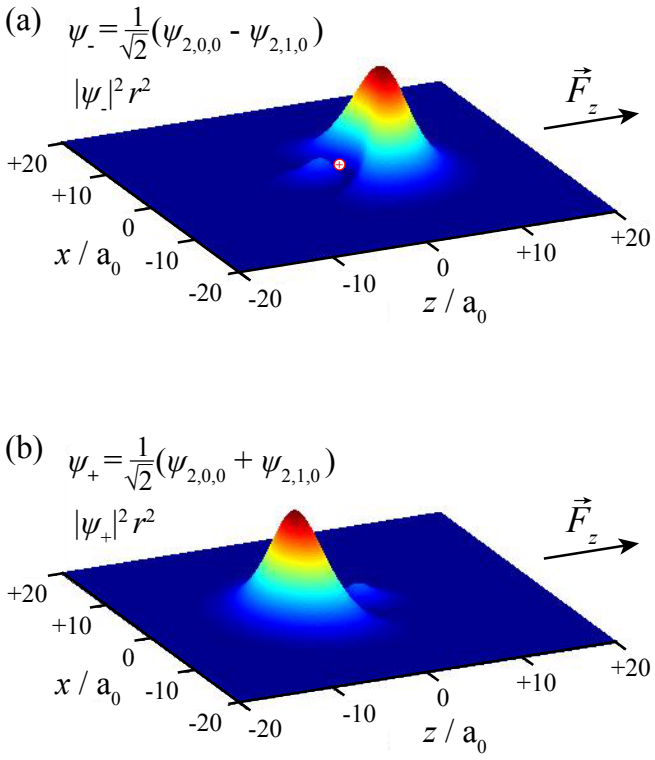

Figure 9.5: Electron charge distributions in (a) the ψ_-, and (b) ψ_+ $n = 2$ Stark states in the H atom. In each figure the proton is located at the origin of the coordinate system indicated by the '$\oplus$' symbol in (a).

operator in the direction of an applied field

$$V(z) = V_C(z) + V_F \tag{9.38}$$

$$= -\frac{e^2}{4\pi\epsilon_0 z} + eF_z z. \tag{9.39}$$

This can be seen in Figure 9.6 in which the pure Coulomb potential associated with the H atom containing excited states with high values of n is displayed, together with the potential in the presence of a field $\vec{F} = (0, 0, -F_z)$. From this figure it can be seen that for the field considered, states with values of $n \geq 28$ lie higher in energy that the saddle point of the continuous curve. Therefore if the electron is in one of these states when the field is applied it will no longer remain bound to the proton and will instead be ionised.

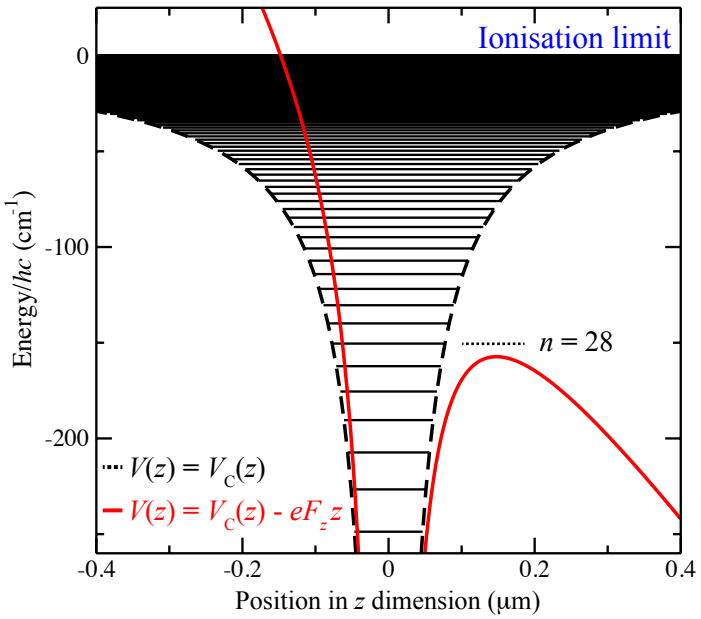

Figure 9.6: The pure Coulomb potential, V_C, experienced by the electron in the H atom (dashed black curve), with the positions of excited states with high values of n indicated. The potential that results when this potential is modified by an external electric field $\vec{F} = (0, 0, -F_z)$ is indicated by the continuous red curve.

The minimum electric field required to ionise an electron in a state with a particular value of n can be determined by equating the position of the saddle point in the potential in the presence of the field with the binding energy of the state. To calculate this field consider the situation in Figure 9.6 in which $\vec{F} = (0, 0, -F_z)$, in this case

$$V(z) = -\frac{e^2}{4\pi\epsilon_0 z} - eF_z z. \tag{9.40}$$

To determine the value of n at the saddle point in the positive z direction

$$\frac{\mathrm{d}V(z)}{\mathrm{d}z} = \frac{e^2}{4\pi\epsilon_0 z^2} - eF_z \tag{9.41}$$

$$= 0, \tag{9.42}$$

and so the position of the saddle point, z_{saddle}, is

$$z_{\text{saddle}} = \sqrt{\frac{e}{4\pi\epsilon_0 F_z}}. \tag{9.43}$$

Therefore, substituting this back into Equation 9.40, the potential energy, $V_{\text{saddle}}(z)$, of the saddle point is

$$V_{\text{saddle}}(z) = -\frac{e^2}{4\pi\epsilon_0}\sqrt{\frac{4\pi\epsilon_0 F_z}{e}} - eF_z\sqrt{\frac{e}{4\pi\epsilon_0 F_z}} \tag{9.44}$$

$$= -2\sqrt{\frac{e^3 F_z}{4\pi\epsilon_0}}. \tag{9.45}$$

To find the state with its binding energy equal to the energy of the saddle point, $V_{\text{saddle}}(z)$ can be set to equal the binding energy given by the Rydberg formula such that

$$V_{\text{saddle}}(z) = -\frac{hc\,R_{\text{H}}}{n^2}, \tag{9.46}$$

with the result that for any value of n the ionisation field, F_{ion}, is

$$F_{\text{ion}} = \frac{\pi\epsilon_0 (hc\,R_{\text{H}})^2}{e^3\,n^4} \tag{9.47}$$

and therefore

$$F_{\text{ion}} \propto \frac{1}{n^4}. \tag{9.48}$$

From this the electric field required to ionise a ground state H atom is

$$F_{\text{ion}}(n=1) \simeq 3\times 10^{10}\ \text{V/m} \tag{9.49}$$

while the electric field required to ionise a H atom in a state with $n = 100$, is

$$F_{\text{ion}}(n=100) \simeq 300\ \text{V/m} \quad (\equiv 3\ \text{V/cm}). \tag{9.50}$$

Part IV

Scattering

Chapter 10

Low-energy particle scattering

10.1 Introduction

Collisions between atoms, molecules, ions and electrons are described in general as scattering processes. In scattering processes that occur at low collision energies the quantised energy-level structure of the particles involved must be accounted for, together with their wave nature (de Broglie wavelength).

Low-energy particle scattering is of importance in the production of antihydrogen and positronium atoms, and in chemical processes at low temperatures. Low energy scattering of positrons and positronium from biomolecules also plays a role in medical imaging [positron emission tomography (PET)].

10.2 Total collision cross-section

The *total collision cross-section*, σ_T, in a scattering process is the effective area, normal to the direction of incidence, of the target in the interaction with an incoming projectile. For example, in Figure 10.1 the large target particle has a diameter of $2r$ and therefore the effective area of the target from the perspective of the incoming projectile is $\sigma_T = \pi r^2$.

In a classical scattering process between two hard spheres, the target can be considered to have hard edges with the total cross-section as de-

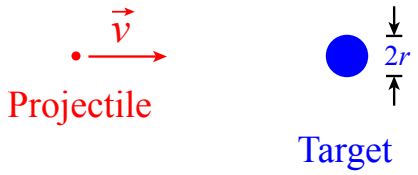

Figure 10.1: The collision of a projectile with a target particle of diameter of $2r$ leading to a total collision cross-section of $\sigma_T = \pi r^2$.

picted in Figure 10.1. However, in collisions in which charged particles are involved, e.g., in collisions of electrons and protons, or collisions of electrons with atoms with their outer electron clouds, the total cross-section can be larger than that in the classical case. This is because of the Coulomb interactions between the charges.

10.3 Beer-Lambert Law

To identify the role of the total collision cross-section in a scattering experiment consider the situation depicted schematically in Figure 10.2. In such an experiment, a beam of projectiles, labelled A, with an intensity I (Note: the intensity of the beam is the number of particles per unit area per unit time) passes through a cell of length l containing the target particles, B, at a number density n_B.

As the beam of projectiles passes through the cell the number of incident particles that are scattered or lost from the beam must be proportional to the number of target particles with which the beam interacts, i.e.,

$$\frac{dI}{I} \propto -n_B \, dz. \tag{10.1}$$

This can also be expressed as

$$\frac{dI}{I} = -\sigma_T \, n_B \, dz, \tag{10.2}$$

where the total collision cross-section, σ_T, is the constant of proportionality.

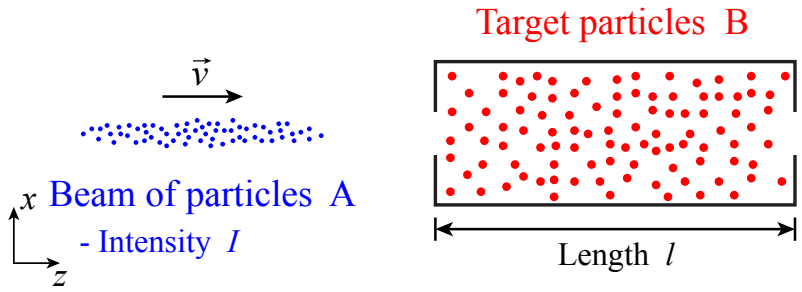

Figure 10.2: Schematic diagram of a particle scattering experiment in which a beam of projectiles, A, passes through a cell of length l filled with target particles, B. The intensity of the beam is denoted I, while the number density of target particles in the cell is n_B.

Integrating Equation 10.2 over the length of the target cell leads to

$$\int_{I_0}^{I(l)} \frac{dI}{I} = -\sigma_T n_B \int_0^l dz, \tag{10.3}$$

$$\ln(I)\Big|_{I_0}^{I(l)} = -\sigma_T n_B z\Big|_0^l \tag{10.4}$$

$$\ln[I(l)] - \ln[I_0] = -\sigma_T n_B (l - 0) \tag{10.5}$$

$$\ln\left[\frac{I(l)}{I_0}\right] = -\sigma_T n_B l, \tag{10.6}$$

and so

$$I(l) = I_0 \exp(-\sigma_T n_B l). \tag{10.7}$$

This expression, Equation 10.7, for the projectile intensity after travelling a distance l through a cell filled with target particles is known as the *Beer-Lambert Law*. By performing measurements with an apparatus of the kind depicted in Figure 10.2 at different relative collision energies the energy dependence of σ_T can be determined. Contributions from the collision energy to the total collision cross-section arise as a result of (1) the corresponding change in the interaction time, i.e., in collisions at higher energy the interaction times between the projectiles and the target are small while at lower

energy, the interaction times are longer; (2) effects of the wave nature of the particles when colliding with low energies, since the de Broglie wavelength $\lambda_{dB} = h/p$ depends on the particles momenta the increase in this wavelength at low collision energies must be considered; and (3) resonances associated with the energy level structure of the particles.

As noted above, σ_T does not represent the physical size of the target atom or molecule because of the effects of long range interactions: *Coulomb interactions*, *dipole-dipole interactions*, or *van der Waals interactions*.

The Coulomb interaction, V_C, occurs between two charged particles and and scales as

$$V_C \propto \frac{1}{R}, \tag{10.8}$$

where R is the distance between the two particles. As a result if the projectile and target particles are both charged σ_T is significantly greater than the physical size of the particles because of the effects of the long-range Coulomb interactions.

Dipole-dipole interactions, V_{dd}, occur between pairs of particles with intrinsic electric dipole moments, i.e., ionically bound ground state molecules, and scale as

$$V_{dd} \propto \frac{1}{R^3}. \tag{10.9}$$

The dipole-dipole interaction does not extend over as large a range of inter-particle distances as the Coulomb interaction, so while dipole-dipole interactions do increase σ_T compared to the physical size of the particles, in general it is not increased as significantly as in the case of the Coulomb interaction.

The van der Waals interaction, V_{vdW}, occurs between pairs of polarizable particles that do not possess intrinsic electric dipole moments. This interaction is therefore more strongly dependent on the inter-particle distance and scales as

$$V_{vdW} \propto \frac{1}{R^6}. \tag{10.10}$$

Such interactions do also increase the value of σ_T when compared to the physical size of the interaction particles, however, this increase is smaller

than that associated with either Coulomb interactions or dipole-dipole interactions.

These interactions are often said to be '*soft*' in that they soften the physical edges of two colliding hard spheres. In this sense the Coulomb interaction between two charged particles is 'softer' than the van der Waals interaction between two neutral particles.

10.4 Cross-sections

Collisions between pairs of particles can be categorised as *elastic* or *inelastic*. In elastic scattering processes only the momenta of the particles change but not the internal states, while in inelastic scattering processes the internal energy can change together with the particle momenta. For example, in the case of an electron scattering from a particle A,

Elastic scattering:

$$\mathrm{e}^- + \mathrm{A} \longrightarrow \mathrm{e}^- + \mathrm{A} \tag{10.11}$$

Inelastic scattering:

$$\begin{aligned} \mathrm{e}^- + \mathrm{A} &\longrightarrow \mathrm{e}^- + \mathrm{A}^* && (10.12)\\ &\longrightarrow \mathrm{e}^- + \mathrm{A}^+ + \mathrm{e}^- && (10.13)\\ &\longrightarrow \mathrm{A}^- + h\nu && (10.14) \end{aligned}$$

where A^* and $h\nu$ represent the particle A in an excited state, and a photon, respectively.

Because inelastic scattering processes lead to changes in the internal quantum states of the target a *total inelastic cross-section*, σ_{if}, can be associated with any pair of initial, i, and final, f, states of the target. This represents the effective area associated with a scattering event in which the target atom is transferred from state i to state f. In these processes the momenta of the colliding particles can also change.

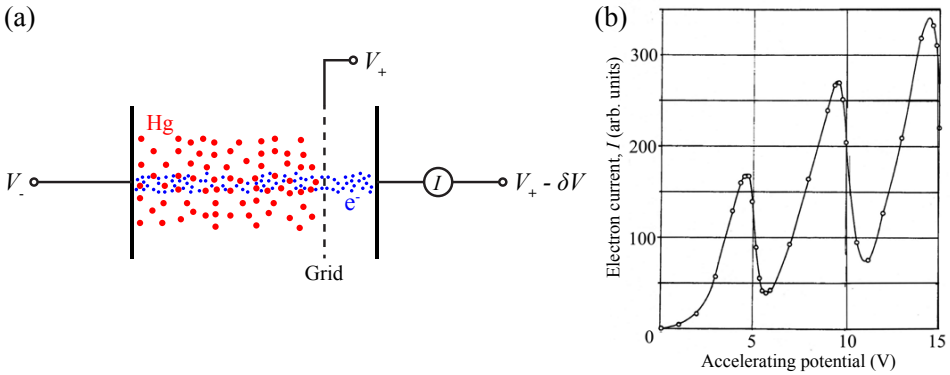

Figure 10.3: (a) Schematic diagram of the experimental apparatus used by Franck and Hertz to study inelastic scattering of electrons from Hg vapour. (b) Observed changes in electron current recorded at the anode in (a) as the accelerating potential, $V_+ - V_-$, was increased. The sharp drops in current at multiples of 4.9 V indicate an inelastic scattering resonance close to this energy.

Inelastic electron scattering was first demonstrated in a classic experiment of Franck and Hertz[1]. In their experiment, depicted schematically in Figure 10.3(a), electrons from a heated cathode operated at a potential V_- were accelerated toward a metal grid through a potential difference $V_+ - V_-$ before the resulting current, I, was measured on an anode. As the accelerating potential was increased from 0 V the electron current initially increased as expected, however, for an accelerating potential of $\sim$ 4.9 V an abrupt drop in current was observed. This reduction in electron current indicated that as the electrons passed through the Hg vapor lost kinetic energy. The resonant behaviour of this loss suggested that the energy at which it occured corresponded to the energy difference between two electronic states in Hg, and that in the electron scattering process the Hg atoms were being excited. This was later confirmed by determining the wavelength of the light, $\lambda = 254$ nm, emitted by the Hg vapor at this resonant collision energy

[1]J. Franck and G. Hertz, Über Zusammenstöße zwischen Elektronen und Molekülen des Quecksilberdampfes und die Ionisierungsspannung desselben [On the collisions between electrons and molecules of mercury vapor and the ionization potential of the same], *Verhandlungen der Deutschen Physikalischen Gesellschaft* **16** 457 (1914).

of $E/e = 4.9$ eV.

10.5 X-ray spectra

In the experiments of Franck and Hertz electrons were accelerated to kinetic energies of a few electron volts. As a result the relevant inelastic scattering processes involved the excitation of atomic electrons in the outer, most weakly bound, orbitals of Hg. Transitions involving these outer-shell electrons typically occur at photon energies corresponding to 1–10 eV, or wavelengths in the visible or ultraviolet regions of the electromagnetic spectrum.

However, if accelerated to higher energies, e.g., 1–100 keV, inelastic electron scattering can be exploited to excite tightly-bound inner-shell electrons in atoms. For example, in the Ne atom with the ground state configuration $1s^2\,2s^2\,2p^6$, the inner-shell electrons are those in the 1s orbital. Transitions involving these electrons typically occur at wavelengths from 0.1 Å to 10 Å, in the extreme ultraviolet or X-ray regions of the electromagnetic spectrum. It is difficult to generate laser radiation at these wavelengths, however, high energy inelastic electron scattering can be exploited to study transitions involving inner-shell electrons in atoms and molecules, and to generate X-ray radiation.

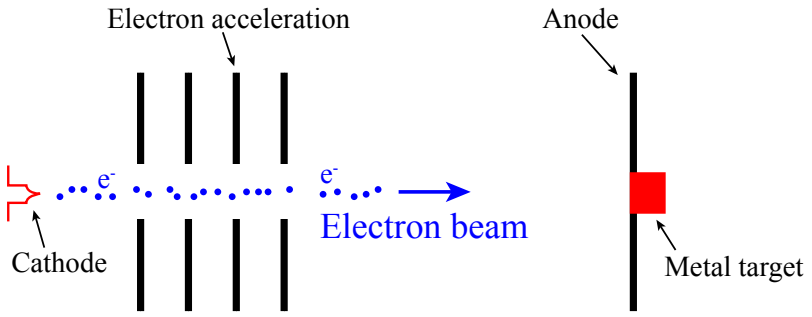

Figure 10.4: Schematic diagram of apparatus used for high energy electron bombardment of metal targets, and X-ray generation.

To study transitions driven by electron bombardment of metal tar-

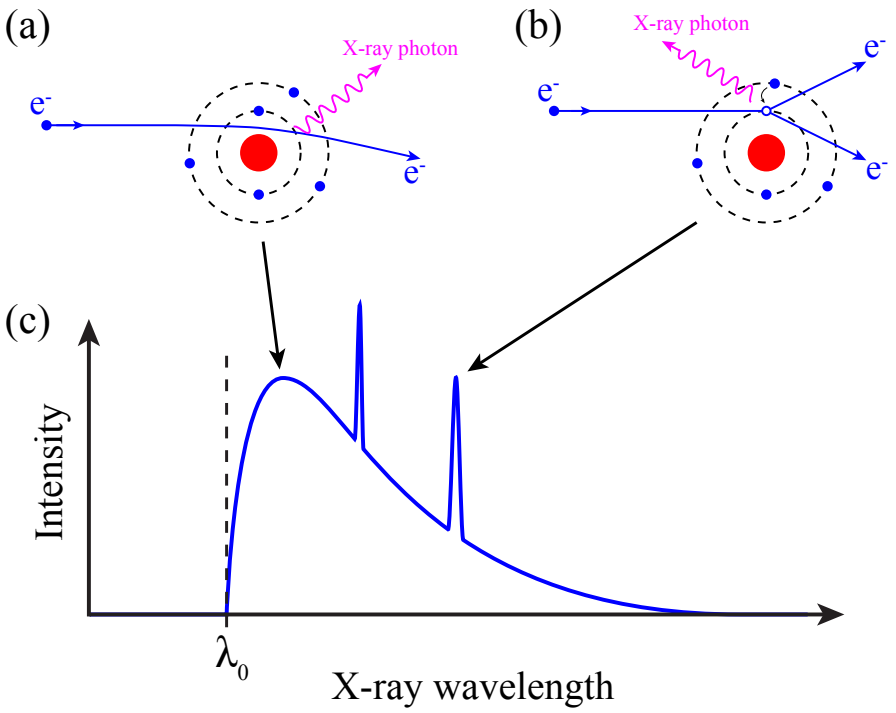

Figure 10.5: (a) The electron acceleration in the Coulomb field of the nucleus that gives rise to the broad background continuum in an X-ray spectrum. (b) The inner-shell excitation process that gives rise the sharp features in an X-ray spectrum. (c) A schematic X-ray spectrum.

gets, experimental arrangements of the kind depicted schematically in Figure 10.4 are typically employed. The excitation of inner-shell electrons by inelastic electron scattering leads to the emission of X-ray photons. The resulting X-ray spectra have two components (1) a broad background continuum, and (2) sharp features characteristic of the target atom or molecule. These components can be seen in Figure 10.5(c).

Continuous spectrum: The broad background continuum in an X-ray spectrum arises as a result of the acceleration of an incoming electron in the Coulomb field of the positively charged nucleus [see Figure 10.5(a)]. In general if accelerated a charged particle emits radiation. This emission is not quantised and appears as a continuous component of the complete X-ray spectrum [see Figure 10.5(c)]. The maximum X-ray

photon energy corresponds to the incoming electron being decelerated to a stand-still as it passes the nucleus of the target atom. When this occurs the wavelength of the emitted photon, λ_0, is

$$\lambda_0 = \frac{hc}{E_{\rm i}}, \tag{10.15}$$

where $E_{\rm i}$ is the initial kinetic energy of the incident electron.

Discrete spectrum: The discrete (sharp) components of an X-ray spectrum result from an incident electron colliding with an inner-shell electron in the atom leaving a *hole* [see Figure 10.5(b)]. When this occurs the electronic configuration of the atom is no longer the lowest in energy for the remaining electrons. Consequently, the electrons rearrange and an electron from a higher orbital can decay to fill the hole. In this process an X-ray photon is emitted. This photon has an energy equal to the energy difference between the excited state from which the atomic electron decayed, and the state containing the hole. This process results in the sharp features in Figure 10.5(c). The photon energies at which these sharp features appear are dependent on the energy level structure of the target atom.

A first approximation to the energies of the sharp features in X-ray spectra can be obtained by assuming that they can be described by an equation similar to the Rydberg formula. In this case, the energy, ΔE, associated with each sharp line corresponds to the difference in energy between an initial state, E_i, and a final state, E_f, such that

$$\frac{\Delta E}{hc} = \frac{E_i - E_f}{hc} \tag{10.16}$$

$$\simeq R_\infty Z_{\rm eff}^2 \left[\frac{1}{n_f^2} - \frac{1}{n_i^2}\right], \tag{10.17}$$

where $Z_{\rm eff} = Z_{\rm nucl} - S$, with $Z_{\rm nucl}$ the nuclear charge, and S a screening constant.

X-ray transitions therefore form series each of which is associated with the decay to a particular final state. Transitions for which $n_f = 1$ form a

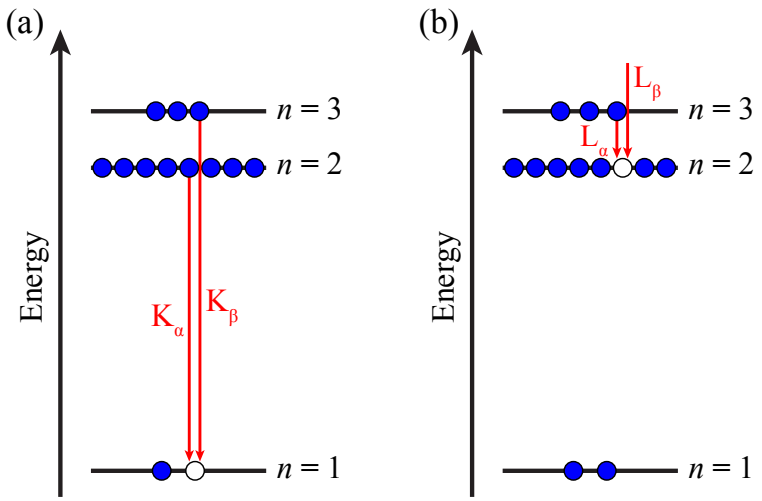

Figure 10.6: Schematic diagrams indicating the $\Delta n = -1$, α, and $\Delta n = -2$, β, transitions in (a) the K series, and (b) the L series of X-ray spectral lines.

series known as the K series, while transitions for which $n_f = 2$ form a series known as the L series, and transitions for which $n_f = 3$ form the M series etc. . . In each series, transitions with $\Delta n = -1$, $\Delta n = -2$. . . are known as the α, β, . . . , respectively. For example

$$n_i = 2 \longrightarrow n_f = 1 \Rightarrow \mathrm{K}_\alpha \text{ line} \tag{10.18}$$

$$n_i = 3 \longrightarrow n_f = 1 \Rightarrow \mathrm{K}_\beta \text{ line} \tag{10.19}$$

$$n_i = 3 \longrightarrow n_f = 2 \Rightarrow \mathrm{L}_\alpha \text{ line} \tag{10.20}$$

$$n_i = 5 \longrightarrow n_f = 2 \Rightarrow \mathrm{L}_\gamma \text{ line} \tag{10.21}$$

10.6 Moseley's Law

An empirical expression for the frequencies, ν_{if}, of sharp X-ray spectral lines (see Figure 10.7) was identified by Henry Moseley and is known as *Moseley's law*[2]. Moseley's expression for these frequencies takes the form

$$\nu_{if} = [C\,(Z_{\mathrm{nucl}} - S)]^2\,, \tag{10.22}$$

[2]H. G. J. Moseley, The High-Frequency Spectra of the Elements, *Phil. Mag* **27**, 703 (1914).

where C is a constant which is independent of the nuclear charge Z_{nucl}. The screening constant S is different for each series, e.g., $S_{\text{K}} = 1$, $S_{\text{L}} = 7.4, \ldots$ Following the identification of this expression Moseley successfully predicted elements that had not been identified at the time, technetium (Tc, $Z_{\text{nucl}} = 43$), promethium (Pm, $Z_{\text{nucl}} = 61$), and Rhenium (Re, $Z_{\text{nucl}} = 75$).

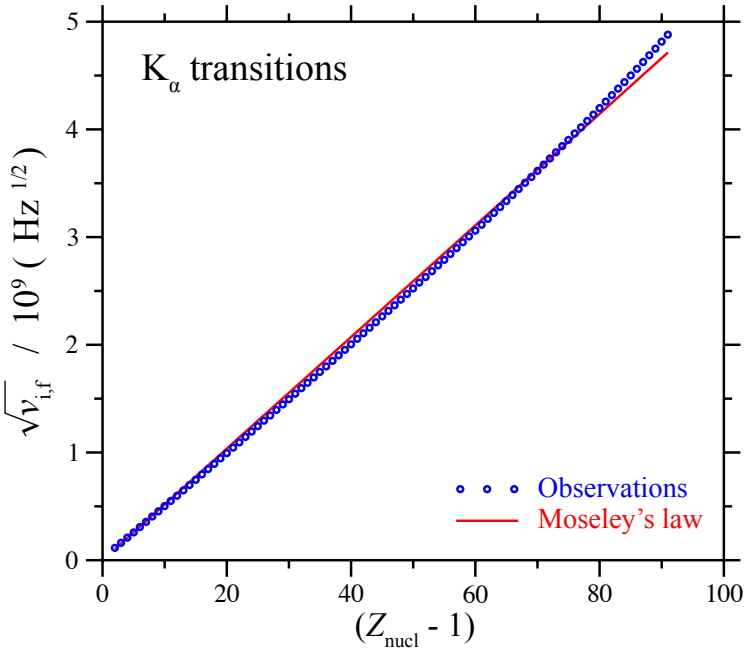

Figure 10.7: Observed values of $\sqrt{\nu_{i,f}}$ for the K_α transitions in the elements from Li to U (circles)[3]. A linear fit according to Moseley's law is overlaid (continuous curve). For the K_α transitions $S = 1$.

10.7 Rutherford scattering

In scattering experiments with α-particles (He nuclei $\equiv$ He^{2+}), Ernest Rutherford observed that most scattering events lead to a deflection of the projectiles from their initial direction of travel by only a small angle, and only a few collision resulting in the projectile particles being scattered backwards. Because He nuclei are heavy, $\sim$ 7000 times heavier than an

[3] J. A. Bearden, X-Ray Wavelengths, *Rev. Mod. Phys.* **39**, 78 (1967).

electron, in a collision with a neutral atom they interact primarily with the nucleus and are not significantly affected by the surrounding electron charge distribution. From his observations Rutherford therefore concluded that the heavy nucleus of an atom with its positive charge was localised at a particular point in space. Collisions between the beams of He nuclei with this localised heavy positive charged of a target atom gave rise to the few back-scattered projectiles, while for the majority of scattering events the projectiles passed through the electron cloud and were only weakly deflected. This demonstrated that the direction into which a projectile is scattered contains information on the properties of the target. The direction in which the scattered projectiles travel after a collision is given by the *differential cross-section*.

10.7.1 Differential cross-section

The differential cross-section in particle scattering experiments is denoted

$$\frac{\mathrm{d}\sigma}{\mathrm{d}\Omega} \equiv \frac{\text{Particle flux scattered into solid angle } \mathrm{d}\Omega}{\text{Incoming projectile intensity}}, \tag{10.23}$$

where the particle flux is the number of particles per second. In Rutherford's scattering experiments the α-particle flux, $\mathrm{d}N$, within a small solid angle, $\mathrm{d}\Omega$, was measured such that

$$\mathrm{d}N \propto N\, n_{\mathrm{t}}\, l\, \mathrm{d}\Omega, \tag{10.24}$$

$$\mathrm{d}N = \frac{\mathrm{d}\sigma}{\mathrm{d}\Omega} N\, n_{\mathrm{t}}\, l\, \mathrm{d}\Omega, \tag{10.25}$$

where N is the flux of incident projectiles, n_{t} is the number density of target particles, l is the interaction length, and the constant of proportionality is the differential cross-section. If the flux is integrated over all scattering directions the total cross-section is obtained, i.e.,

$$\sigma_{\mathrm{T}} = \int \frac{\mathrm{d}\sigma(\theta,\phi)}{\mathrm{d}\Omega}\, \mathrm{d}\Omega \tag{10.26}$$

$$= \int_0^{2\pi}\int_0^{\pi} \frac{\mathrm{d}\sigma(\theta,\phi)}{\mathrm{d}\Omega} \sin\theta\, \mathrm{d}\theta\, \mathrm{d}\phi, \tag{10.27}$$

since $d\Omega = \sin\theta\, d\theta\, d\phi$. However, because collisions involving atoms and molecules in free space have cylindrical symmetry, the differential cross-section must be independent of ϕ, therefore

$$\sigma_T = 2\pi \int_0^{\pi} \frac{d\sigma(\theta)}{d\Omega} \sin\theta\, d\theta \tag{10.28}$$